Czech Technical University in Prague
Faculty of Mechanical Engineering
Department of Technical Mathematics

Diploma thesis

Stabilization of finite element method for solving incompressible viscous flows

Jakub Šístek

Specialization
Mathematical Modelling in Technology

Advisor
Doc. RNDr. Pavel Burda, CSc.

Consultant
RNDr. Jaroslav Novotný, PhD.

Prague, 2004

Abstract

The topic of the thesis is an advanced application of the finite element method (FEM) to the solution of flows of viscous incompressible fluids. The aim is to extend the applicability of conventional methods to higher Reynolds numbers.

The derivation and the verification of the algorithm for stabilizing the FEM are considered by the author as the main achievement of the work presented. By applying it, we are able to increase the 'critical' Reynolds number of the flow, which can be succesfully solved by the FEM.

Motivation and main goals are described in the introductory chapter, together with the recent state of the research in this field. The problem of flow of incompressible Newtonian fluid in a two-dimensional domain is introduced. Following part is devoted to the FEM solution and problems of discretization in general. Stabilized methods based on the FEM for the scalar advective-diffusive equation are described, followed by the extension to the flow problem.

Next chapter is the principal part of the thesis. It contains a careful derivation of a FEM algorithm based on stabilization known as Galerkin Least-Squares (GLS) method. The algorithm is applied to several problems, and results of the experiments are presented.

Following chapter is devoted to the aspect of accuracy of the FEM solution. It presents work aimed on the application of a priori error estimates of FEM. Estimates are applied to the generation of the mesh, and cheap and precise computing of the solution even in domains with corner-like singularities is reached. Numerical results are included for two channels with sharp nonconvex inner corners.

Conclusions are summarized, including achievements and topics for further research.

Acknowledgements

I greatly thank Mr Pavel Burda, my advisor, proofreader, consultant, teacher, and friendly colleague in one personality. He came up with the idea of performing the following research and interested me in the finite element method. He kept his optimism when everything went wrong, was helpful anytime I needed it, and his friendship with me has been beyond the role of mere advisor.

No less do I thank Mr Jaroslav Novotný. None of used program implementations would have been developed without his assistance. He spent huge amounts of his time working on my problems and helping me to realize my ideas. He also has had many useful comments which have helped to orient me in problems of computational fluid dynamics. I thank him also for providing his frontal solver for systems of linear equations. It has helped to save a lot of time.

I also thank my parents who have supported me in studies.

Jakub Šístek

This research has been realized as a part of the project supported by the GAAV Grant No. IAA2120201/02.

Contents

1 Introduction

Application of the finite element method (FEM) in engeneering has made a rapid progress, and it is widely used in industry as well as in research centers today. Well-established commercial software based on the FEM helps with performing more complex simulations to make developments of products of desired properties cheaper.

When application of the FEM in structure mechanics is now clear enough for solving common tasks, and only special problems remain to be resolved, fluid dynamics still includes amount of open and not well handled problems. One of them is reliable modelling of flows for high Reynolds numbers, which appear in engineering practice.

The idea of stabilizing the FEM is not quite new in comparison to history of FEM itself. Many researchers are involved in this area and have already presented many techniques and results. Some of them have provided theroretical basis for the problem from the mathematical point of view, others presented often better results but usually with quite unclear background.

Let us briefly review several publications related to the area. T.J.R. Hughes, L.P. Franca, and M. Balestra [20] presented the stable Petrov-Galerkin formulation of the Stokes problem in 1986. J. Douglas, Jr. and J. Wang [10] introduced another stabilized method for the Stokes problem in 1988. In the same year, T.J.R. Hughes, L.P. Franca, and G.M. Hulbert [21] presented SUPG and GLS stabilized finite element methods for the advective-diffusive equation. Their ideas were extended to the Navier-Stokes equations and completed by L.P. Franca and S.L. Frey [12], L.P. Franca and T.J.R. Hughes [14], L.P. Franca and A.L. Madureira [15], and L.P. Franca, S.L. Frey, and A.L. Madureira [13]. Work of T.E. Tezduyar (e.g. [27]) and work of G. Lube and his co-workers (e.g. [16]) can be listed as a recent research in the stabilization of the FEM for fluid dynamics. R. Glowinski investigates another approach to stabilization (e.g. [18]). It uses spliting of the Navier-Stokes equations into the Stokes problem and the advective-diffusive equation.

Work of L.P. Franca and T.J.R. Hughes provides the theoretical basis for the presented research. The goal of it was to develop an algorithm based on the FEM stabilized by the technique introduced in [21] as Galerkin Least-Squares (GLS) method.

Let us mention the structure of the thesis. Flow of an incompressible viscous fluid described by the Navier-Stokes equations is introduced in Chapter 2. In Chapter 3, FEM formulation of the Navier-Stokes problem is described, together with difficulties accompanying numerical solution. An overview of stabilization techniques, especially GLS is presented in Chapter 4. This stabilization is applied to the advective-diffusive equation and to the Navier-Stokes equations. Chapter 5 is the principal part of the work. It contains a careful derivation of the algorithm based on the FEM. The algorithm is derived for the steady case and then extended to the unsteady case. Several numerical experiments are presented in Chapter 6. They are selected and sorted in order to show all positive as well as negative aspects of the stabilization, and of solving the Navier-Stokes equations in general. Whereas most of the thesis (Chapters 2-6) is concerned with the stability and therefore convergence of the FEM solution of fluid flow for high Reynolds numbers, Chapter 7 is devoted more to the aspect of accuracy of the FEM applied to flow in channels with sharp nonconvex inner corners. It deals with the application of a priori error estimates of the FEM to mesh generation. This approach offers quite cheap and precise computing of selected problems. Numerical results are demonstrated on two examples. Chapter 8 includes main achievements and topics for further research.

2 Navier-Stokes equations for incompressible viscous fluids

Let Ω be an open bounded domain in $\mathbb{R}^2$ filled with a fluid, and let Γ be its boundary. The generic point of $\mathbb{R}^2$ is denoted by $\mathbf{x} = (x_1, x_2)^T$ considered in meters, and t denotes time variable considered in seconds.

2.1 Unsteady two-dimensional flow

In this work, we deal with isothermal flow of Newtonian viscous fluids with constant density. Such flow is modelled by the following Navier-Stokes system of partial differential equations (nonconservative form)

$$\rho\left(\frac{\partial \mathbf{u}}{\partial t} + (\mathbf{u}\cdot\nabla)\mathbf{u}\right) - \mu\Delta\mathbf{u} + \nabla p_r = \rho\mathbf{f} \quad \text{in } \Omega\times[0,T] \tag{2.1}$$

$$\nabla\cdot\mathbf{u} = 0 \quad \text{in } \Omega\times[0,T] \tag{2.2}$$

where

- $\mathbf{u} = (u_1, u_2)^T$ denotes the vector of flow velocity considered in m/s, which is a function of $\mathbf{x}$ and t
- p_r denotes the pressure considered in Pa, which is a function of $\mathbf{x}$ and t
- ρ denotes the density of the fluid considered in kg/m^3
- μ denotes the dynamic viscosity of the fluid considered in $Pa\cdot s$, which is supposed to be constant
- $\mathbf{f}$ denotes the density of volume forces per mass unit considered in N/kg, which could be a function of $\mathbf{x}$ and t,

Let us divide both sides of the momentum equation (2.1) by ρ and leave the continuity equation (2.2) unchanged. Then we obtain

$$\frac{\partial \mathbf{u}}{\partial t} + (\mathbf{u}\cdot\nabla)\mathbf{u} - \nu\Delta\mathbf{u} + \nabla p = \mathbf{f} \quad \text{in } \Omega\times[0,T] \tag{2.3}$$

$$\nabla\cdot\mathbf{u} = 0 \quad \text{in } \Omega\times[0,T] \tag{2.4}$$

where

- $p = \frac{p_r}{\rho}$ denotes the pressure divided by the density considered in $Pa\cdot m^3/kg$
- $\nu = \frac{\mu}{\rho}$ denotes the kinematic viscosity of the fluid considered in m^2/s

The system introduced is not sufficient to define a flow since it has an infinity of solutions. To restrict the number of solutions, we have to consider further conditions, such as the initial condition

$$\mathbf{u} = \mathbf{u}_0 \ \text{ in } \Omega,\ t = 0 \tag{2.5}$$

where $\nabla\cdot\mathbf{u}_0 = 0$, and the boundary conditions

$$\mathbf{u} = \mathbf{g} \ \text{ on } \Gamma_g\times[0,T] \tag{2.6}$$

$$-\nu(\nabla\mathbf{u})\mathbf{n} + p\mathbf{n} = \mathbf{0} \ \text{ on } \Gamma_h\times[0,T] \tag{2.7}$$

where

- Γ_g and Γ_h are two subsets of Γ satisfying $\overline{\Gamma} = \overline{\Gamma}_g \cup \overline{\Gamma}_h,\ \mu_{\mathbb{R}^1}(\Gamma_g \cap \Gamma_h) = 0$
- $\mathbf{n}$ denotes an outer normal vector to the boundary Γ with unit lenght

Introduced $\mathbf{g}$ is a given function of $\mathbf{x}$ and t satisfying in the case of $\Gamma = \Gamma_g$ for all $t \in [0, T]$

$$\int_\Gamma \mathbf{g} \cdot \mathbf{n} \mathrm{d}\Gamma = 0$$

2.2 Steady two-dimensional flow

For the case of steady flow, the time derivative in (2.3) becomes zero. Then the Navier-Stokes equations are reduced to

$$(\mathbf{u} \cdot \nabla)\mathbf{u} - \nu\Delta\mathbf{u} + \nabla p = \mathbf{f} \quad \text{in } \Omega \tag{2.8}$$

$$\nabla \cdot \mathbf{u} = 0 \quad \text{in } \Omega \tag{2.9}$$

and boundary conditions to

$$\mathbf{u} = \mathbf{g} \quad \text{on } \Gamma_g \tag{2.10}$$

$$-\nu(\nabla\mathbf{u})\mathbf{n} + p\mathbf{n} = \mathbf{0} \quad \text{on } \Gamma_h \tag{2.11}$$

Initial condition is not present, and $\mathbf{u}$, p, $\mathbf{f}$, and $\mathbf{g}$ are no more functions of t.

2.3 Unsteady axisymmetric flow

Let us now consider the system of Navier-Stokes equations for incompressible viscous fluid in three dimensions, cf. [18]. After performing transformation of the cartesian system of coordinates $\{x_1, x_2, x_3\}$ into the cylindrical system of coordinates $\{r, \varphi, z\}$ where

$$x_1 = r\cos\varphi;\ x_2 = r\sin\varphi;\ x_3 = z,$$

and considering axialy symmetric flow, i.e. variables are independent of φ, we obtain Navier-Stokes equations in the form (cf. e.g. [5])

$$\frac{\partial u}{\partial t} + v\frac{\partial u}{\partial r} + u\frac{\partial u}{\partial z} - \nu\left(\frac{\partial^2 u}{\partial r^2} + \frac{1}{r}\frac{\partial u}{\partial r} + \frac{\partial^2 u}{\partial z^2}\right) + \frac{\partial p}{\partial z} = f_z \quad \text{in } \Omega \times [0, T] \tag{2.12}$$

$$\frac{\partial v}{\partial t} + v\frac{\partial v}{\partial r} + u\frac{\partial v}{\partial z} - \nu\left(\frac{\partial^2 v}{\partial r^2} + \frac{1}{r}\frac{\partial v}{\partial r} - \frac{v}{r^2} + \frac{\partial^2 v}{\partial z^2}\right) + \frac{\partial p}{\partial r} = f_r \quad \text{in } \Omega \times [0, T] \tag{2.13}$$

$$\frac{\partial v}{\partial r} + \frac{v}{r} + \frac{\partial u}{\partial z} = 0 \quad \text{in } \Omega \times [0, T] \tag{2.14}$$

where

- u denotes the axial component of velocity (direction of z-coordinate) considered in m/s, which is a function of $\mathbf{x}$ and t
- v denotes the radial component of velocity (direction of r-coordinate) considered in m/s, which is a function of $\mathbf{x}$ and t
- $\mathbf{f} = (f_z, f_r)^T$ denotes the density of volume forces per mass unit considered in N/m^3, which could be a function of $\mathbf{x}$ and t

Equations (2.12)-(2.14) govern the axisymmetric flow in a domain $\Omega \subset \mathbb{R}^2$, where the generic point of $\mathbb{R}^2$ is now denoted by $\mathbf{x} = (z, r)^T$ for arbitrary φ.

2.4 Variational formulation of Navier-Stokes equations

We need to introduce several function spaces for further derivations. Note, that all integrals are considered in the Lebesque sense. Let $L_2(\Omega)$ be the space of square integrable functions on Ω, and let $L_2(\Omega)/\mathbb{R}$ be the space of functions in $L_2(\Omega)$ ignoring an additive constant. Let $H^1(\Omega)$ and $H_0^1(\Omega)$ be the Sobolev spaces defined as

$$\begin{aligned} H^1(\Omega) &= \left\{ v \mid v \in L^2(\Omega), \frac{\partial v}{\partial x_i} \in L^2(\Omega), i = 1, 2 \right\} \\ H_0^1(\Omega) &= \left\{ v \mid v \in H^1(\Omega), \mathbf{Tr}\ v = 0 \right\} \end{aligned}$$

where $\mathbf{Tr}$ is the trace operator $\mathbf{Tr}:\ H^1(\Omega) \longrightarrow L_2(\Gamma_g)$, and derivatives are considered in the weak sense.

The norm of function v in the space $L_2(\Omega)$ is considered as

$$\|v\|^2_{L_2(\Omega)} = \int_\Omega v^2 \mathrm{d}\Omega$$

and the norm of function v in the Sobolev space $H^1(\Omega)$ is considered as

$$\|v\|^2_{H^1(\Omega)} = \int_\Omega \left(v^2 + \sum_{k=1}^{2} \left(\frac{\partial v}{\partial x_k} \right)^2 \right) \mathrm{d}\Omega$$

Sometimes, the notation $\|\cdot\|_{L_2(\Omega)}$ is shortened to $\|\cdot\|_0$ and $\|\cdot\|_{H^1(\Omega)}$ to $\|\cdot\|_1$.

The inner product of two functions u and v in the space $L_2(\Omega)$ is considered as

$$(u, v)_{L_2(\Omega)} = \int_\Omega uv \ \mathrm{d}\Omega$$

Similarly, the notation $(u, v)_{L_2(\Omega)}$ is shortened to $(u, v)_0$. For more about Sobolev spaces and their properties, see e.g. [11].

Let us define vector function spaces V_g and V by

$$\begin{aligned} V_g &= \left\{ \mathbf{v} = (v_1, v_2)^T \mid \mathbf{v} \in [H^1(\Omega)]^2; \mathbf{Tr}\ v_i = g_i, i = 1, 2 \right\} \\ V &= \left\{ \mathbf{v} = (v_1, v_2)^T \mid \mathbf{v} \in [H_0^1(\Omega)]^2 \right\} \end{aligned}$$

Let us note, that the norm of vector function $\mathbf{v}$ in the space V_g and V is then

$$\|\mathbf{v}\|^2_{[H^1(\Omega)]^2} = \sum_{i=1}^{2} \int_\Omega \left(v_i^2 + \sum_{k=1}^{2} \left(\frac{\partial v_i}{\partial x_k} \right)^2 \right) \mathrm{d}\Omega$$

and the norm of vector function $\mathbf{v}$ in the space $[L_2(\Omega)]^2$ is

$$\|\mathbf{v}\|^2_{[L_2(\Omega)]^2} = \sum_{i=1}^{2} \int_\Omega v_i^2 \mathrm{d}\Omega$$

Let us derive the weak formulation of the Navier-Stokes equations (2.3)-(2.4) in the way of mixed methods, i.e. usage of different function spaces of test functions for the momentum equation and for the continuity equation (cf. [17]). To derive it, we suppose for a while, that the functions appearing in the system are sufficiently smooth. Then for any $t \in [0, T]$, we have

$$\int_\Omega \frac{\partial \mathbf{u}}{\partial t} \cdot \mathbf{v} \mathrm{d}\Omega + \int_\Omega (\mathbf{u} \cdot \nabla)\mathbf{u} \cdot \mathbf{v} \mathrm{d}\Omega - \nu \int_\Omega \Delta \mathbf{u} \cdot \mathbf{v} \mathrm{d}\Omega + \int_\Omega \nabla p \cdot \mathbf{v} \mathrm{d}\Omega = \int_\Omega \mathbf{f} \cdot \mathbf{v} \mathrm{d}\Omega \quad (2.15)$$

$$\int_\Omega \psi \nabla \cdot \mathbf{u} \mathrm{d}\Omega = 0 \quad (2.16)$$

$$\mathbf{u} - \mathbf{u}_g \in V \quad (2.17)$$

for any $\mathbf{v} \in V$ and $\psi \in L^2(\Omega)$ where $\mathbf{u}_g \in V_g$ is a representation of the Dirichlet boundary condition $\mathbf{g}$ in (2.6). We assume $\mathbf{g} \in [L_2(\Gamma_g)]^2$ and $\mathbf{f} \in [L_2(\Omega)]^2$.

Using Green's formula on the third and the fourth term of equation (2.15), we obtain

$$\int_\Omega \frac{\partial \mathbf{u}}{\partial t} \cdot \mathbf{v} \mathrm{d}\Omega + \int_\Omega (\mathbf{u} \cdot \nabla)\mathbf{u} \cdot \mathbf{v} \mathrm{d}\Omega - \nu \int_\Gamma (\nabla \mathbf{u})\mathbf{v} \cdot \mathbf{n} \mathrm{d}\Gamma + \nu \int_\Omega \nabla \mathbf{u} : \nabla \mathbf{v} \mathrm{d}\Omega +$$
$$+ \int_\Gamma p \mathbf{v} \cdot \mathbf{n} \mathrm{d}\Gamma - \int_\Omega p \nabla \cdot \mathbf{v} \mathrm{d}\Omega = \int_\Omega \mathbf{f} \cdot \mathbf{v} \mathrm{d}\Omega \quad (2.18)$$

$$\int_\Omega \psi \nabla \cdot \mathbf{u} \mathrm{d}\Omega = 0 \quad (2.19)$$

$$\mathbf{u} - \mathbf{u}_g \in V \quad (2.20)$$

The integrals over boundary in (2.18) vanish for considered boundary conditions. The operation $\nabla \mathbf{u} : \nabla \mathbf{v}$ is defined in Appendix.

Then the *weak unsteady Navier-Stokes problem* means seeking of $\mathbf{u}(t) = (u_1(t), u_2(t))^T \in V_g$ and $p(t) \in L_2(\Omega)/\mathbb{R}$ satisfying for any $t \in [0, T]$

$$\int_\Omega \frac{\partial \mathbf{u}}{\partial t} \cdot \mathbf{v} \mathrm{d}\Omega + \int_\Omega (\mathbf{u} \cdot \nabla)\mathbf{u} \cdot \mathbf{v} \mathrm{d}\Omega + \nu \int_\Omega \nabla \mathbf{u} : \nabla \mathbf{v} \mathrm{d}\Omega - \int_\Omega p \nabla \cdot \mathbf{v} \mathrm{d}\Omega = \int_\Omega \mathbf{f} \cdot \mathbf{v} \mathrm{d}\Omega \quad (2.21)$$

$$\int_\Omega \psi \nabla \cdot \mathbf{u} \mathrm{d}\Omega = 0 \quad (2.22)$$

$$\mathbf{u} - \mathbf{u}_g \in V \quad (2.23)$$

for $\mathbf{v} \in V$ and $\psi \in L^2(\Omega)$.

Similarly, the *weak steady Navier-Stokes problem* reads:

Seek $\mathbf{u} = (u_1, u_2)^T \in V_g$ and $p \in L_2(\Omega)/\mathbb{R}$ satisfying

$$\int_\Omega (\mathbf{u} \cdot \nabla)\mathbf{u} \cdot \mathbf{v} \mathrm{d}\Omega + \nu \int_\Omega \nabla \mathbf{u} : \nabla \mathbf{v} \mathrm{d}\Omega - \int_\Omega p \nabla \cdot \mathbf{v} \mathrm{d}\Omega = \int_\Omega \mathbf{f} \cdot \mathbf{v} \mathrm{d}\Omega \quad (2.24)$$

$$\int_\Omega \psi \nabla \cdot \mathbf{u} \mathrm{d}\Omega = 0 \quad (2.25)$$

$$\mathbf{u} - \mathbf{u}_g \in V \quad (2.26)$$

for $\mathbf{v} \in V$ and $\psi \in L^2(\Omega)$.

3 Finite element methods for Navier-Stokes equations

Let us divide the domain Ω (supposed now polygonal) into N elements T_K of a triangulation $\mathcal{T}$ such that

$$\begin{aligned} \bigcup_{K=1}^{N} \overline{T}_K &= \overline{\Omega} \\ \mu_{\mathbb{R}^2}\left(T_K \cap T_L\right) &= 0, K \neq L \end{aligned}$$

Let h_K mean the largest distance in element T_K.

3.1 Function spaces for velocity and pressure approximation

Difficult problem in solving the Navier-Stokes equations by the FEM consists in a proper choice of function spaces for velocity and pressure approximation. Appart from spectral finite element methods, polynomial approximation is commonly used in the FEM in general. To solve the Navier-Stokes equations, it is possible to choose different polynomial approximation for velocities and for pressure. Equal order approximation is easy to implement, but pressure exhibits instability. Approximation with different order is more suitable for practical computing, cf. [1].

The following properties of desired solution are linked with the variational formulation of the Navier-Stokes equations (2.21)-(2.23) or (2.24)-(2.26):

- each component of velocity is a square integrable function of $\mathbf{x}$, and at least its first derivative by any coordinate (in the weak sense) exists
- pressure is a square integrable function of $\mathbf{x}$

There is an effort for using higher order approximations induced by p-methods and hp-methods. But this is not straightforward for the Navier-Stokes equations. I. Babuška and F. Brezzi proved a condition (also called inf-sup condition) limitting the choice of combinations of approximation

$$\exists_{C_B>0,const.}\ \forall_{q_h \in Q_h}\ \exists_{\mathbf{v}_h \in V_{gh}}\ (q_h, \nabla \cdot \mathbf{v}_h)_0 \geq C_B \|q_h\|_0 \|\mathbf{v}_h\|_1 \tag{3.1}$$

where Q_h and V_{gh} are the function spaces for approximation of pressure and velocity. This is an important stability result. It has been shown, that there are big difficulties with applying approximations, which do not satisfy the Babuška-Brezzi condition, cf. e.g. [1].

Chosen combination of final polynomial approximation is achieved by usage of corresponding finite elements. There are several finite elements (in 2D as well as in 3D) which do satisfy the BB-condition. Following list is not complete.

Finite elements satisfying the Babuška-Brezzi condition (cf. [1])

- $P_1^+ P_1$ (mini element)
- $P_2 P_1$ (Hood-Taylor, 1973)
- $P_2^+ P_1$
- $P_2^+ P_{-1}$ (Crouzeix-Raviart)
- $Q_2 Q_1$ (Hood-Taylor)
- $Q_2 P_{-1}$

3.2 Hood-Taylor finite elements

For their application in this work, Hood-Taylor finite elements on triangles and quadrilaterals are described more precisely. Values of velocity are aproximated in corner nodes and in midsides, and values of pressure in corner nodes (Figure 3.1). It corresponds to the following function spaces on element T_K:

- *triangle*

$$\begin{aligned} v_i &\in P_2(T_K),\ i = 1, 2, \quad \text{i.e. polynomial of the second order} \\ p &\in P_1(T_K) \quad \text{i.e. linear polynomial} \end{aligned}$$

- *quadrilateral*

$$\begin{aligned} v_i &\in Q_2(T_K),\ i = 1, 2, \quad \text{i.e. polynomial of the second order for each coordinate} \\ p &\in Q_1(T_K) \quad \text{i.e. bilinear polynomial} \end{aligned}$$

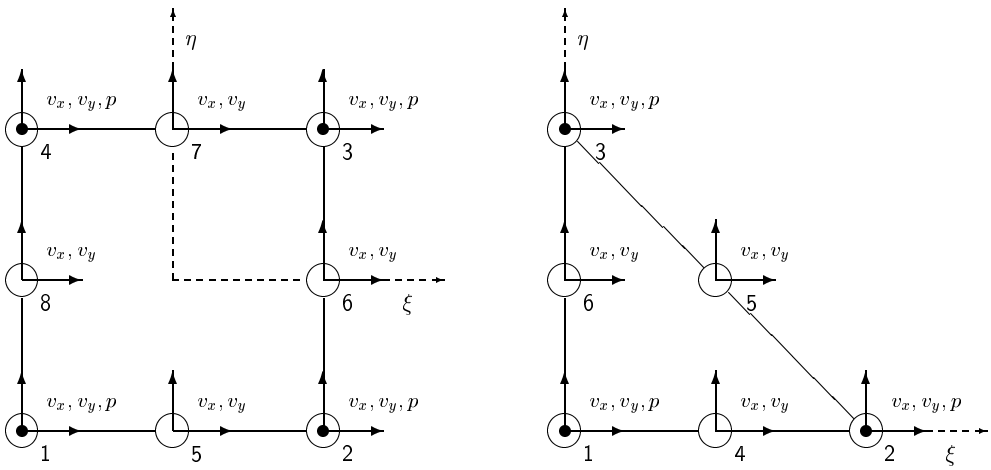

Figure 3.1: Hood-Taylor reference elements

The approximation leads to the following shape functions written in local coordinate system $\{\xi, \eta\}$:

- *triangle*
  Space functions for approximation of velocity component

$$\begin{aligned} N_1 &= 1/2 \cdot (2 - \xi - \eta)(1 - \xi - \eta) \\ N_2 &= 1/2 \cdot \xi(\xi - 1) \\ N_3 &= 1/2 \cdot \eta(\eta - 1) \\ N_4 &= \xi(2 - \xi - \eta) \\ N_5 &= \xi\eta \\ N_6 &= \eta(2 - \xi - \eta) \end{aligned}$$

Space functions for approximation of pressure

$$\begin{aligned} M_1 &= 1/2 \cdot (2 - \xi - \eta) \\ M_2 &= 1/2 \cdot \xi \\ M_3 &= 1/2 \cdot \eta \end{aligned}$$

- *quadrilateral*
  Space functions for approximation of velocity component

$$\begin{aligned} N_1 &= 1/4 \cdot (1-\xi)(1-\eta)(-\xi-\eta-1) \\ N_2 &= 1/4 \cdot (1+\xi)(1-\eta)(\xi-\eta-1) \\ N_3 &= 1/4 \cdot (1+\xi)(1+\eta)(\xi+\eta-1) \\ N_4 &= 1/4 \cdot (1-\xi)(1+\eta)(-\xi+\eta-1) \\ N_5 &= 1/2 \cdot (1-\xi^2)(1-\eta) \\ N_6 &= 1/2 \cdot (1-\eta^2)(1+\xi) \\ N_7 &= 1/2 \cdot (1-\xi^2)(1+\eta) \\ N_8 &= 1/2 \cdot (1-\eta^2)(1-\xi) \end{aligned}$$

  Space functions for approximation of pressure

$$\begin{aligned} M_1 &= 1/4 \cdot (1-\xi)(1-\eta) \\ M_2 &= 1/4 \cdot (1+\xi)(1-\eta) \\ M_3 &= 1/4 \cdot (1+\xi)(1+\eta) \\ M_4 &= 1/4 \cdot (1-\xi)(1+\eta) \end{aligned}$$

3.3 Discretization of steady Navier-Stokes equations by FEM

Let us consider the variational formulation of the steady Navier-Stokes equations (2.24)-(2.26). For isoparametric finite elements, velocities and pressure on each element are given as

$$\begin{aligned} v_x &= \sum_{i=1}^{N_u} v_{x_i} N_i \\ v_y &= \sum_{i=1}^{N_u} v_{y_i} N_i \\ p &= \sum_{i=1}^{N_p} p_i M_i \end{aligned}$$

where

- v_x denotes the component of velocity in the direction of x-coordinate
- v_y denotes the component of velocity in the direction of y-coordinate
- p denotes pressure
- v_{x_i} is the value of velocity v_x in the node i

- v_{y_i} is the value of velocity v_y in the node i
- p_i is the value of pressure in the node i
- N_u is the number of nodes with value of velocity on element given (in the case of Hood-Taylor elements, $N_u = 8$ for quadrilateral and $N_u = 6$ for triangle)
- N_p is the number of nodes with value of pressure on element given (in the case of Hood-Taylor elements, $N_p = 4$ for quadrilateral, $N_p = 3$ for triangle)

Let us employ the notation

$$R_m(\overline{T_K}) = \begin{cases} P_m(\overline{T_K}), & \text{if } T_K \text{ is a triangle} \\ Q_m(\overline{T_K}), & \text{if } T_K \text{ is a quadrilateral} \end{cases}$$

and let $\mathcal{C}(\overline{\Omega})$ denote the space of continuous functions on $\overline{\Omega}$.

Application of Hood-Taylor finite elements leads to the final approximation on the domain Ω satisfying $\mathbf{u}_h \in V_{gh}$ and $p_h \in Q_h$ where

$$\begin{aligned} V_{gh} &= \Big\{ \mathbf{v}_h = (v_{h_1}, v_{h_2})^T \in [\mathcal{C}(\overline{\Omega})]^2;\ v_{h_i}\,|_{T_K} \in R_2(\overline{T_K}),\ K = 1, \ldots, N,\ i = 1, 2,\ \mathbf{v}_h = \mathbf{g} \\ &\qquad \text{in nodes on } \Gamma_g \Big\} \\ Q_h &= \Big\{ \psi_h \in \mathcal{C}(\overline{\Omega});\ \psi_h\,|_{T_K} \in R_1(\overline{T_K}),\ K = 1, \ldots, N \Big\} \end{aligned}$$

For further reasons, we introduce the space

$$\begin{aligned} V_h &= \Big\{ \mathbf{v}_h = (v_{h_1}, v_{h_2})^T \in [\mathcal{C}(\overline{\Omega})]^2;\ v_{h_i}\,|_{T_K} \in R_2(\overline{T_K}),\ K = 1, \ldots, N,\ i = 1, 2,\ \mathbf{v}_h = \mathbf{0} \\ &\qquad \text{in nodes on } \Gamma_g \Big\} \end{aligned}$$

Since these function spaces satisfy $V_{gh} \subset V_g$, $V_h \subset V$, and $Q_h \subset L_2(\Omega)/\mathbb{R}$ for prescribed arbitrary value of pressure (e.g. $p_h = 0$) in one node, we can introduce *approximate steady Navier-Stokes problem*:

Seek $\mathbf{u}_h \in V_{gh}$ and $p_h \in Q_h$ satisfying

$$\int_\Omega (\mathbf{u}_h \cdot \nabla)\mathbf{u}_h \cdot \mathbf{v}_h \mathrm{d}\Omega + \nu \int_\Omega \nabla \mathbf{u}_h : \nabla \mathbf{v}_h \mathrm{d}\Omega - \int_\Omega p_h \nabla \cdot \mathbf{v}_h \mathrm{d}\Omega = \int_\Omega \mathbf{f} \cdot \mathbf{v}_h \mathrm{d}\Omega,\ \forall \mathbf{v}_h \in V_h \tag{3.2}$$

$$\int_\Omega \psi_h \nabla \cdot \mathbf{u}_h \mathrm{d}\Omega = 0,\ \forall \psi_h \in Q_h \tag{3.3}$$

$$\mathbf{u}_h - \mathbf{u}_{gh} \in V_h \tag{3.4}$$

where $\mathbf{u}_{gh} \in V_{gh}$ is the projection of $\mathbf{u}_g$ onto the space V_{gh}.

Using the shape regular triangulation and refining the mesh such that $h_{max} \to 0$ where

$$h_{max} = \max_K h_K,$$

the solution of the approximated problem converges to the solution of the continuous problem (for more cf. e.g. [1]).

3.4 Discretization of unsteady Navier-Stokes equations

To solve the unsteady Navier-Stokes equations (2.21)-(2.23), we need to discretize the system both in space and time. Two techniques are avaiable:

- Method of lines (MOL)
  1. step – semidiscretization in space (e.g. by FEM)
  2. step – discretization in time (e.g. by the Euler method)
- Rothe's method
  1. step – semidiscretization in time
  2. step – discretization in space

3.5 Space semidiscretization of unsteady Navier-Stokes equations by FEM

Let us perform space semidiscretization of the system (2.21)-(2.23) by the FEM in the context of the MOL. Extending derivations for the steady case in Chapter 3.3, we introduce the problem:

Seek $\mathbf{u}_h(t) \in V_{gh},\ t \in [0,T]$ and $p_h(t) \in Q_h,\ t \in [0,T]$ satisfying

$$\begin{aligned}
\int_\Omega \frac{\partial \mathbf{u}_h}{\partial t} \cdot \mathbf{v}_h \mathrm{d}\Omega + \int_\Omega (\mathbf{u}_h \cdot \nabla)\mathbf{u}_h \cdot \mathbf{v}_h \mathrm{d}\Omega \quad &+ \quad \nu \int_\Omega \nabla \mathbf{u}_h : \nabla \mathbf{v}_h \mathrm{d}\Omega - \\
- \int_\Omega p_h \nabla \cdot \mathbf{v}_h \mathrm{d}\Omega \quad &= \quad \int_\Omega \mathbf{f} \cdot \mathbf{v}_h \mathrm{d}\Omega,\ \forall \mathbf{v}_h \in V_h \qquad (3.5)\\
\int_\Omega \psi_h \nabla \cdot \mathbf{u}_h \mathrm{d}\Omega \quad &= \quad 0,\ \forall \psi_h \in Q_h \qquad (3.6)\\
\mathbf{u}_h - \mathbf{u}_{gh} \quad &\in \quad V_h \qquad (3.7)
\end{aligned}$$

3.6 Time discretization of unsteady Navier-Stokes equations by the Euler method

In the unsteady case of the Navier-Stokes system of equations, the approximation of time is needed. As for discretization in space, several possibilities are avaiable. Let us restrict to those introducing discrete time layers, in which the solution is seeked. These methods can be divided into explicit, semi-imlicit, and implicit families.

Employing MOL leads to solving system of ordinary differential equations (ODE) after semidiscretization in space. We can choose from various numerical methods known from solving ODE systems, starting from the Euler methods to the Runge-Kutta methods of high order approximation.

Very sophisticated way was introduced by R. Glowinski (e.g. in [18]). It is based on fractional steps methods, therefore represents the family of Rothe's methods.

In this thesis, we consider partition of the time interval $[0,T]$ into M time intervals with $M+1$ time layers. The time step between n-th time layer and $(n+1)$-st time layer is assumed constant and is denoted by ϑ.

We employ the implicit Euler method (also known as the backward difference method) for time discretization of the Navier-Stokes system (3.5)-(3.7), i.e. time derivative is substituted as

$$\frac{\partial \mathbf{u}_h}{\partial t} \approx \frac{\mathbf{u}_h^{n+1} - \mathbf{u}_h^n}{\vartheta}.$$

This leads to fully implicit method for seeking $\mathbf{u}_h$ in $(n+1)$-st time layer. The problem then reads:

Seek $\mathbf{u}_h^{n+1} \in V_{gh}$ and $p_h^{n+1} \in Q_h$ satisfying

$$\begin{aligned}
\frac{1}{\vartheta}\int_\Omega \mathbf{u}_h^{n+1}\cdot\mathbf{v}_h \mathrm{d}\Omega + \int_\Omega (\mathbf{u}_h^{n+1}\cdot\nabla)\mathbf{u}_h^{n+1}\cdot\mathbf{v}_h \mathrm{d}\Omega &+ \nu\int_\Omega \nabla\mathbf{u}_h^{n+1} : \nabla\mathbf{v}_h \mathrm{d}\Omega - \\
-\int_\Omega p_h^{n+1}\nabla\cdot\mathbf{v}_h \mathrm{d}\Omega - \frac{1}{\vartheta}\int_\Omega \mathbf{u}_h^n\cdot\mathbf{v}_h \mathrm{d}\Omega &= \int_\Omega \mathbf{f}^{n+1}\cdot\mathbf{v}_h \mathrm{d}\Omega,\ \forall \mathbf{v}_h \in V_h \qquad (3.8)\\
\int_\Omega \psi_h \nabla\cdot\mathbf{u}_h^{n+1} \mathrm{d}\Omega &= 0,\ \forall \psi_h \in Q_h \qquad (3.9)\\
\mathbf{u}_h^{n+1} - \mathbf{u}_{gh}^{n+1} &\in V_h \qquad (3.10)
\end{aligned}$$

4 Stabilization techniques for finite element method

Stability of numerical methods for solving partial differential equations is restricted, e.g. for the Navier-Stokes equations by the Reynolds number. In the effort for computing 'behind this line', a lot of researchers presented methods improving stability of numerical schemes. For the finite element method, let us mention work of T.J.R. Hughes, L.P. Franca, and their co-workers in [12],[13],[14],[15],[20], and [21], which gives the basis for this work.

4.1 Advection-diffusion equation

Let us consider for a moment the problem of finding $u = u(x)$, $x \in \overline{\Omega}$ satisfying

$$\begin{aligned} \mathcal{L} &\equiv -\nabla \cdot \sigma(u) = f \quad \text{in } \Omega \\ \sigma &= -\mathbf{a}u + \kappa \nabla u \end{aligned}$$

where

- $\mathbf{a}$ denotes given flow velocity assumed solenoidal, i.e. $\nabla \cdot \mathbf{a} = 0$ in Ω
- $\kappa > 0$ denotes diffusivity

combined with sufficient boundary conditions (see [4] for details).

Variational formulation of this problem reads:
Seek $u \in V_g$ such that

$$B(u, w) = L(w), \quad \forall w \in V$$

where

$$\begin{aligned} B(u,w) &= (-\mathbf{a}u + \kappa \nabla u, \nabla w)_\Omega + (a_n^+ u, w)_{\Gamma_h} \\ L(w) &= (f, w)_\Omega + (h, w)_{\Gamma_h} \\ V_g &= \{w \in H^1(\Omega), w = g \text{ on } \Gamma_g \text{ in the sense of traces}\} \\ V &= \{w \in H^1(\Omega), w = 0 \text{ on } \Gamma_g \text{ in the sense of traces}\} \\ a_n^+ u &= \frac{\mathbf{a} \cdot \mathbf{n} + |\mathbf{a} \cdot \mathbf{n}|}{2} \end{aligned}$$

Let us consider a partition of Ω into finite elements. Let Ω_K be the interior of the $K-$th element. Denote

$$\widetilde{\Omega} = \bigcup_K \Omega_K \quad \text{(element interiors)}$$

Let $V_{gh} \subset V_g, V_h \subset V$ be finite element spaces consisting of continuous piecewise polynomials of order k.

Classical Galerkin method means:

Seek $u_h \in V_{gh}$ such that

$$B(u_h, w_h) = L(w_h), \quad \forall w_h \in V_h$$

Hughes, Franca, and Hulbert presented two methods with improved stability properties for the advection-diffusion equation in [21]:

Streamline Upwind Petrov-Galerkin (SUPG)

$$\begin{aligned} B_{SUPG}(u_h, w_h) &= L_{SUPG}(w_h), \quad \forall w_h \in V_h \\ B_{SUPG}(u_h, w_h) &\equiv B(u_h, w_h) + \tau(\mathcal{L}u_h, \mathbf{a} \cdot \nabla w_h)_{\tilde{\Omega}} \\ L_{SUPG}(w_h) &\equiv L(w_h) + \tau(f, \mathbf{a} \cdot \nabla w_h)_{\tilde{\Omega}} \end{aligned}$$

Galerkin Least-Squares (GLS)

$$\begin{aligned} B_{GLS}(u_h, w_h) &= L_{GLS}(w_h), \quad \forall w_h \in V_h \\ B_{GLS}(u_h, w_h) &\equiv B(u_h, w_h) + \tau(\mathcal{L}u_h, \mathcal{L}w_h)_{\tilde{\Omega}} \\ L_{GLS}(w_h) &\equiv L(w_h) + \tau(f, \mathcal{L}w_h)_{\tilde{\Omega}} \end{aligned}$$

where τ is positive parameter and is function of element Peclet number α. The authors assume the following:

$$\begin{aligned} \alpha &= \frac{h|\mathbf{a}|}{2\kappa} \\ \tau &= O(\frac{h}{|\mathbf{a}|}) \text{ for } \alpha \text{ large} \\ \tau &= O(\frac{h^2}{\kappa}) \text{ for } \alpha \text{ small} \end{aligned}$$

Both SUPG and GLS methods have modifications for the Navier-Stokes equations.

4.2 Navier-Stokes equations

L.P. Franca and T.J.R. Hughes [14] analyze modification of the GLS method to stabilize the steady *linearized* Navier-Stokes equations given by

$$(\nabla \mathbf{u})\mathbf{a} + \nabla p - \nu \Delta \mathbf{u} = \mathbf{f} \text{ in } \Omega \tag{4.1}$$

$$\nabla \cdot \mathbf{u} = 0 \text{ in } \Omega \tag{4.2}$$

$$\mathbf{u} = \mathbf{0} \text{ on } \Gamma \tag{4.3}$$

where $\nabla \cdot \mathbf{a} = 0$. They define the norm on $V_{gh} \times Q_h$ as

$$|||\{\mathbf{u}, p\}|||^2 \equiv \nu \|\nabla \mathbf{u}\|_{0,\Omega}^2 + \sum_K \tau \|(\nabla \mathbf{u})\mathbf{a} + \nabla p - \nu \Delta \mathbf{u}\|_{0,K}^2 + \sum_K \delta \|\nabla \cdot \mathbf{u}\|_{0,K}^2 \tag{4.4}$$

and they prove the following lemma:

Lemma 4.1 (Stability) *The bilinear form of the linearized problem (4.1)-(4.3) satisfies*

$$B_{GLS}(\mathbf{u}_h, p_h; \mathbf{u}_h, p_h) = |||\{\mathbf{u}_h, p_h\}|||^2.$$

For the Stokes problem, the following estimate is proved in [14]

$$|||\{\mathbf{u}_h, p_h\}|||^2 \geq \frac{\nu}{2}\|\nabla \mathbf{u}\|^2_{0,\Omega} + \frac{1}{2}\sum_K \tau\|\nabla p\|^2_{0,K} + \sum_K \delta\|\nabla\cdot\mathbf{u}\|^2_{0,K} \tag{4.5}$$

Notice, that the choice $\delta = 0$ also gives stability. It is important in further derivations (Chapter 5).

Using stability, the following convergence theorem is proved in [14]:

Theorem (Convergence) *Assuming constant viscosity ν, the solution $\{\mathbf{u}_h, p_h\}$ obtained by the GLS method converges to the solution $\{\mathbf{u}, p\}$ of (4.1)-(4.3) as follows:*

$$\begin{aligned} |||\{\mathbf{u}_h, p_h\} - \{\mathbf{u}, p\}|||^2 \;\leq\; & C\sum_K \Bigg[H(Re_K - 1)\left(\sup_{x\in T_K}|a|_q h_K^{2k+1}|\mathbf{u}|^2_{k+1,T_K} + \sup_{x\in T_K}|a|_q^{-1}h_K^{2l+1}|p|^2_{l+1,T_K}\right) \\ + \;& H(1 - Re_K)\left(\nu h_K^{2k}|\mathbf{u}|^2_{k+1,T_K} + \nu^{-1}h_K^{2l+2}|p|^2_{l+1,T_K}\right)\Bigg] \end{aligned}$$

where $H(\cdot)$ is the Heaviside function given by

$$H(x-y) = \begin{cases} 0, & x < y \\ 1, & x > y \end{cases}$$

and Re_K is local Reynolds number on element K.

L.P. Franca and A.L. Madureira [15] consider slightly different formulation of the steady problem than is considered in this work up to here, given by

$$\begin{aligned} (\nabla\mathbf{u})\mathbf{u} - 2\nu\nabla\cdot\varepsilon(\mathbf{u}) + \nabla p &= \mathbf{f} \;\text{ in } \Omega \\ \nabla\cdot\mathbf{u} &= 0 \;\text{ in } \Omega \\ \mathbf{u} &= \mathbf{0} \;\text{ on } \Gamma \end{aligned}$$

where $\varepsilon(\mathbf{u})_{ij} = \frac{1}{2}\left(\frac{\partial u_i}{\partial x_j} + \frac{\partial u_j}{\partial x_i}\right)$.

The stabilized problem reads:

Seek $\mathbf{u}_h \in V_{gh}$ and $p_h \in Q_h$ satisfying in Ω

$$B_{GLS}(\mathbf{u}_h, p_h; \mathbf{v}_h, \psi_h) = L_{GLS}(\mathbf{v}_h, \psi_h), \quad \forall \mathbf{v}_h \in V_h, \quad \forall \psi_h \in Q_h$$

where

$$\begin{aligned} & B_{GLS}(\mathbf{u}_h, p_h; \mathbf{v}_h, \psi_h) \equiv \\ \equiv\; & ((\mathbf{u}_h\cdot\nabla)\mathbf{u}_h, \mathbf{v}_h)_0 + (2\nu\varepsilon(\mathbf{u}_h), \varepsilon(\mathbf{v}_h))_0 - (p_h, \nabla\cdot\mathbf{v}_h)_0 + \\ +\; & (\psi_h, \nabla\cdot\mathbf{u}_h)_0 + (\nabla\cdot\mathbf{u}_h, \delta\nabla\cdot\mathbf{v}_h)_0 + \\ +\; & \sum_K \big((\mathbf{u}_h\cdot\nabla)\mathbf{u}_h + \nabla p_h - 2\nu\nabla\cdot\varepsilon(\mathbf{u}_h), \tau((\mathbf{u}_h\cdot\nabla)\mathbf{v}_h + \nabla\psi_h - 2\nu\nabla\cdot\varepsilon(\mathbf{v}_h))\big)_{T_K} \end{aligned}$$

$$L_{GLS}(\mathbf{v}_h, \psi_h) \;\equiv\; (\mathbf{f}, \mathbf{v}_h)_0 + \sum_K \big(\mathbf{f}, \tau((\mathbf{u}_h\cdot\nabla)\mathbf{v}_h + \nabla\psi_h - 2\nu\nabla\cdot\varepsilon(\mathbf{v}_h))\big)_{T_K}$$

Franca and Madureira [15] suggest stabilization parameters τ and δ as

$$\delta = \frac{\mid \mathbf{u}(\mathbf{x}) \mid_p}{\sqrt{\lambda_K}} \xi(\mathrm{Re}_K(\mathbf{x})) \tag{4.6}$$

$$\tau = \frac{\xi(\mathrm{Re}_K(\mathbf{x}))}{\sqrt{\lambda_K} \mid \mathbf{u}(\mathbf{x}) \mid_p} \tag{4.7}$$

where

$$\begin{aligned}
\mathrm{Re}_K(\mathbf{x}) &= \frac{\mid \mathbf{u}(\mathbf{x}) \mid_p}{4\sqrt{\lambda_K}\nu} \\
\xi(\mathrm{Re}_K(\mathbf{x})) &= \begin{cases} \mathrm{Re}_K(\mathbf{x}), & 0 \leq \mathrm{Re}_K(\mathbf{x}) < 1 \\ 1, & \mathrm{Re}_K(\mathbf{x}) \geq 1 \end{cases} \\
\lambda_K &= \max_{0 \neq \mathbf{v} \in (R_k(T_K)/\mathbb{R})^N} \frac{\|\nabla \cdot \varepsilon(\mathbf{v}_h)\|^2_{0,T_K}}{\|\varepsilon(\mathbf{v}_h)\|^2_{0,T_K}} \\
\mid \mathbf{u}(\mathbf{x}) \mid_p &= \begin{cases} \left(\sum_{i=1}^{N} \mid u_i(\mathbf{x}) \mid^p \right)^{\frac{1}{p}}, & 1 \leq p < \infty \\ \max_{i=1,N} \mid u_i(\mathbf{x}) \mid, & p = \infty \end{cases}
\end{aligned}$$

Recommended way of computing λ_K is to find the largest eigenvalue of the problem

$$(\nabla \cdot \varepsilon(\mathbf{w}_h), \nabla \cdot \varepsilon(\mathbf{v}_h)) - \lambda_K(\nabla \mathbf{w}_h, \nabla \mathbf{v}_h) = 0, \quad \forall \mathbf{v}_h \in (R_k(T_K)/\mathbb{R})^N$$

for each element once the mesh is set up.

5 Algorithm for solving Navier-Stokes equations based on GLS

In this chapter, the algorithm for solving Navier-Stokes equations is derived. We employ the finite element method equipped with the Galerkin Least-Squares (GLS) stabilization. We assume application of the Newton method for solving resulting system of nonlinear equations. First, we derive the algorithm for the steady case of the Navier-Stokes equtions, and then we extend it to the unsteady case. Note, that vector operations are defined in Appendix.

5.1 Stabilizing terms for steady Navier-Stokes equations

Let us remind the mixed FEM formulation of the steady Navier-Stokes equations (3.2)-(3.4):

Seek $\mathbf{u}_h \in V_{gh}$ and $p_h \in Q_h$ satisfying

$$\int_\Omega (\mathbf{u}_h \cdot \nabla)\mathbf{u}_h \cdot \mathbf{v}_h \mathrm{d}\Omega + \nu \int_\Omega \nabla \mathbf{u}_h : \nabla \mathbf{v}_h \mathrm{d}\Omega - \int_\Omega p_h \nabla \cdot \mathbf{v}_h \mathrm{d}\Omega = \int_\Omega \mathbf{f} \cdot \mathbf{v}_h \mathrm{d}\Omega, \ \forall \mathbf{v}_h \in V_h \quad (5.1)$$

$$\int_\Omega \psi_h \nabla \cdot \mathbf{u}_h \mathrm{d}\Omega = 0, \ \forall \psi_h \in Q_h \quad (5.2)$$

$$\mathbf{u}_h - \mathbf{u}_{gh} \in V_h \quad (5.3)$$

We apply stabilization based on the GLS method. We combine ideas of Hughes and Franca ([21],[15]) with two modifications:

1. Stabilization term with parameter δ is not considered. Since most problems are caused by the advective term, we find stabilization of it as most important. We consider as redundant to stabilize the continuity equation, which is represened by the term with δ. In spite of it, we performed several experiments with δ applied, but the results were disastrous.

2. Formulas by Franca and Madureira (Chapter 4.2) are derived for the considered formulation (5.1)-(5.3) of the problem. This formulation makes the derivations much simpler, therefore less mistakes can be made and stay undetected. As long as we tried to employ the Franca's formulation, we were not able to obtain contributive results.

Let us add 'zero' to the left side of the momentum equation (5.1) as

$$\begin{aligned}
& \sum_{K=1}^{N} \int_{T_K} [(\mathbf{u}_h \cdot \nabla)\mathbf{u}_h - \nu \Delta \mathbf{u}_h + \nabla p_h - \mathbf{f}_h] \cdot \tau [(\mathbf{u}_h \cdot \nabla)\mathbf{v}_h - \nu \Delta \mathbf{v}_h + \nabla \psi_h] \mathrm{d}\Omega = \\
= & \sum_{K=1}^{N} \Bigg\{ \int_{T_K} \tau (\mathbf{u}_h \cdot \nabla)\mathbf{u}_h \cdot (\mathbf{u}_h \cdot \nabla)\mathbf{v}_h \mathrm{d}\Omega - \nu \int_{T_K} \tau (\mathbf{u}_h \cdot \nabla)\mathbf{u}_h \cdot \Delta \mathbf{v}_h \mathrm{d}\Omega + \\
+ & \int_{T_K} \tau (\mathbf{u}_h \cdot \nabla)\mathbf{u}_h \cdot \nabla \psi_h \mathrm{d}\Omega - \nu \int_{T_K} \tau \Delta \mathbf{u}_h \cdot (\mathbf{u}_h \cdot \nabla)\mathbf{v}_h \mathrm{d}\Omega + \\
+ & \nu^2 \int_{T_K} \tau \Delta \mathbf{u}_h \cdot \Delta \mathbf{v}_h \mathrm{d}\Omega - \nu \int_{T_K} \tau \Delta \mathbf{u}_h \cdot \nabla \psi_h \mathrm{d}\Omega + \\
+ & \int_{T_K} \tau \nabla p_h \cdot (\mathbf{u}_h \cdot \nabla)\mathbf{v}_h \mathrm{d}\Omega - \nu \int_{T_K} \tau \nabla p_h \cdot \Delta \mathbf{v}_h \mathrm{d}\Omega + \int_{T_K} \tau \nabla p_h \cdot \nabla \psi_h \mathrm{d}\Omega - \\
- & \int_{T_K} \tau \mathbf{f}_h \cdot (\mathbf{u}_h \cdot \nabla)\mathbf{v}_h \mathrm{d}\Omega + \nu \int_{T_K} \tau \mathbf{f}_h \cdot \Delta \mathbf{v}_h \mathrm{d}\Omega - \int_{T_K} \tau \mathbf{f}_h \cdot \nabla \psi_h \mathrm{d}\Omega \Bigg\}
\end{aligned}$$

where τ denotes the positive stabilization parameter. In Chapter 5.7, we show how to determine it.

5.2 Functionals for the Newton method and their differentials in steady case

Note: Since only finite element functions $\mathbf{u}_h$, $\mathbf{v}_h$, p_h, and ψ_h are considered in this chapter, index h is omitted in what follows.

Let us introduce functionals $F_1(\mathbf{u}, p)$ and $F_2(\mathbf{u}, p)$ for Newton's minimization. $F_1(\mathbf{u}, p)$ is derived for the enriched momentum equation (5.1) and $F_2(\mathbf{u}, p)$ for the continuity equation (5.2).

$$
\begin{aligned}
F_1(\mathbf{u}, p) &= \int_\Omega (\mathbf{u}\cdot\nabla)\mathbf{u}\cdot\mathbf{v}\mathrm{d}\Omega + \nu\int_\Omega \nabla\mathbf{u} : \nabla\mathbf{v}\mathrm{d}\Omega - \int_\Omega p\nabla\cdot\mathbf{v}\mathrm{d}\Omega - \int_\Omega \mathbf{f}\cdot\mathbf{v}\mathrm{d}\Omega + \\
&+ \sum_{K=1}^{N}\left\{\int_{T_K} \tau(\mathbf{u}\cdot\nabla)\mathbf{u}\cdot(\mathbf{u}\cdot\nabla)\mathbf{v}\mathrm{d}\Omega - \nu\int_{T_K}\tau(\mathbf{u}\cdot\nabla)\mathbf{u}\cdot\Delta\mathbf{v}\mathrm{d}\Omega + \right. \\
&+ \int_{T_K}\tau(\mathbf{u}\cdot\nabla)\mathbf{u}\cdot\nabla\psi\mathrm{d}\Omega - \nu\int_{T_K}\tau\Delta\mathbf{u}\cdot(\mathbf{u}\cdot\nabla)\mathbf{v}\mathrm{d}\Omega + \nu^2\int_{T_K}\tau\Delta\mathbf{u}\cdot\Delta\mathbf{v}\mathrm{d}\Omega - \\
&- \nu\int_{T_K}\tau\Delta\mathbf{u}\cdot\nabla\psi\mathrm{d}\Omega + \int_{T_K}\tau\nabla p\cdot(\mathbf{u}\cdot\nabla)\mathbf{v}\mathrm{d}\Omega - \nu\int_{T_K}\tau\nabla p\cdot\Delta\mathbf{v}\mathrm{d}\Omega + \\
&+ \int_{T_K}\tau\nabla p\cdot\nabla\psi\mathrm{d}\Omega - \int_{T_K}\tau\mathbf{f}\cdot(\mathbf{u}\cdot\nabla)\mathbf{v}\mathrm{d}\Omega + \\
&+ \left.\nu\int_{T_K}\tau\mathbf{f}\cdot\Delta\mathbf{v}\mathrm{d}\Omega - \int_{T_K}\tau\mathbf{f}\cdot\nabla\psi\mathrm{d}\Omega\right\} \\
F_2(\mathbf{u}, p) &= \int_\Omega \psi\nabla\cdot\mathbf{u}\mathrm{d}\Omega
\end{aligned}
$$

We need Frechet's differentials of functionals $F_1(\mathbf{u},p)$ and $F_2(\mathbf{u},p)$ for using the Newton method. We can find them by evaluating Gateaux's differentials since we assume that both exist.

$$< DF_1(\mathbf{u},p),[\mathbf{h},q] >=$$

$$\begin{aligned}
&= \lim_{t\to 0}\frac{1}{t}\Bigg[\int_\Omega [(\mathbf{u}+t\mathbf{h})\cdot\nabla](\mathbf{u}+t\mathbf{h})\cdot\mathbf{v}\mathrm{d}\Omega + \nu\int_\Omega \nabla(\mathbf{u}+t\mathbf{h}):\nabla\mathbf{v}\mathrm{d}\Omega - \\
&- \int_\Omega (p+tq)\nabla\cdot\mathbf{v}\mathrm{d}\Omega - \int_\Omega \mathbf{f}\cdot\mathbf{v}\mathrm{d}\Omega + \\
&+ \sum_{K=1}^{N}\Bigg\{\int_{T_K}\tau[(\mathbf{u}+t\mathbf{h})\cdot\nabla](\mathbf{u}+t\mathbf{h})\cdot[(\mathbf{u}+t\mathbf{h})\cdot\nabla]\mathbf{v}\mathrm{d}\Omega - \\
&- \nu\int_{T_K}\tau[(\mathbf{u}+t\mathbf{h})\cdot\nabla](\mathbf{u}+t\mathbf{h})\cdot\Delta\mathbf{v}\mathrm{d}\Omega + \int_{T_K}\tau[(\mathbf{u}+t\mathbf{h})\cdot\nabla](\mathbf{u}+t\mathbf{h})\cdot\nabla\psi\mathrm{d}\Omega - \\
&- \nu\int_{T_K}\tau\Delta(\mathbf{u}+t\mathbf{h})\cdot[(\mathbf{u}+t\mathbf{h})\cdot\nabla]\mathbf{v}\mathrm{d}\Omega + \nu^2\int_{T_K}\tau\Delta(\mathbf{u}+t\mathbf{h})\cdot\Delta\mathbf{v}\mathrm{d}\Omega - \\
&- \nu\int_{T_K}\tau\Delta(\mathbf{u}+t\mathbf{h})\cdot\nabla\psi\mathrm{d}\Omega + \int_{T_K}\tau\nabla(p+tq)\cdot[(\mathbf{u}+t\mathbf{h})\cdot\nabla]\mathbf{v}\mathrm{d}\Omega - \\
&- \nu\int_{T_K}\tau\nabla(p+tq)\cdot\Delta\mathbf{v}\mathrm{d}\Omega + \int_{T_K}\tau\nabla(p+tq)\cdot\nabla\psi\mathrm{d}\Omega - \\
&- \int_{T_K}\tau\mathbf{f}\cdot[(\mathbf{u}+t\mathbf{h})\cdot\nabla]\mathbf{v}\mathrm{d}\Omega + \nu\int_{T_K}\tau\mathbf{f}\cdot\Delta\mathbf{v}\mathrm{d}\Omega - \int_{T_K}\tau\mathbf{f}\cdot\nabla\psi\mathrm{d}\Omega\Bigg\} - \\
&- \int_\Omega (\mathbf{u}\cdot\nabla)\mathbf{u}\cdot\mathbf{v}\mathrm{d}\Omega - \nu\int_\Omega \nabla\mathbf{u}:\nabla\mathbf{v}\mathrm{d}\Omega + \int_\Omega p\nabla\cdot\mathbf{v}\mathrm{d}\Omega + \int_\Omega \mathbf{f}\cdot\mathbf{v}\mathrm{d}\Omega - \\
&- \sum_{K=1}^{N}\Bigg\{\int_{T_K}\tau(\mathbf{u}\cdot\nabla)\mathbf{u}\cdot(\mathbf{u}\cdot\nabla)\mathbf{v}\mathrm{d}\Omega - \nu\int_{T_K}\tau(\mathbf{u}\cdot\nabla)\mathbf{u}\cdot\Delta\mathbf{v}\mathrm{d}\Omega + \\
&+ \int_{T_K}\tau(\mathbf{u}\cdot\nabla)\mathbf{u}\cdot\nabla\psi\mathrm{d}\Omega - \nu\int_{T_K}\tau\Delta\mathbf{u}\cdot(\mathbf{u}\cdot\nabla)\mathbf{v}\mathrm{d}\Omega + \\
&+ \nu^2\int_{T_K}\tau\Delta\mathbf{u}\cdot\Delta\mathbf{v}\mathrm{d}\Omega - \nu\int_{T_K}\tau\Delta\mathbf{u}\cdot\nabla\psi\mathrm{d}\Omega + \\
&+ \int_{T_K}\tau\nabla p\cdot(\mathbf{u}\cdot\nabla)\mathbf{v}\mathrm{d}\Omega - \nu\int_{T_K}\tau\nabla p\cdot\Delta\mathbf{v}\mathrm{d}\Omega + \\
&+ \int_{T_K}\tau\nabla p\cdot\nabla\psi\mathrm{d}\Omega - \int_{T_K}\tau\mathbf{f}\cdot(\mathbf{u}\cdot\nabla)\mathbf{v}\mathrm{d}\Omega + \\
&+ \nu\int_{T_K}\tau\mathbf{f}\cdot\Delta\mathbf{v}\mathrm{d}\Omega - \int_{T_K}\tau\mathbf{f}\cdot\nabla\psi\mathrm{d}\Omega\Bigg\}\Bigg]
\end{aligned}$$

$$< DF_2(\mathbf{u},p),[\mathbf{h},q] >= \lim_{t\to 0}\frac{1}{t}\left[\int_\Omega \psi\nabla\cdot(\mathbf{u}+t\mathbf{h})\mathrm{d}\Omega - \int_\Omega \psi\nabla\cdot\mathbf{u}\mathrm{d}\Omega\right]$$

After letting $t \to 0$, we get the following lemma.

Lemma 5.1 *Assume all functions sufficiently smooth. Then the Frechet's differentials of functionals $F_1(\mathbf{u}, p)$ and $F_2(\mathbf{u}, p)$ are*

$$< DF_1(\mathbf{u}, p), [\mathbf{h}, q] >=$$

$$\begin{aligned}
= & \int_\Omega (\mathbf{h}\cdot\nabla)\mathbf{u}\cdot\mathbf{v}\mathrm{d}\Omega + \int_\Omega (\mathbf{u}\cdot\nabla)\mathbf{h}\cdot\mathbf{v}\mathrm{d}\Omega + \nu\int_\Omega \nabla\mathbf{h} : \nabla\mathbf{v}\mathrm{d}\Omega - \int_\Omega q\nabla\cdot\mathbf{v}\mathrm{d}\Omega + \\
+ & \sum_{K=1}^{N}\Bigg\{ \int_{T_K} \tau(\mathbf{h}\cdot\nabla)\mathbf{u}\cdot(\mathbf{u}\cdot\nabla)\mathbf{v}\mathrm{d}\Omega + \int_{T_K} \tau(\mathbf{u}\cdot\nabla)\mathbf{h}\cdot(\mathbf{u}\cdot\nabla)\mathbf{v}\mathrm{d}\Omega + \\
+ & \int_{T_K} \tau(\mathbf{u}\cdot\nabla)\mathbf{u}\cdot(\mathbf{h}\cdot\nabla)\mathbf{v}\mathrm{d}\Omega - \nu\int_{T_K} \tau(\mathbf{h}\cdot\nabla)\mathbf{u}\cdot\Delta\mathbf{v}\mathrm{d}\Omega - \nu\int_{T_K} \tau(\mathbf{u}\cdot\nabla)\mathbf{h}\cdot\Delta\mathbf{v}\mathrm{d}\Omega + \\
+ & \int_{T_K} \tau(\mathbf{h}\cdot\nabla)\mathbf{u}\cdot\nabla\psi\mathrm{d}\Omega + \int_{T_K} \tau(\mathbf{u}\cdot\nabla)\mathbf{h}\cdot\nabla\psi\mathrm{d}\Omega - \nu\int_{T_K} \tau\Delta\mathbf{h}\cdot(\mathbf{u}\cdot\nabla)\mathbf{v}\mathrm{d}\Omega - \\
- & \nu\int_{T_K} \tau\Delta\mathbf{u}\cdot(\mathbf{h}\cdot\nabla)\mathbf{v}\mathrm{d}\Omega + \nu^2\int_{T_K} \tau\Delta\mathbf{h}\cdot\Delta\mathbf{v}\mathrm{d}\Omega - \nu\int_{T_K} \tau\Delta\mathbf{h}\cdot\nabla\psi\mathrm{d}\Omega + \\
+ & \int_{T_K} \tau\nabla q\cdot(\mathbf{u}\cdot\nabla)\mathbf{v}\mathrm{d}\Omega + \int_{T_K} \tau\nabla p\cdot(\mathbf{h}\cdot\nabla)\mathbf{v}\mathrm{d}\Omega - \nu\int_{T_K} \tau\nabla q\cdot\Delta\mathbf{v}\mathrm{d}\Omega + \\
+ & \int_{T_K} \tau\nabla q\cdot\nabla\psi\mathrm{d}\Omega - \int_{T_K} \tau\mathbf{f}\cdot(\mathbf{h}\cdot\nabla)\mathbf{v}\mathrm{d}\Omega \Bigg\}
\end{aligned}$$

and

$$< DF_2(\mathbf{u}, p), [\mathbf{h}, q] >= \int_\Omega \psi\nabla\cdot\mathbf{h}\mathrm{d}\Omega.$$

Let us formally introduce the functional

$$\mathcal{F}(\mathbf{u}, p) = F_1(\mathbf{u}, p) + F_2(\mathbf{u}, p) \tag{5.4}$$

and its differential

$$< D\mathcal{F}(\mathbf{u}, p), [\mathbf{h}, q] >=< DF_1(\mathbf{u}, p), [\mathbf{h}, q] > + < DF_2(\mathbf{u}, p), [\mathbf{h}, q] > . \tag{5.5}$$

The algorithm consists of the following steps

1. solution of the equation system (the zth iteration of the Newton method) for $\mathbf{h}$, q:

$$< D\mathcal{F}(\mathbf{u}, p), [\mathbf{h}, q] >= -\mathcal{F}(\mathbf{u}, p) \tag{5.6}$$

2. correction of the solution $\mathbf{u}$, p:

$$\begin{aligned}
\mathbf{u}^{z+1} &= \mathbf{u}^z + \mathbf{h} \\
p^{z+1} &= p^z + q
\end{aligned}$$

5.3 Matrices for the finite element method in steady case

Let us derive matrices for the finite element method. We substitute

$$\begin{aligned} h_x &= \sum_{i=1}^{N_u} h_{xi} N_i \\ h_y &= \sum_{i=1}^{N_u} h_{y_i} N_i \\ q &= \sum_{i=1}^{N_p} q_i M_i \end{aligned}$$

and reduce all test functions to

$$\begin{aligned} \mathbf{v} &= (N_j, 0),\ \mathbf{v} = (0, N_j), \\ \psi &= M_j \end{aligned}$$

where

- $N_j,\ j = 1, \ldots, N_u$ are the basis functions of space V_h for each component
- $M_j,\ j = 1, \ldots, N_p$ are the basis functions of space Q_h

Then, we derive three equations for each node from the scalar equation (5.6) by input in turn the following combinations of test functions

$$\begin{aligned} \mathbf{v} &= (N_j, 0), \psi = 0; \\ \mathbf{v} &= (0, N_j), \psi = 0; \\ \mathbf{v} &= (0, 0), \psi = M_j. \end{aligned}$$

These equations read for the node j

$$< D\mathcal{F}(\mathbf{u}, p), [\mathbf{h}, q] >_{j_1} = -\mathcal{F}(\mathbf{u}, p)_{j_1} \tag{5.7}$$

$$< D\mathcal{F}(\mathbf{u}, p), [\mathbf{h}, q] >_{j_2} = -\mathcal{F}(\mathbf{u}, p)_{j_2} \tag{5.8}$$

$$< D\mathcal{F}(\mathbf{u}, p), [\mathbf{h}, q] >_{j_3} = -\mathcal{F}(\mathbf{u}, p)_{j_3} \tag{5.9}$$

where by Lemma 5.1 we obtain following terms:

$$< D\mathcal{F}(\mathbf{u},p),[\mathbf{h},q] >_{j_1} =$$

$$
\begin{aligned}
= & \sum_{i=1}^{N_u}\int_\Omega \left(h_{x_i}N_i\frac{\partial u_x}{\partial x}+h_{y_i}N_i\frac{\partial u_x}{\partial y}\right)N_j\mathrm{d}\Omega+\sum_{i=1}^{N_u}\int_\Omega h_{x_i}\left(u_x\frac{\partial N_i}{\partial x}+u_y\frac{\partial N_i}{\partial y}\right)N_j\mathrm{d}\Omega+\\
+ & \sum_{i=1}^{N_u}\nu\int_\Omega h_{x_i}\left(\frac{\partial N_i}{\partial x}\frac{\partial N_j}{\partial x}+\frac{\partial N_i}{\partial y}\frac{\partial N_j}{\partial y}\right)\mathrm{d}\Omega-\sum_{i=1}^{N_p}\int_\Omega q_iM_i\frac{\partial N_j}{\partial x}\mathrm{d}\Omega+\\
+ & \sum_{i=1}^{N_u}\sum_K\left\{\int_{T_K}\tau\left(h_{x_i}N_i\frac{\partial u_x}{\partial x}+h_{y_i}N_i\frac{\partial u_x}{\partial y}\right)\left(u_x\frac{\partial N_j}{\partial x}+u_y\frac{\partial N_j}{\partial y}\right)\mathrm{d}\Omega+\right.\\
+ & \int_{T_K}\tau h_{x_i}\left(u_x\frac{\partial N_i}{\partial x}+u_y\frac{\partial N_i}{\partial y}\right)\left(u_x\frac{\partial N_j}{\partial x}+u_y\frac{\partial N_j}{\partial y}\right)\mathrm{d}\Omega+\\
+ & \int_{T_K}\tau\left(u_x\frac{\partial u_x}{\partial x}+u_y\frac{\partial u_x}{\partial y}\right)\left(h_{x_i}N_i\frac{\partial N_j}{\partial x}+h_{y_i}N_i\frac{\partial N_j}{\partial y}\right)\mathrm{d}\Omega-\\
- & \nu\int_{T_K}\tau\left(h_{x_i}N_i\frac{\partial u_x}{\partial x}+h_{y_i}N_i\frac{\partial u_x}{\partial y}\right)\left(\frac{\partial^2 N_j}{\partial x^2}+\frac{\partial^2 N_j}{\partial y^2}\right)\mathrm{d}\Omega-\\
- & \nu\int_{T_K}\tau h_{x_i}\left(u_x\frac{\partial N_i}{\partial x}+u_y\frac{\partial N_i}{\partial y}\right)\left(\frac{\partial^2 N_j}{\partial x^2}+\frac{\partial^2 N_j}{\partial y^2}\right)\mathrm{d}\Omega-\\
- & \nu\int_{T_K}\tau h_{x_i}\left(\frac{\partial^2 N_i}{\partial x^2}+\frac{\partial^2 N_i}{\partial y^2}\right)\left(u_x\frac{\partial N_j}{\partial x}+u_y\frac{\partial N_j}{\partial y}\right)\mathrm{d}\Omega-\\
- & \nu\int_{T_K}\tau\left(\frac{\partial^2 u_x}{\partial x^2}+\frac{\partial^2 u_x}{\partial y^2}\right)\left(h_{x_i}N_i\frac{\partial N_j}{\partial x}+h_{y_i}N_i\frac{\partial N_j}{\partial y}\right)\mathrm{d}\Omega+\\
+ & \nu^2\int_{T_K}\tau h_{x_i}\left(\frac{\partial^2 N_i}{\partial x^2}+\frac{\partial^2 N_i}{\partial y^2}\right)\left(\frac{\partial^2 N_j}{\partial x^2}+\frac{\partial^2 N_j}{\partial y^2}\right)\mathrm{d}\Omega+\\
+ & \int_{T_K}\tau\frac{\partial p}{\partial x}\left(h_{x_i}N_i\frac{\partial N_j}{\partial x}+h_{y_i}N_i\frac{\partial N_j}{\partial y}\right)\mathrm{d}\Omega-\\
- & \left.\int_{T_K}\tau f_x\left(h_{x_i}N_i\frac{\partial N_j}{\partial x}+h_{y_i}N_i\frac{\partial N_j}{\partial y}\right)\mathrm{d}\Omega\right\}+\\
+ & \sum_{i=1}^{N_p}\sum_K\left\{\int_{T_K}\tau q_i\frac{\partial M_i}{\partial x}\left(u_x\frac{\partial N_j}{\partial x}+u_y\frac{\partial N_j}{\partial y}\right)\mathrm{d}\Omega-\right.\\
- & \left.\nu\int_{T_K}\tau q_i\frac{\partial M_i}{\partial x}\left(\frac{\partial^2 N_j}{\partial x^2}+\frac{\partial^2 N_j}{\partial y^2}\right)\mathrm{d}\Omega\right\}
\end{aligned}
$$

$$< D\mathcal{F}(\mathbf{u},p),[\mathbf{h},q] >_{j_2}=$$

$$
\begin{aligned}
= & \sum_{i=1}^{N_u}\int_\Omega\left(h_{x_i}N_i\frac{\partial u_y}{\partial x}+h_{y_i}N_i\frac{\partial u_y}{\partial y}\right)N_j\mathrm{d}\Omega+\sum_{i=1}^{N_u}\int_\Omega h_{y_i}\left(u_x\frac{\partial N_i}{\partial x}+u_y\frac{\partial N_i}{\partial y}\right)N_j\mathrm{d}\Omega+\\
+ & \sum_{i=1}^{N_u}\nu\int_\Omega h_{y_i}\left(\frac{\partial N_i}{\partial x}\frac{\partial N_j}{\partial x}+\frac{\partial N_i}{\partial y}\frac{\partial N_j}{\partial y}\right)\mathrm{d}\Omega-\sum_{i=1}^{N_p}\int_\Omega q_iM_i\frac{\partial N_j}{\partial y}\mathrm{d}\Omega+\\
+ & \sum_{i=1}^{N_u}\sum_K\left\{\int_{T_K}\tau\left(h_{x_i}N_i\frac{\partial u_y}{\partial x}+h_{y_i}N_i\frac{\partial u_y}{\partial y}\right)\left(u_x\frac{\partial N_j}{\partial x}+u_y\frac{\partial N_j}{\partial y}\right)\mathrm{d}\Omega+\right.\\
+ & \int_{T_K}\tau h_{y_i}\left(u_x\frac{\partial N_i}{\partial x}+u_y\frac{\partial N_i}{\partial y}\right)\left(u_x\frac{\partial N_j}{\partial x}+u_y\frac{\partial N_j}{\partial y}\right)\mathrm{d}\Omega+\\
+ & \int_{T_K}\tau\left(u_x\frac{\partial u_y}{\partial x}+u_y\frac{\partial u_y}{\partial y}\right)\left(h_{x_i}N_i\frac{\partial N_j}{\partial x}+h_{y_i}N_i\frac{\partial N_j}{\partial y}\right)\mathrm{d}\Omega-\\
- & \nu\int_{T_K}\tau\left(h_{x_i}N_i\frac{\partial u_y}{\partial x}+h_{y_i}N_i\frac{\partial u_y}{\partial y}\right)\left(\frac{\partial^2 N_j}{\partial x^2}+\frac{\partial^2 N_j}{\partial y^2}\right)\mathrm{d}\Omega-\\
- & \nu\int_{T_K}\tau h_{y_i}\left(u_x\frac{\partial N_i}{\partial x}+u_y\frac{\partial N_i}{\partial y}\right)\left(\frac{\partial^2 N_j}{\partial x^2}+\frac{\partial^2 N_j}{\partial y^2}\right)\mathrm{d}\Omega-\\
- & \nu\int_{T_K}\tau h_{y_i}\left(\frac{\partial^2 N_i}{\partial x^2}+\frac{\partial^2 N_i}{\partial y^2}\right)\left(u_x\frac{\partial N_j}{\partial x}+u_y\frac{\partial N_j}{\partial y}\right)\mathrm{d}\Omega-\\
- & \nu\int_{T_K}\tau\left(\frac{\partial^2 u_y}{\partial x^2}+\frac{\partial^2 u_y}{\partial y^2}\right)\left(h_{x_i}N_i\frac{\partial N_j}{\partial x}+h_{y_i}N_i\frac{\partial N_j}{\partial y}\right)\mathrm{d}\Omega+\\
+ & \nu^2\int_{T_K}\tau h_{y_i}\left(\frac{\partial^2 N_i}{\partial x^2}+\frac{\partial^2 N_i}{\partial y^2}\right)\left(\frac{\partial^2 N_j}{\partial x^2}+\frac{\partial^2 N_j}{\partial y^2}\right)\mathrm{d}\Omega+\\
+ & \int_{T_K}\tau\frac{\partial p}{\partial y}\left(h_{x_i}N_i\frac{\partial N_j}{\partial x}+h_{y_i}N_i\frac{\partial N_j}{\partial y}\right)\mathrm{d}\Omega-\\
- & \left.\int_{T_K}\tau f_y\left(h_{x_i}N_i\frac{\partial N_j}{\partial x}+h_{y_i}N_i\frac{\partial N_j}{\partial y}\right)\mathrm{d}\Omega\right\}+\\
+ & \sum_{i=1}^{N_p}\sum_K\left\{\int_{T_K}\tau q_i\frac{\partial M_i}{\partial y}\left(u_x\frac{\partial N_j}{\partial x}+u_y\frac{\partial N_j}{\partial y}\right)\mathrm{d}\Omega-\right.\\
- & \left.\nu\int_{T_K}\tau q_i\frac{\partial M_i}{\partial y}\left(\frac{\partial^2 N_j}{\partial x^2}+\frac{\partial^2 N_j}{\partial y^2}\right)\mathrm{d}\Omega\right\}
\end{aligned}
$$

$$< D\mathcal{F}(\mathbf{u},p),[\mathbf{h},q] >_{j_3}=$$

$$
\begin{aligned}
= & \sum_{i=1}^{N_u}\int_\Omega\left(h_{x_i}\frac{\partial N_i}{\partial x}+h_{y_i}\frac{\partial N_i}{\partial y}\right)M_j\mathrm{d}\Omega+\\
+ & \sum_{i=1}^{N_u}\sum_K\left\{\int_{T_K}\tau\left(h_{x_i}N_i\frac{\partial u_x}{\partial x}+h_{y_i}N_i\frac{\partial u_x}{\partial y}\right)\frac{\partial M_j}{\partial x}\mathrm{d}\Omega+\right.\\
+ & \int_{T_K}\tau\left(h_{x_i}N_i\frac{\partial u_y}{\partial x}+h_{y_i}N_i\frac{\partial u_y}{\partial y}\right)\frac{\partial M_j}{\partial y}\mathrm{d}\Omega+\\
+ & \int_{T_K}\tau h_{x_i}\left(u_x\frac{\partial N_i}{\partial x}+u_y\frac{\partial N_i}{\partial y}\right)\frac{\partial M_j}{\partial x}\mathrm{d}\Omega+\int_{T_K}\tau h_{y_i}\left(u_x\frac{\partial N_i}{\partial x}+u_y\frac{\partial N_i}{\partial y}\right)\frac{\partial M_j}{\partial y}\mathrm{d}\Omega-\\
- & \left.\nu\int_{T_K}\tau h_{x_i}\left(\frac{\partial^2 N_i}{\partial x^2}+\frac{\partial^2 N_i}{\partial y^2}\right)\frac{\partial M_j}{\partial x}\mathrm{d}\Omega-\nu\int_{T_K}\tau h_{y_i}\left(\frac{\partial^2 N_i}{\partial x^2}+\frac{\partial^2 N_i}{\partial y^2}\right)\frac{\partial M_j}{\partial y}\mathrm{d}\Omega\right\}+\\
+ & \sum_{i=1}^{N_p}\sum_K\int_{T_K}\tau q_i\left(\frac{\partial M_i}{\partial x}\frac{\partial M_j}{\partial x}+\frac{\partial M_i}{\partial y}\frac{\partial M_j}{\partial y}\right)\mathrm{d}\Omega
\end{aligned}
$$

$$
\begin{aligned}
\mathcal{F}(\mathbf{u},p)_{j_1} = & \int_\Omega\left(u_x\frac{\partial u_x}{\partial x}+u_y\frac{\partial u_x}{\partial y}\right)N_j\mathrm{d}\Omega+\nu\int_\Omega\left(\frac{\partial u_x}{\partial x}\frac{\partial N_j}{\partial x}+\frac{\partial u_x}{\partial y}\frac{\partial N_j}{\partial y}\right)\mathrm{d}\Omega-\\
- & \int_\Omega p\frac{\partial N_j}{\partial x}\mathrm{d}\Omega-\int_\Omega f_x N_j\mathrm{d}\Omega+\\
+ & \sum_K\left\{\int_K\tau\left(u_x\frac{\partial u_x}{\partial x}+u_y\frac{\partial u_x}{\partial y}\right)\left(u_x\frac{\partial N_j}{\partial x}+u_y\frac{\partial N_j}{\partial y}\right)\mathrm{d}\Omega-\right.\\
- & \nu\int_{T_K}\tau\left(u_x\frac{\partial u_x}{\partial x}+u_y\frac{\partial u_x}{\partial y}\right)\left(\frac{\partial^2 N_j}{\partial x^2}+\frac{\partial^2 N_j}{\partial y^2}\right)\mathrm{d}\Omega-\\
- & \nu\int_{T_K}\tau\left(\frac{\partial^2 u_x}{\partial x^2}+\frac{\partial^2 u_x}{\partial y^2}\right)\left(u_x\frac{\partial N_j}{\partial x}+u_y\frac{\partial N_j}{\partial y}\right)\mathrm{d}\Omega+\\
+ & \nu^2\int_{T_K}\tau\left(\frac{\partial^2 u_x}{\partial x^2}+\frac{\partial^2 u_x}{\partial y^2}\right)\left(\frac{\partial^2 N_j}{\partial x^2}+\frac{\partial^2 N_j}{\partial y^2}\right)\mathrm{d}\Omega+\\
+ & \int_{T_K}\tau\frac{\partial p}{\partial x}\left(u_x\frac{\partial N_j}{\partial x}+u_y\frac{\partial N_j}{\partial y}\right)\mathrm{d}\Omega-\\
- & \nu\int_{T_K}\tau\frac{\partial p}{\partial x}\left(\frac{\partial^2 N_j}{\partial x^2}+\frac{\partial^2 N_j}{\partial y^2}\right)\mathrm{d}\Omega-\\
- & \int_{T_K}\tau f_x\left(u_x\frac{\partial N_j}{\partial x}+u_y\frac{\partial N_j}{\partial y}\right)\mathrm{d}\Omega+\\
+ & \left.\nu\int_{T_K}\tau f_x\left(\frac{\partial^2 N_j}{\partial x^2}+\frac{\partial^2 N_j}{\partial y^2}\right)\mathrm{d}\Omega\right\}
\end{aligned}
$$

$$
\begin{aligned}
\mathcal{F}(\mathbf{u},p)_{j_2} &= \int_\Omega \left(u_x\frac{\partial u_y}{\partial x}+u_y\frac{\partial u_y}{\partial y}\right)N_j\mathrm{d}\Omega+\nu\int_\Omega\left(\frac{\partial u_y}{\partial x}\frac{\partial N_j}{\partial x}+\frac{\partial u_y}{\partial y}\frac{\partial N_j}{\partial y}\right)\mathrm{d}\Omega - \\
&- \int_\Omega p\frac{\partial N_j}{\partial y}\mathrm{d}\Omega-\int_\Omega f_y N_j\mathrm{d}\Omega + \\
&+ \sum_K\left\{\int_{T_K}\tau\left(u_x\frac{\partial u_y}{\partial x}+u_y\frac{\partial u_y}{\partial y}\right)\left(u_x\frac{\partial N_j}{\partial x}+u_y\frac{\partial N_j}{\partial y}\right)\mathrm{d}\Omega - \right. \\
&- \nu\int_{T_K}\tau\left(u_x\frac{\partial u_y}{\partial x}+u_y\frac{\partial u_y}{\partial y}\right)\left(\frac{\partial^2 N_j}{\partial x^2}+\frac{\partial^2 N_j}{\partial y^2}\right)\mathrm{d}\Omega - \\
&- \nu\int_{T_K}\tau\left(\frac{\partial^2 u_y}{\partial x^2}+\frac{\partial^2 u_y}{\partial y^2}\right)\left(u_x\frac{\partial N_j}{\partial x}+u_y\frac{\partial N_j}{\partial y}\right)\mathrm{d}\Omega + \\
&+ \nu^2\int_{T_K}\tau\left(\frac{\partial^2 u_y}{\partial x^2}+\frac{\partial^2 u_y}{\partial y^2}\right)\left(\frac{\partial^2 N_j}{\partial x^2}+\frac{\partial^2 N_j}{\partial y^2}\right)\mathrm{d}\Omega + \\
&+ \int_{T_K}\tau\frac{\partial p}{\partial y}\left(u_x\frac{\partial N_j}{\partial x}+u_y\frac{\partial N_j}{\partial y}\right)\mathrm{d}\Omega - \\
&- \nu\int_{T_K}\tau\frac{\partial p}{\partial y}\left(\frac{\partial^2 N_j}{\partial x^2}+\frac{\partial^2 N_j}{\partial y^2}\right)\mathrm{d}\Omega - \\
&- \int_{T_K}\tau f_y\left(u_x\frac{\partial N_j}{\partial x}+u_y\frac{\partial N_j}{\partial y}\right)\mathrm{d}\Omega + \\
&+ \left.\nu\int_{T_K}\tau f_y\left(\frac{\partial^2 N_j}{\partial x^2}+\frac{\partial^2 N_j}{\partial y^2}\right)\mathrm{d}\Omega\right\}
\end{aligned}
$$

$$
\begin{aligned}
\mathcal{F}(\mathbf{u},p)_{j_3} &= \int_\Omega\left(\frac{\partial u_x}{\partial x}+\frac{\partial u_y}{\partial y}\right)M_j\mathrm{d}\Omega + \\
&+ \sum_K\left\{\int_{T_K}\tau\left(u_x\frac{\partial u_x}{\partial x}+u_y\frac{\partial u_x}{\partial y}\right)\frac{\partial M_j}{\partial x}\mathrm{d}\Omega + \right. \\
&+ \int_{T_K}\tau\left(u_x\frac{\partial u_y}{\partial x}+u_y\frac{\partial u_y}{\partial y}\right)\frac{\partial M_j}{\partial y}\mathrm{d}\Omega - \\
&- \nu\int_{T_K}\tau\left(\frac{\partial^2 u_x}{\partial x^2}+\frac{\partial^2 u_x}{\partial y^2}\right)\frac{\partial M_j}{\partial x}\mathrm{d}\Omega - \\
&- \nu\int_{T_K}\tau\left(\frac{\partial^2 u_y}{\partial x^2}+\frac{\partial^2 u_y}{\partial y^2}\right)\frac{\partial M_j}{\partial y}\mathrm{d}\Omega + \\
&+ \int_{T_K}\tau\frac{\partial p}{\partial x}\frac{\partial M_j}{\partial x}\mathrm{d}\Omega+\int_{T_K}\tau\frac{\partial p}{\partial y}\frac{\partial M_j}{\partial y}\mathrm{d}\Omega - \\
&- \left.\int_{T_K}\tau f_x\frac{\partial M_j}{\partial x}\mathrm{d}\Omega-\int_{T_K}\tau f_y\frac{\partial M_j}{\partial y}\mathrm{d}\Omega\right\}
\end{aligned}
$$

Now, we can 'peck out' the elements of the ji-submatrix $\mathbf{K}_{ji}$ of the element stiffness matrix $\mathbf{K}^e$ (cf. Figure 5.1).

$$
\begin{aligned}
K_{ji_{11}}(\mathbf{u},p) &= \int_\Omega N_i \frac{\partial u_x}{\partial x} N_j \mathrm{d}\Omega + \int_\Omega \left(u_x \frac{\partial N_i}{\partial x} + u_y \frac{\partial N_i}{\partial y} \right) N_j \mathrm{d}\Omega + \\
&+ \nu \int_\Omega \left(\frac{\partial N_i}{\partial x}\frac{\partial N_j}{\partial x} + \frac{\partial N_i}{\partial y}\frac{\partial N_j}{\partial y} \right) \mathrm{d}\Omega + \\
&+ \sum_K \left\{ \int_{T_K} \tau N_i \frac{\partial u_x}{\partial x} \left(u_x \frac{\partial N_j}{\partial x} + u_y \frac{\partial N_j}{\partial y} \right) \mathrm{d}\Omega + \right. \\
&+ \int_{T_K} \tau \left(u_x \frac{\partial N_i}{\partial x} + u_y \frac{\partial N_i}{\partial y} \right) \left(u_x \frac{\partial N_j}{\partial x} + u_y \frac{\partial N_j}{\partial y} \right) \mathrm{d}\Omega + \\
&+ \int_{T_K} \tau \left(u_x \frac{\partial u_x}{\partial x} + u_y \frac{\partial u_x}{\partial y} \right) N_i \frac{\partial N_j}{\partial x} \mathrm{d}\Omega - \\
&- \nu \int_{T_K} \tau N_i \frac{\partial u_x}{\partial x} \left(\frac{\partial^2 N_j}{\partial x^2} + \frac{\partial^2 N_j}{\partial y^2} \right) \mathrm{d}\Omega - \\
&- \nu \int_{T_K} \tau \left(u_x \frac{\partial N_i}{\partial x} + u_y \frac{\partial N_i}{\partial y} \right) \left(\frac{\partial^2 N_j}{\partial x^2} + \frac{\partial^2 N_j}{\partial y^2} \right) \mathrm{d}\Omega - \\
&- \nu \int_{T_K} \tau \left(\frac{\partial^2 N_i}{\partial x^2} + \frac{\partial^2 N_i}{\partial y^2} \right) \left(u_x \frac{\partial N_j}{\partial x} + u_y \frac{\partial N_j}{\partial y} \right) \mathrm{d}\Omega - \\
&- \nu \int_{T_K} \tau \left(\frac{\partial^2 u_x}{\partial x^2} + \frac{\partial^2 u_x}{\partial y^2} \right) N_i \frac{\partial N_j}{\partial x} \mathrm{d}\Omega + \\
&+ \nu^2 \int_{T_K} \tau \left(\frac{\partial^2 N_i}{\partial x^2} + \frac{\partial^2 N_i}{\partial y^2} \right) \left(\frac{\partial^2 N_j}{\partial x^2} + \frac{\partial^2 N_j}{\partial y^2} \right) \mathrm{d}\Omega + \\
&+ \left. \int_{T_K} \tau \frac{\partial p}{\partial x} N_i \frac{\partial N_j}{\partial x} \mathrm{d}\Omega - \int_{T_K} \tau f_x N_i \frac{\partial N_j}{\partial x} \mathrm{d}\Omega \right\}
\end{aligned}
$$

$$
\begin{aligned}
K_{ji_{12}}(\mathbf{u},p) &= \int_\Omega N_i \frac{\partial u_x}{\partial y} N_j \mathrm{d}\Omega + \\
&+ \sum_K \left\{ \int_{T_K} \tau N_i \frac{\partial u_x}{\partial y} \left(u_x \frac{\partial N_j}{\partial x} + u_y \frac{\partial N_j}{\partial y} \right) \mathrm{d}\Omega + \right. \\
&+ \int_{T_K} \tau \left(u_x \frac{\partial u_x}{\partial x} + u_y \frac{\partial u_x}{\partial y} \right) N_i \frac{\partial N_j}{\partial y} \mathrm{d}\Omega - \\
&- \nu \int_{T_K} \tau N_i \frac{\partial u_x}{\partial y} \left(\frac{\partial^2 N_j}{\partial x^2} + \frac{\partial^2 N_j}{\partial y^2} \right) \mathrm{d}\Omega - \\
&- \nu \int_{T_K} \tau \left(\frac{\partial^2 u_x}{\partial x^2} + \frac{\partial^2 u_x}{\partial y^2} \right) N_i \frac{\partial N_j}{\partial y} \mathrm{d}\Omega + \\
&+ \left. \int_{T_K} \tau \frac{\partial p}{\partial x} N_i \frac{\partial N_j}{\partial y} \mathrm{d}\Omega - \int_{T_K} \tau f_x N_i \frac{\partial N_j}{\partial y} \mathrm{d}\Omega \right\}
\end{aligned}
$$

$$
\begin{aligned}
K_{ji_{13}}(\mathbf{u},p) &= -\int_\Omega M_i \frac{\partial N_j}{\partial x} \mathrm{d}\Omega + \\
&+ \sum_K \left\{ \int_{T_K} \tau \frac{\partial M_i}{\partial x} \left(u_x \frac{\partial N_j}{\partial x} + u_y \frac{\partial N_j}{\partial y} \right) \mathrm{d}\Omega - \right. \\
&- \left. \nu \int_{T_K} \tau \frac{\partial M_i}{\partial x} \left(\frac{\partial^2 N_j}{\partial x^2} + \frac{\partial^2 N_j}{\partial y^2} \right) \mathrm{d}\Omega \right\}
\end{aligned}
$$

$$
\begin{aligned}
K_{ji_{21}}(\mathbf{u},p) &= \int_\Omega N_i \frac{\partial u_y}{\partial x} N_j \mathrm{d}\Omega + \\
&+ \sum_K \left\{ \int_{T_K} \tau N_i \frac{\partial u_y}{\partial x} \left(u_x \frac{\partial N_j}{\partial x} + u_y \frac{\partial N_j}{\partial y} \right) \mathrm{d}\Omega + \right. \\
&+ \int_{T_K} \tau \left(u_x \frac{\partial u_y}{\partial x} + u_y \frac{\partial u_y}{\partial y} \right) N_i \frac{\partial N_j}{\partial x} \mathrm{d}\Omega - \\
&- \nu \int_{T_K} \tau N_i \frac{\partial u_y}{\partial x} \left(\frac{\partial^2 N_j}{\partial x^2} + \frac{\partial^2 N_j}{\partial y^2} \right) \mathrm{d}\Omega - \\
&- \nu \int_{T_K} \tau \left(\frac{\partial^2 u_y}{\partial x^2} + \frac{\partial^2 u_y}{\partial y^2} \right) N_i \frac{\partial N_j}{\partial x} \mathrm{d}\Omega + \\
&+ \left. \int_{T_K} \tau \frac{\partial p}{\partial y} N_i \frac{\partial N_j}{\partial x} \mathrm{d}\Omega - \int_{T_K} \tau f_y N_i \frac{\partial N_j}{\partial x} \mathrm{d}\Omega \right\}
\end{aligned}
$$

$$
\begin{aligned}
K_{ji_{22}}(\mathbf{u},p) &= \int_\Omega N_i \frac{\partial u_y}{\partial y} N_j \mathrm{d}\Omega + \int_\Omega \left(u_x \frac{\partial N_i}{\partial x} + u_y \frac{\partial N_i}{\partial y} \right) N_j \mathrm{d}\Omega + \\
&+ \nu \int_\Omega \left(\frac{\partial N_i}{\partial x} \frac{\partial N_j}{\partial x} + \frac{\partial N_i}{\partial y} \frac{\partial N_j}{\partial y} \right) \mathrm{d}\Omega + \\
&+ \sum_K \left\{ \int_{T_K} \tau N_i \frac{\partial u_y}{\partial y} \left(u_x \frac{\partial N_j}{\partial x} + u_y \frac{\partial N_j}{\partial y} \right) \mathrm{d}\Omega + \right. \\
&+ \int_{T_K} \tau \left(u_x \frac{\partial N_i}{\partial x} + u_y \frac{\partial N_i}{\partial y} \right) \left(u_x \frac{\partial N_j}{\partial x} + u_y \frac{\partial N_j}{\partial y} \right) \mathrm{d}\Omega + \\
&+ \int_{T_K} \tau \left(u_x \frac{\partial u_y}{\partial x} + u_y \frac{\partial u_y}{\partial y} \right) N_i \frac{\partial N_j}{\partial y} \mathrm{d}\Omega - \\
&- \nu \int_{T_K} \tau N_i \frac{\partial u_y}{\partial y} \left(\frac{\partial^2 N_j}{\partial x^2} + \frac{\partial^2 N_j}{\partial y^2} \right) \mathrm{d}\Omega - \\
&- \nu \int_K \tau \left(u_x \frac{\partial N_i}{\partial x} + u_y \frac{\partial N_i}{\partial y} \right) \left(\frac{\partial^2 N_j}{\partial x^2} + \frac{\partial^2 N_j}{\partial y^2} \right) \mathrm{d}\Omega - \\
&- \nu \int_{T_K} \tau \left(\frac{\partial^2 N_i}{\partial x^2} + \frac{\partial^2 N_i}{\partial y^2} \right) \left(u_x \frac{\partial N_j}{\partial x} + u_y \frac{\partial N_j}{\partial y} \right) \mathrm{d}\Omega - \\
&- \nu \int_{T_K} \tau \left(\frac{\partial^2 u_y}{\partial x^2} + \frac{\partial^2 u_y}{\partial y^2} \right) N_i \frac{\partial N_j}{\partial y} \mathrm{d}\Omega + \\
&+ \nu^2 \int_{T_K} \tau \left(\frac{\partial^2 N_i}{\partial x^2} + \frac{\partial^2 N_i}{\partial y^2} \right) \left(\frac{\partial^2 N_j}{\partial x^2} + \frac{\partial^2 N_j}{\partial y^2} \right) \mathrm{d}\Omega + \\
&+ \left. \int_{T_K} \tau \frac{\partial p}{\partial y} N_i \frac{\partial N_j}{\partial y} \mathrm{d}\Omega - \int_{T_K} \tau f_y N_i \frac{\partial N_j}{\partial y} \mathrm{d}\Omega \right\}
\end{aligned}
$$

$$
\begin{aligned}
K_{ji_{23}}(\mathbf{u},p) &= -\int_\Omega M_i \frac{\partial N_j}{\partial y}\mathrm{d}\Omega + \\
&+ \sum_K \left\{ \int_{T_K} \tau \frac{\partial M_i}{\partial y}\left(u_x \frac{\partial N_j}{\partial x} + u_y \frac{\partial N_j}{\partial y}\right)\mathrm{d}\Omega - \right. \\
&- \left. \nu \int_{T_K} \tau \frac{\partial M_i}{\partial y}\left(\frac{\partial^2 N_j}{\partial x^2} + \frac{\partial^2 N_j}{\partial y^2}\right)\mathrm{d}\Omega \right\}
\end{aligned}
$$

$$
\begin{aligned}
K_{ji_{31}}(\mathbf{u},p) &= \int_\Omega \frac{\partial N_i}{\partial x} M_j \mathrm{d}\Omega + \\
&+ \sum_K \left\{ \int_{T_K} \tau N_i \frac{\partial u_x}{\partial x}\frac{\partial M_j}{\partial x}\mathrm{d}\Omega + \int_{T_K} \tau N_i \frac{\partial u_y}{\partial x}\frac{\partial M_j}{\partial y}\mathrm{d}\Omega + \right. \\
&+ \left. \int_{T_K} \tau \left(u_x \frac{\partial N_i}{\partial x} + u_y \frac{\partial N_i}{\partial y}\right)\frac{\partial M_j}{\partial x}\mathrm{d}\Omega - \nu \int_{T_K} \tau \left(\frac{\partial^2 N_i}{\partial x^2} + \frac{\partial^2 N_i}{\partial y^2}\right)\frac{\partial M_j}{\partial x}\mathrm{d}\Omega \right\}
\end{aligned}
$$

$$
\begin{aligned}
K_{ji_{32}}(\mathbf{u},p) &= \int_\Omega \frac{\partial N_i}{\partial y} M_j \mathrm{d}\Omega + \\
&+ \sum_K \left\{ \int_{T_K} \tau N_i \frac{\partial u_x}{\partial y}\frac{\partial M_j}{\partial x}\mathrm{d}\Omega + \int_{T_K} \tau N_i \frac{\partial u_y}{\partial y}\frac{\partial M_j}{\partial y}\mathrm{d}\Omega + \right. \\
&+ \left. \int_{T_K} \tau \left(u_x \frac{\partial N_i}{\partial x} + u_y \frac{\partial N_i}{\partial y}\right)\frac{\partial M_j}{\partial y}\mathrm{d}\Omega - \nu \int_{T_K} \tau \left(\frac{\partial^2 N_i}{\partial x^2} + \frac{\partial^2 N_i}{\partial y^2}\right)\frac{\partial M_j}{\partial y}\mathrm{d}\Omega \right\}
\end{aligned}
$$

$$
K_{ji_{33}}(\mathbf{u},p) = \sum_K \int_{T_K} \tau \left(\frac{\partial M_i}{\partial x}\frac{\partial M_j}{\partial x} + \frac{\partial M_i}{\partial y}\frac{\partial M_j}{\partial y}\right)\mathrm{d}\Omega
$$

Matrix $\mathbf{K}_{ji}$ can be written as

$$
\mathbf{K}_{ji} = \begin{bmatrix} K_{ji_{11}} & K_{ji_{12}} & K_{ji_{13}} \\ K_{ji_{21}} & K_{ji_{22}} & K_{ji_{23}} \\ K_{ji_{31}} & K_{ji_{32}} & K_{ji_{33}} \end{bmatrix}.
$$

Let us define vector of the right hand side as

$$
\mathbf{R_j} = \begin{bmatrix} -\mathcal{F}(\mathbf{u},p)_{j_1} \\ -\mathcal{F}(\mathbf{u},p)_{j_2} \\ -\mathcal{F}(\mathbf{u},p)_{j_3} \end{bmatrix}
$$

and vector of solution as

$$
\mathbf{H_i} = \begin{bmatrix} h_{x_i} \\ h_{y_i} \\ q_i \end{bmatrix}.
$$

This way, we obtain element stiffness matrix $\mathbf{K}^e$ and element vector of the right hand side $\mathbf{R}^e$ (cf. Figure 5.1). After conventional assemblage procedure of stiffness matrix $\mathbf{K}$ and the right hand side $\mathbf{R}$, we solve the system of linear equations

$$
\mathbf{KH} = \mathbf{R}
$$

in each iteration of the Newton method.

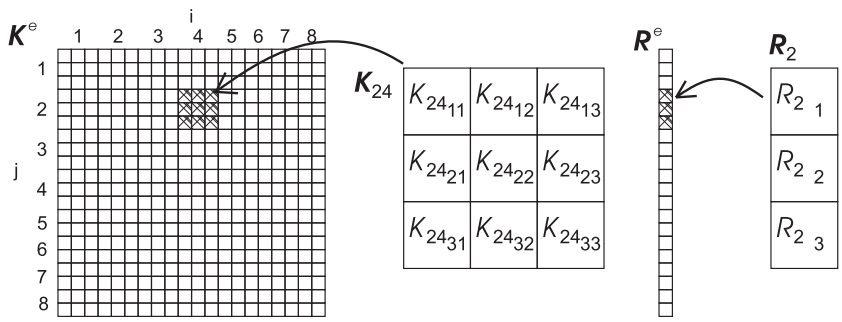

Figure 5.1: Structure of element stiffnes matrix for quadrilateral element

5.4 Stabilizing terms for unsteady Navier-Stokes equations

Remind the unsteady Navier-Stokes problem after space semidiscretization (3.5)-(3.7):

Seek $\mathbf{u}_h(t) \in V_{gh},\ t \in [0,T]$ and $p_h(t) \in Q_h,\ t \in [0,T]$ satisfying

$$\begin{aligned}
\int_\Omega \frac{\partial \mathbf{u}_h}{\partial t} \cdot \mathbf{v}_h \mathrm{d}\Omega + \int_\Omega (\mathbf{u}_h \cdot \nabla)\mathbf{u}_h \cdot \mathbf{v}_h \mathrm{d}\Omega \ &+\ \nu \int_\Omega \nabla \mathbf{u}_h : \nabla \mathbf{v}_h \mathrm{d}\Omega - \\
-\int_\Omega p_h \nabla \cdot \mathbf{v}_h \mathrm{d}\Omega \ &=\ \int_\Omega \mathbf{f} \cdot \mathbf{v}_h \mathrm{d}\Omega,\ \forall \mathbf{v}_h \in V_h && (5.10)\\
\int_\Omega \psi_h \nabla \cdot \mathbf{u}_h \mathrm{d}\Omega \ &=\ 0,\ \forall \psi_h \in Q_h && (5.11)\\
\mathbf{u}_h - \mathbf{u}_{gh} \ &\in\ V_h && (5.12)
\end{aligned}$$

Let us add stabilization terms in the same manner as for the steady case

$$\sum_{K=1}^{N} \int_{T_K} \left[\frac{\partial \mathbf{u}_h}{\partial t} + (\mathbf{u}_h \cdot \nabla)\mathbf{u}_h - \nu \Delta \mathbf{u}_h + \nabla p_h - \mathbf{f}_h \right] \cdot \tau \left[\frac{\partial \mathbf{v}_h}{\partial t} + (\mathbf{u}_h \cdot \nabla)\mathbf{v}_h - \nu \Delta \mathbf{v}_h + \nabla \psi_h \right] \mathrm{d}\Omega =$$

$$\begin{aligned}
= \ & \sum_{K=1}^{N} \left\{ \int_{T_K} \tau \frac{\partial \mathbf{u}_h}{\partial t} \cdot (\mathbf{u}_h \cdot \nabla)\mathbf{v}_h \mathrm{d}\Omega - \nu \int_{T_K} \tau \frac{\partial \mathbf{u}_h}{\partial t} \cdot \Delta \mathbf{v}_h \mathrm{d}\Omega + \int_{T_K} \tau \frac{\partial \mathbf{u}_h}{\partial t} \cdot \nabla \psi_h \mathrm{d}\Omega + \right. \\
+ \ & \int_{T_K} \tau (\mathbf{u}_h \cdot \nabla)\mathbf{u}_h \cdot (\mathbf{u}_h \cdot \nabla)\mathbf{v}_h \mathrm{d}\Omega - \nu \int_{T_K} \tau (\mathbf{u}_h \cdot \nabla)\mathbf{u}_h \cdot \Delta \mathbf{v}_h \mathrm{d}\Omega + \\
+ \ & \int_{T_K} \tau (\mathbf{u}_h \cdot \nabla)\mathbf{u}_h \cdot \nabla \psi_h \mathrm{d}\Omega - \nu \int_{T_K} \tau \Delta \mathbf{u}_h \cdot (\mathbf{u}_h \cdot \nabla)\mathbf{v}_h \mathrm{d}\Omega + \\
+ \ & \nu^2 \int_{T_K} \tau \Delta \mathbf{u}_h \cdot \Delta \mathbf{v}_h \mathrm{d}\Omega - \nu \int_{T_K} \tau \Delta \mathbf{u}_h \cdot \nabla \psi_h \mathrm{d}\Omega + \\
+ \ & \int_{T_K} \tau \nabla p_h \cdot (\mathbf{u}_h \cdot \nabla)\mathbf{v}_h \mathrm{d}\Omega - \nu \int_{T_K} \tau \nabla p_h \cdot \Delta \mathbf{v}_h \mathrm{d}\Omega + \int_{T_K} \tau \nabla p_h \cdot \nabla \psi_h \mathrm{d}\Omega - \\
- \ & \left. \int_{T_K} \tau \mathbf{f}_h \cdot (\mathbf{u}_h \cdot \nabla)\mathbf{v}_h \mathrm{d}\Omega + \nu \int_{T_K} \tau \mathbf{f}_h \cdot \Delta \mathbf{v}_h \mathrm{d}\Omega - \int_{T_K} \tau \mathbf{f}_h \cdot \nabla \psi_h \mathrm{d}\Omega \right\}
\end{aligned}$$

where we presumed $\frac{\partial \mathbf{v}_h}{\partial t} = \mathbf{0}$.

Note: As in the steady case, index h is omitted in the following text.

Let us approximate the time derivative in the $(n+1)$-st time layer as

$$\frac{\partial \mathbf{u}}{\partial t} \approx \frac{\mathbf{u}^{n+1} - \mathbf{u}^n}{\vartheta}$$

where ϑ is a constant time step.

5.5 Functionals for the Newton method and their differentials in unsteady case

Functionals for the Newton method are defined as

$$\begin{aligned}
F_1(\mathbf{u}^{n+1}, p^{n+1}) &= \frac{1}{\vartheta}\int_\Omega \mathbf{u}^{n+1}\cdot\mathbf{v}\mathrm{d}\Omega + \int_\Omega (\mathbf{u}^{n+1}\cdot\nabla)\mathbf{u}^{n+1}\cdot\mathbf{v}\mathrm{d}\Omega + \\
&+ \nu\int_\Omega \nabla\mathbf{u}^{n+1} : \nabla\mathbf{v}\mathrm{d}\Omega - \int_\Omega p^{n+1}\nabla\cdot\mathbf{v}\mathrm{d}\Omega - \\
&- \int_\Omega \mathbf{f}^{n+1}\cdot\mathbf{v}\mathrm{d}\Omega - \frac{1}{\vartheta}\int_\Omega \mathbf{u}^n\cdot\mathbf{v}\mathrm{d}\Omega + \\
&+ \sum_{K=1}^{N}\left\{\frac{1}{\vartheta}\int_{T_K}\tau\mathbf{u}^{n+1}\cdot(\mathbf{u}^{n+1}\cdot\nabla)\mathbf{v}\mathrm{d}\Omega - \frac{\nu}{\vartheta}\int_{T_K}\tau\mathbf{u}^{n+1}\cdot\Delta\mathbf{v}\mathrm{d}\Omega + \right. \\
&+ \frac{1}{\vartheta}\int_{T_K}\tau\mathbf{u}^{n+1}\cdot\nabla\psi\mathrm{d}\Omega + \int_{T_K}\tau(\mathbf{u}^{n+1}\cdot\nabla)\mathbf{u}^{n+1}\cdot(\mathbf{u}^{n+1}\cdot\nabla)\mathbf{v}\mathrm{d}\Omega - \\
&- \nu\int_{T_K}\tau(\mathbf{u}^{n+1}\cdot\nabla)\mathbf{u}^{n+1}\cdot\Delta\mathbf{v}\mathrm{d}\Omega + \int_{T_K}\tau(\mathbf{u}^{n+1}\cdot\nabla)\mathbf{u}^{n+1}\cdot\nabla\psi\mathrm{d}\Omega - \\
&- \nu\int_{T_K}\tau\Delta\mathbf{u}^{n+1}\cdot(\mathbf{u}^{n+1}\cdot\nabla)\mathbf{v}\mathrm{d}\Omega + \nu^2\int_{T_K}\tau\Delta\mathbf{u}^{n+1}\cdot\Delta\mathbf{v}\mathrm{d}\Omega - \\
&- \nu\int_{T_K}\tau\Delta\mathbf{u}^{n+1}\cdot\nabla\psi\mathrm{d}\Omega + \int_{T_K}\tau\nabla p^{n+1}\cdot(\mathbf{u}^{n+1}\cdot\nabla)\mathbf{v}\mathrm{d}\Omega - \\
&- \nu\int_{T_K}\tau\nabla p^{n+1}\cdot\Delta\mathbf{v}\mathrm{d}\Omega + \int_{T_K}\tau\nabla p^{n+1}\cdot\nabla\psi\mathrm{d}\Omega - \\
&- \int_{T_K}\tau\mathbf{f}^{n+1}\cdot(\mathbf{u}^{n+1}\cdot\nabla)\mathbf{v}\mathrm{d}\Omega + \nu\int_{T_K}\tau\mathbf{f}^{n+1}\cdot\Delta\mathbf{v}\mathrm{d}\Omega - \\
&- \int_{T_K}\tau\mathbf{f}^{n+1}\cdot\nabla\psi\mathrm{d}\Omega - \frac{1}{\vartheta}\int_{T_K}\tau\mathbf{u}^n\cdot(\mathbf{u}^{n+1}\cdot\nabla)\mathbf{v}\mathrm{d}\Omega + \\
&+ \left.\frac{\nu}{\vartheta}\int_{T_K}\tau\mathbf{u}^n\cdot\Delta\mathbf{v}\mathrm{d}\Omega - \frac{1}{\vartheta}\int_{T_K}\tau\mathbf{u}^n\cdot\nabla\psi\mathrm{d}\Omega\right\} \\
F_2(\mathbf{u}^{n+1}, p^{n+1}) &= \int_\Omega \psi\nabla\cdot\mathbf{u}^{n+1}\mathrm{d}\Omega
\end{aligned}$$

Note: Another simplification of notation is employed in the following derivations. We omit index $n+1$, and then $\mathbf{u}$ and p denote variables in the $(n+1)$-st time layer. Index of time layer is preserved at variables from other time layers, e.g. $\mathbf{u}^n$.

Lemma 5.2 *Assume all functions sufficiently smooth. Then the Frechet's differentials of functionals $F_1(\mathbf{u},p)$ and $F_2(\mathbf{u},p)$ are*

$$< DF_1(\mathbf{u},p),[\mathbf{h},q] >=$$

$$\begin{aligned}
= & \frac{1}{\vartheta}\int_\Omega \mathbf{h}\cdot\mathbf{v}\mathrm{d}\Omega + \int_\Omega (\mathbf{h}\cdot\nabla)\mathbf{u}\cdot\mathbf{v}\mathrm{d}\Omega + \int_\Omega (\mathbf{u}\cdot\nabla)\mathbf{h}\cdot\mathbf{v}\mathrm{d}\Omega + \nu\int_\Omega \nabla\mathbf{h}:\nabla\mathbf{v}\mathrm{d}\Omega - \int_\Omega q\nabla\cdot\mathbf{v}\mathrm{d}\Omega + \\
+ & \sum_{K=1}^{N}\left\{\frac{1}{\vartheta}\int_{T_K}\tau\mathbf{h}\cdot(\mathbf{u}\cdot\nabla)\mathbf{v}\mathrm{d}\Omega + \frac{1}{\vartheta}\int_{T_K}\tau\mathbf{u}\cdot(\mathbf{h}\cdot\nabla)\mathbf{v}\mathrm{d}\Omega - \frac{\nu}{\vartheta}\int_{T_K}\tau\mathbf{h}\cdot\Delta\mathbf{v}\mathrm{d}\Omega + \right. \\
+ & \frac{1}{\vartheta}\int_{T_K}\tau\mathbf{h}\cdot\nabla\psi\mathrm{d}\Omega + \int_{T_K}\tau(\mathbf{h}\cdot\nabla)\mathbf{u}\cdot(\mathbf{u}\cdot\nabla)\mathbf{v}\mathrm{d}\Omega + \int_{T_K}\tau(\mathbf{u}\cdot\nabla)\mathbf{h}\cdot(\mathbf{u}\cdot\nabla)\mathbf{v}\mathrm{d}\Omega + \\
+ & \int_{T_K}\tau(\mathbf{u}\cdot\nabla)\mathbf{u}\cdot(\mathbf{h}\cdot\nabla)\mathbf{v}\mathrm{d}\Omega - \nu\int_{T_K}\tau(\mathbf{h}\cdot\nabla)\mathbf{u}\cdot\Delta\mathbf{v}\mathrm{d}\Omega - \nu\int_{T_K}\tau(\mathbf{u}\cdot\nabla)\mathbf{h}\cdot\Delta\mathbf{v}\mathrm{d}\Omega + \\
+ & \int_{T_K}\tau(\mathbf{h}\cdot\nabla)\mathbf{u}\cdot\nabla\psi\mathrm{d}\Omega + \int_{T_K}\tau(\mathbf{u}\cdot\nabla)\mathbf{h}\cdot\nabla\psi\mathrm{d}\Omega - \nu\int_{T_K}\tau\Delta\mathbf{h}\cdot(\mathbf{u}\cdot\nabla)\mathbf{v}\mathrm{d}\Omega - \\
- & \nu\int_{T_K}\tau\Delta\mathbf{u}\cdot(\mathbf{h}\cdot\nabla)\mathbf{v}\mathrm{d}\Omega + \nu^2\int_{T_K}\tau\Delta\mathbf{h}\cdot\Delta\mathbf{v}\mathrm{d}\Omega - \nu\int_{T_K}\tau\Delta\mathbf{h}\cdot\nabla\psi\mathrm{d}\Omega + \\
+ & \int_{T_K}\tau\nabla q\cdot(\mathbf{u}\cdot\nabla)\mathbf{v}\mathrm{d}\Omega + \int_{T_K}\tau\nabla p\cdot(\mathbf{h}\cdot\nabla)\mathbf{v}\mathrm{d}\Omega - \nu\int_{T_K}\tau\nabla q\cdot\Delta\mathbf{v}\mathrm{d}\Omega + \\
+ & \left.\int_{T_K}\tau\nabla q\cdot\nabla\psi\mathrm{d}\Omega - \int_{T_K}\tau\mathbf{f}\cdot(\mathbf{h}\cdot\nabla)\mathbf{v}\mathrm{d}\Omega - \frac{1}{\vartheta}\int_{T_K}\tau\mathbf{u}^n(\mathbf{h}\cdot\nabla)\mathbf{v}\mathrm{d}\Omega\right\}
\end{aligned}$$

and

$$< DF_2(\mathbf{u},p),[\mathbf{h},q] >= \int_\Omega \psi\nabla\cdot\mathbf{h}\mathrm{d}\Omega.$$

As for the steady case, we formally introduce the functional

$$\mathcal{F}(\mathbf{u},p) = F_1(\mathbf{u},p) + F_2(\mathbf{u},p) \tag{5.13}$$

and its differential

$$< D\mathcal{F}(\mathbf{u},p),[\mathbf{h},q] >=< DF_1(\mathbf{u},p),[\mathbf{h},q] > + < DF_2(\mathbf{u},p),[\mathbf{h},q] > . \tag{5.14}$$

5.6 Matrices for the finite element method in unsteady case

Let us derive matrices for the finite element method. We substitute h_x, h_y, and q as in Chapter 5.3 and use the basis functions as test functions.

We obtain elements of the ji-submatrix $\mathbf{K}_{ji}$ of the element stiffness matrix $\mathbf{K}^e$:

$$
\begin{aligned}
K_{ji_{11}}(\mathbf{u},p) &= \frac{1}{\vartheta}\int_\Omega N_i N_j \mathrm{d}\Omega + \int_\Omega N_i \frac{\partial u_x}{\partial x} N_j \mathrm{d}\Omega + \int_\Omega \left(u_x \frac{\partial N_i}{\partial x} + u_y \frac{\partial N_i}{\partial y}\right) N_j \mathrm{d}\Omega + \\
&+ \nu \int_\Omega \left(\frac{\partial N_i}{\partial x}\frac{\partial N_j}{\partial x} + \frac{\partial N_i}{\partial y}\frac{\partial N_j}{\partial y}\right) \mathrm{d}\Omega + \\
&+ \sum_K \left\{ \frac{1}{\vartheta}\int_{T_K} \tau N_i \left(u_x \frac{\partial N_j}{\partial x} + u_y \frac{\partial N_j}{\partial y}\right) \mathrm{d}\Omega + \frac{1}{\vartheta}\int_{T_K} \tau u_x N_i \frac{\partial N_j}{\partial x} \mathrm{d}\Omega - \right. \\
&- \frac{\nu}{\vartheta}\int_{T_K} \tau N_i \left(\frac{\partial^2 N_j}{\partial x^2} + \frac{\partial^2 N_j}{\partial y^2}\right) \mathrm{d}\Omega + \\
&+ \int_{T_K} \tau N_i \frac{\partial u_x}{\partial x} \left(u_x \frac{\partial N_j}{\partial x} + u_y \frac{\partial N_j}{\partial y}\right) \mathrm{d}\Omega + \\
&+ \int_{T_K} \tau \left(u_x \frac{\partial N_i}{\partial x} + u_y \frac{\partial N_i}{\partial y}\right) \left(u_x \frac{\partial N_j}{\partial x} + u_y \frac{\partial N_j}{\partial y}\right) \mathrm{d}\Omega + \\
&+ \int_{T_K} \tau \left(u_x \frac{\partial u_x}{\partial x} + u_y \frac{\partial u_x}{\partial y}\right) N_i \frac{\partial N_j}{\partial x} \mathrm{d}\Omega - \\
&- \nu \int_{T_K} \tau N_i \frac{\partial u_x}{\partial x} \left(\frac{\partial^2 N_j}{\partial x^2} + \frac{\partial^2 N_j}{\partial y^2}\right) \mathrm{d}\Omega - \\
&- \nu \int_{T_K} \tau \left(u_x \frac{\partial N_i}{\partial x} + u_y \frac{\partial N_i}{\partial y}\right) \left(\frac{\partial^2 N_j}{\partial x^2} + \frac{\partial^2 N_j}{\partial y^2}\right) \mathrm{d}\Omega - \\
&- \nu \int_{T_K} \tau \left(\frac{\partial^2 N_i}{\partial x^2} + \frac{\partial^2 N_i}{\partial y^2}\right) \left(u_x \frac{\partial N_j}{\partial x} + u_y \frac{\partial N_j}{\partial y}\right) \mathrm{d}\Omega - \\
&- \nu \int_{T_K} \tau \left(\frac{\partial^2 u_x}{\partial x^2} + \frac{\partial^2 u_x}{\partial y^2}\right) N_i \frac{\partial N_j}{\partial x} \mathrm{d}\Omega + \\
&+ \nu^2 \int_{T_K} \tau \left(\frac{\partial^2 N_i}{\partial x^2} + \frac{\partial^2 N_i}{\partial y^2}\right) \left(\frac{\partial^2 N_j}{\partial x^2} + \frac{\partial^2 N_j}{\partial y^2}\right) \mathrm{d}\Omega + \\
&+ \left. \int_{T_K} \tau \frac{\partial p}{\partial x} N_i \frac{\partial N_j}{\partial x} \mathrm{d}\Omega - \int_{T_K} \tau f_x N_i \frac{\partial N_j}{\partial x} \mathrm{d}\Omega - \frac{1}{\vartheta}\int_{T_K} \tau u_x^n N_i \frac{\partial N_j}{\partial x} \mathrm{d}\Omega \right\}
\end{aligned}
$$

$$
\begin{aligned}
K_{ji_{12}}(\mathbf{u},p) &= \int_\Omega N_i \frac{\partial u_x}{\partial y} N_j \mathrm{d}\Omega + \\
&+ \sum_K \left\{ \frac{1}{\vartheta}\int_{T_K} \tau u_x N_i \frac{\partial N_j}{\partial y} \mathrm{d}\Omega + \int_{T_K} \tau N_i \frac{\partial u_x}{\partial y} \left(u_x \frac{\partial N_j}{\partial x} + u_y \frac{\partial N_j}{\partial y}\right) \mathrm{d}\Omega + \right. \\
&+ \int_{T_K} \tau \left(u_x \frac{\partial u_x}{\partial x} + u_y \frac{\partial u_x}{\partial y}\right) N_i \frac{\partial N_j}{\partial y} \mathrm{d}\Omega - \\
&- \nu \int_{T_K} \tau N_i \frac{\partial u_x}{\partial y} \left(\frac{\partial^2 N_j}{\partial x^2} + \frac{\partial^2 N_j}{\partial y^2}\right) \mathrm{d}\Omega - \\
&- \nu \int_{T_K} \tau \left(\frac{\partial^2 u_x}{\partial x^2} + \frac{\partial^2 u_x}{\partial y^2}\right) N_i \frac{\partial N_j}{\partial y} \mathrm{d}\Omega + \\
&+ \left. \int_{T_K} \tau \frac{\partial p}{\partial x} N_i \frac{\partial N_j}{\partial y} \mathrm{d}\Omega - \int_{T_K} \tau f_x N_i \frac{\partial N_j}{\partial y} \mathrm{d}\Omega - \frac{1}{\vartheta}\int_{T_K} \tau u_x^n N_i \frac{\partial N_j}{\partial y} \mathrm{d}\Omega \right\}
\end{aligned}
$$

$$
\begin{aligned}
K_{ji_{13}}(\mathbf{u},p) &= -\int_\Omega M_i \frac{\partial N_j}{\partial x}\mathrm{d}\Omega + \sum_K \left\{ \int_{T_K} \tau \frac{\partial M_i}{\partial x}\left(u_x \frac{\partial N_j}{\partial x} + u_y \frac{\partial N_j}{\partial y}\right)\mathrm{d}\Omega - \right. \\
&- \left. \nu \int_{T_K} \tau \frac{\partial M_i}{\partial x}\left(\frac{\partial^2 N_j}{\partial x^2} + \frac{\partial^2 N_j}{\partial y^2}\right)\mathrm{d}\Omega \right\}
\end{aligned}
$$

$$
\begin{aligned}
K_{ji_{21}}(\mathbf{u},p) &= \int_\Omega N_i \frac{\partial u_y}{\partial x} N_j \mathrm{d}\Omega + \sum_K \left\{ \frac{1}{\vartheta}\int_{T_K} \tau u_y N_i \frac{\partial N_j}{\partial x}\mathrm{d}\Omega + \right. \\
&+ \int_{T_K} \tau N_i \frac{\partial u_y}{\partial x}\left(u_x \frac{\partial N_j}{\partial x} + u_y \frac{\partial N_j}{\partial y}\right)\mathrm{d}\Omega + \\
&+ \int_{T_K} \tau \left(u_x \frac{\partial u_y}{\partial x} + u_y \frac{\partial u_y}{\partial y}\right) N_i \frac{\partial N_j}{\partial x}\mathrm{d}\Omega - \\
&- \nu \int_{T_K} \tau N_i \frac{\partial u_y}{\partial x}\left(\frac{\partial^2 N_j}{\partial x^2} + \frac{\partial^2 N_j}{\partial y^2}\right)\mathrm{d}\Omega - \\
&- \nu \int_{T_K} \tau \left(\frac{\partial^2 u_y}{\partial x^2} + \frac{\partial^2 u_y}{\partial y^2}\right) N_i \frac{\partial N_j}{\partial x}\mathrm{d}\Omega + \\
&+ \left. \int_{T_K} \tau \frac{\partial p}{\partial y} N_i \frac{\partial N_j}{\partial x}\mathrm{d}\Omega - \int_{T_K} \tau f_y N_i \frac{\partial N_j}{\partial x}\mathrm{d}\Omega - \frac{1}{\vartheta}\int_{T_K} \tau u_y^n N_i \frac{\partial N_j}{\partial x}\mathrm{d}\Omega \right\}
\end{aligned}
$$

$$
\begin{aligned}
K_{ji_{22}}(\mathbf{u},p) &= \frac{1}{\vartheta}\int_\Omega N_i N_j \mathrm{d}\Omega + \int_\Omega N_i \frac{\partial u_y}{\partial y} N_j \mathrm{d}\Omega + \int_\Omega \left(u_x \frac{\partial N_i}{\partial x} + u_y \frac{\partial N_i}{\partial y}\right) N_j \mathrm{d}\Omega + \\
&+ \nu \int_\Omega \left(\frac{\partial N_i}{\partial x}\frac{\partial N_j}{\partial x} + \frac{\partial N_i}{\partial y}\frac{\partial N_j}{\partial y}\right)\mathrm{d}\Omega + \\
&+ \sum_K \left\{ \frac{1}{\vartheta}\int_{T_K} \tau N_i \left(u_x \frac{\partial N_j}{\partial x} + u_y \frac{\partial N_j}{\partial y}\right)\mathrm{d}\Omega + \frac{1}{\vartheta}\int_{T_K} \tau u_y N_i \frac{\partial N_j}{\partial y}\mathrm{d}\Omega - \right. \\
&- \frac{\nu}{\vartheta}\int_{T_K} \tau N_i \left(\frac{\partial^2 N_j}{\partial x^2} + \frac{\partial^2 N_j}{\partial y^2}\right)\mathrm{d}\Omega + \int_{T_K} \tau N_i \frac{\partial u_y}{\partial y}\left(u_x \frac{\partial N_j}{\partial x} + u_y \frac{\partial N_j}{\partial y}\right)\mathrm{d}\Omega + \\
&+ \int_{T_K} \tau \left(u_x \frac{\partial N_i}{\partial x} + u_y \frac{\partial N_i}{\partial y}\right)\left(u_x \frac{\partial N_j}{\partial x} + u_y \frac{\partial N_j}{\partial y}\right)\mathrm{d}\Omega + \\
&+ \int_{T_K} \tau \left(u_x \frac{\partial u_y}{\partial x} + u_y \frac{\partial u_y}{\partial y}\right) N_i \frac{\partial N_j}{\partial y}\mathrm{d}\Omega - \nu \int_{T_K} \tau N_i \frac{\partial u_y}{\partial y}\left(\frac{\partial^2 N_j}{\partial x^2} + \frac{\partial^2 N_j}{\partial y^2}\right)\mathrm{d}\Omega - \\
&- \nu \int_K \tau \left(u_x \frac{\partial N_i}{\partial x} + u_y \frac{\partial N_i}{\partial y}\right)\left(\frac{\partial^2 N_j}{\partial x^2} + \frac{\partial^2 N_j}{\partial y^2}\right)\mathrm{d}\Omega - \\
&- \nu \int_{T_K} \tau \left(\frac{\partial^2 N_i}{\partial x^2} + \frac{\partial^2 N_i}{\partial y^2}\right)\left(u_x \frac{\partial N_j}{\partial x} + u_y \frac{\partial N_j}{\partial y}\right)\mathrm{d}\Omega - \\
&- \nu \int_{T_K} \tau \left(\frac{\partial^2 u_y}{\partial x^2} + \frac{\partial^2 u_y}{\partial y^2}\right) N_i \frac{\partial N_j}{\partial y}\mathrm{d}\Omega + \\
&+ \nu^2 \int_{T_K} \tau \left(\frac{\partial^2 N_i}{\partial x^2} + \frac{\partial^2 N_i}{\partial y^2}\right)\left(\frac{\partial^2 N_j}{\partial x^2} + \frac{\partial^2 N_j}{\partial y^2}\right)\mathrm{d}\Omega + \\
&+ \left. \int_{T_K} \tau \frac{\partial p}{\partial y} N_i \frac{\partial N_j}{\partial y}\mathrm{d}\Omega - \int_{T_K} \tau f_y N_i \frac{\partial N_j}{\partial y}\mathrm{d}\Omega - \frac{1}{\vartheta}\int_{T_K} \tau u_y^n N_i \frac{\partial N_j}{\partial y}\mathrm{d}\Omega \right\}
\end{aligned}
$$

$$
\begin{aligned}
K_{ji_{23}}(\mathbf{u},p) &= -\int_\Omega M_i \frac{\partial N_j}{\partial y}\mathrm{d}\Omega + \sum_K \left\{ \int_{T_K} \tau \frac{\partial M_i}{\partial y}\left(u_x \frac{\partial N_j}{\partial x} + u_y \frac{\partial N_j}{\partial y}\right)\mathrm{d}\Omega - \right. \\
&- \left. \nu \int_{T_K} \tau \frac{\partial M_i}{\partial y}\left(\frac{\partial^2 N_j}{\partial x^2} + \frac{\partial^2 N_j}{\partial y^2}\right)\mathrm{d}\Omega \right\}
\end{aligned}
$$

$$
\begin{aligned}
K_{ji_{31}}(\mathbf{u},p) &= \int_\Omega \frac{\partial N_i}{\partial x} M_j \mathrm{d}\Omega + \\
&+ \sum_K \left\{ \frac{1}{\vartheta}\int_{T_K} \tau N_i \frac{\partial M_j}{\partial x}\mathrm{d}\Omega + \int_{T_K} \tau N_i \frac{\partial u_x}{\partial x}\frac{\partial M_j}{\partial x}\mathrm{d}\Omega + \int_{T_K} \tau N_i \frac{\partial u_y}{\partial x}\frac{\partial M_j}{\partial y}\mathrm{d}\Omega + \right. \\
&+ \left. \int_{T_K} \tau \left(u_x \frac{\partial N_i}{\partial x} + u_y \frac{\partial N_i}{\partial y}\right)\frac{\partial M_j}{\partial x}\mathrm{d}\Omega - \nu \int_{T_K} \tau \left(\frac{\partial^2 N_i}{\partial x^2} + \frac{\partial^2 N_i}{\partial y^2}\right)\frac{\partial M_j}{\partial x}\mathrm{d}\Omega \right\}
\end{aligned}
$$

$$
\begin{aligned}
K_{ji_{32}}(\mathbf{u},p) &= \int_\Omega \frac{\partial N_i}{\partial y} M_j \mathrm{d}\Omega + \\
&+ \sum_K \left\{ \frac{1}{\vartheta}\int_{T_K} \tau N_i \frac{\partial M_j}{\partial y}\mathrm{d}\Omega + \int_{T_K} \tau N_i \frac{\partial u_x}{\partial y}\frac{\partial M_j}{\partial x}\mathrm{d}\Omega + \int_{T_K} \tau N_i \frac{\partial u_y}{\partial y}\frac{\partial M_j}{\partial y}\mathrm{d}\Omega + \right. \\
&+ \left. \int_{T_K} \tau \left(u_x \frac{\partial N_i}{\partial x} + u_y \frac{\partial N_i}{\partial y}\right)\frac{\partial M_j}{\partial y}\mathrm{d}\Omega - \nu \int_{T_K} \tau \left(\frac{\partial^2 N_i}{\partial x^2} + \frac{\partial^2 N_i}{\partial y^2}\right)\frac{\partial M_j}{\partial y}\mathrm{d}\Omega \right\}
\end{aligned}
$$

$$
K_{ji_{33}}(\mathbf{u},p) = \sum_K \int_{T_K} \tau \left(\frac{\partial M_i}{\partial x}\frac{\partial M_j}{\partial x} + \frac{\partial M_i}{\partial y}\frac{\partial M_j}{\partial y}\right)\mathrm{d}\Omega
$$

Let us remind matrix $\mathbf{K}_{ji}$

$$
\mathbf{K}_{ji} = \begin{bmatrix} K_{ji_{11}} & K_{ji_{12}} & K_{ji_{13}} \\ K_{ji_{21}} & K_{ji_{22}} & K_{ji_{23}} \\ K_{ji_{31}} & K_{ji_{32}} & K_{ji_{33}} \end{bmatrix},
$$

vector of the right hand side

$$
\mathbf{R_j} = \begin{bmatrix} -\mathcal{F}(\mathbf{u},p)_{j_1} \\ -\mathcal{F}(\mathbf{u},p)_{j_2} \\ -\mathcal{F}(\mathbf{u},p)_{j_3} \end{bmatrix},
$$

and vector of solution

$$
\mathbf{H_i} = \begin{bmatrix} h_{x_i} \\ h_{y_i} \\ q_i \end{bmatrix}.
$$

Elements of the vector of the right hand side are

$$
\begin{aligned}
\mathcal{F}(\mathbf{u},p)_{j_1} &= \frac{1}{\vartheta}\int_\Omega u_x N_j \mathrm{d}\Omega + \int_\Omega \left(u_x\frac{\partial u_x}{\partial x} + u_y\frac{\partial u_x}{\partial y}\right) N_j \mathrm{d}\Omega + \nu\int_\Omega \left(\frac{\partial u_x}{\partial x}\frac{\partial N_j}{\partial x} + \frac{\partial u_x}{\partial y}\frac{\partial N_j}{\partial y}\right)\mathrm{d}\Omega - \\
&- \int_\Omega p\frac{\partial N_j}{\partial x}\mathrm{d}\Omega - \int_\Omega f_x N_j \mathrm{d}\Omega - \frac{1}{\vartheta}\int_\Omega u_x^n N_j \mathrm{d}\Omega + \\
&+ \sum_K \left\{ \frac{1}{\vartheta}\int_{T_K} \tau u_x \left(u_x\frac{\partial N_j}{\partial x} + u_y\frac{\partial N_j}{\partial y}\right)\mathrm{d}\Omega - \frac{\nu}{\vartheta}\int_{T_K}\tau u_x\left(\frac{\partial^2 N_j}{\partial x^2} + \frac{\partial^2 N_j}{\partial y^2}\right)\mathrm{d}\Omega + \right. \\
&+ \int_{T_K}\tau\left(u_x\frac{\partial u_x}{\partial x} + u_y\frac{\partial u_x}{\partial y}\right)\left(u_x\frac{\partial N_j}{\partial x} + u_y\frac{\partial N_j}{\partial y}\right)\mathrm{d}\Omega - \\
&- \nu\int_{T_K}\tau\left(u_x\frac{\partial u_x}{\partial x} + u_y\frac{\partial u_x}{\partial y}\right)\left(\frac{\partial^2 N_j}{\partial x^2} + \frac{\partial^2 N_j}{\partial y^2}\right)\mathrm{d}\Omega - \\
&- \nu\int_{T_K}\tau\left(\frac{\partial^2 u_x}{\partial x^2} + \frac{\partial^2 u_x}{\partial y^2}\right)\left(u_x\frac{\partial N_j}{\partial x} + u_y\frac{\partial N_j}{\partial y}\right)\mathrm{d}\Omega + \\
&+ \nu^2\int_{T_K}\tau\left(\frac{\partial^2 u_x}{\partial x^2} + \frac{\partial^2 u_x}{\partial y^2}\right)\left(\frac{\partial^2 N_j}{\partial x^2} + \frac{\partial^2 N_j}{\partial y^2}\right)\mathrm{d}\Omega + \\
&+ \int_{T_K}\tau\frac{\partial p}{\partial x}\left(u_x\frac{\partial N_j}{\partial x} + u_y\frac{\partial N_j}{\partial y}\right)\mathrm{d}\Omega - \nu\int_{T_K}\tau\frac{\partial p}{\partial x}\left(\frac{\partial^2 N_j}{\partial x^2} + \frac{\partial^2 N_j}{\partial y^2}\right)\mathrm{d}\Omega - \\
&- \int_{T_K}\tau f_x\left(u_x\frac{\partial N_j}{\partial x} + u_y\frac{\partial N_j}{\partial y}\right)\mathrm{d}\Omega + \nu\int_{T_K}\tau f_x\left(\frac{\partial^2 N_j}{\partial x^2} + \frac{\partial^2 N_j}{\partial y^2}\right)\mathrm{d}\Omega - \\
&- \left.\frac{1}{\vartheta}\int_{T_K}\tau u_x^n\left(u_x\frac{\partial N_j}{\partial x} + u_y\frac{\partial N_j}{\partial y}\right)\mathrm{d}\Omega + \frac{\nu}{\vartheta}\int_{T_K}\tau u_x^n\left(\frac{\partial^2 N_j}{\partial x^2} + \frac{\partial^2 N_j}{\partial y^2}\right)\mathrm{d}\Omega\right\}
\end{aligned}
$$

$$
\begin{aligned}
\mathcal{F}(\mathbf{u},p)_{j_2} &= \frac{1}{\vartheta}\int_\Omega u_y N_j \mathrm{d}\Omega + \int_\Omega \left(u_x\frac{\partial u_y}{\partial x} + u_y\frac{\partial u_y}{\partial y}\right) N_j \mathrm{d}\Omega + \nu\int_\Omega \left(\frac{\partial u_y}{\partial x}\frac{\partial N_j}{\partial x} + \frac{\partial u_y}{\partial y}\frac{\partial N_j}{\partial y}\right)\mathrm{d}\Omega - \\
&- \int_\Omega p\frac{\partial N_j}{\partial y}\mathrm{d}\Omega - \int_\Omega f_y N_j \mathrm{d}\Omega - \frac{1}{\vartheta}\int_\Omega u_y^n N_j \mathrm{d}\Omega + \\
&+ \sum_K \left\{ \frac{1}{\vartheta}\int_{T_K} \tau u_y \left(u_x\frac{\partial N_j}{\partial x} + u_y\frac{\partial N_j}{\partial y}\right)\mathrm{d}\Omega - \frac{\nu}{\vartheta}\int_{T_K}\tau u_y\left(\frac{\partial^2 N_j}{\partial x^2} + \frac{\partial^2 N_j}{\partial y^2}\right)\mathrm{d}\Omega + \right. \\
&+ \int_{T_K}\tau\left(u_x\frac{\partial u_y}{\partial x} + u_y\frac{\partial u_y}{\partial y}\right)\left(u_x\frac{\partial N_j}{\partial x} + u_y\frac{\partial N_j}{\partial y}\right)\mathrm{d}\Omega - \\
&- \nu\int_{T_K}\tau\left(u_x\frac{\partial u_y}{\partial x} + u_y\frac{\partial u_y}{\partial y}\right)\left(\frac{\partial^2 N_j}{\partial x^2} + \frac{\partial^2 N_j}{\partial y^2}\right)\mathrm{d}\Omega - \\
&- \nu\int_{T_K}\tau\left(\frac{\partial^2 u_y}{\partial x^2} + \frac{\partial^2 u_y}{\partial y^2}\right)\left(u_x\frac{\partial N_j}{\partial x} + u_y\frac{\partial N_j}{\partial y}\right)\mathrm{d}\Omega + \\
&+ \nu^2\int_{T_K}\tau\left(\frac{\partial^2 u_y}{\partial x^2} + \frac{\partial^2 u_y}{\partial y^2}\right)\left(\frac{\partial^2 N_j}{\partial x^2} + \frac{\partial^2 N_j}{\partial y^2}\right)\mathrm{d}\Omega + \\
&+ \int_{T_K}\tau\frac{\partial p}{\partial y}\left(u_x\frac{\partial N_j}{\partial x} + u_y\frac{\partial N_j}{\partial y}\right)\mathrm{d}\Omega - \nu\int_{T_K}\tau\frac{\partial p}{\partial y}\left(\frac{\partial^2 N_j}{\partial x^2} + \frac{\partial^2 N_j}{\partial y^2}\right)\mathrm{d}\Omega - \\
&- \int_{T_K}\tau f_y\left(u_x\frac{\partial N_j}{\partial x} + u_y\frac{\partial N_j}{\partial y}\right)\mathrm{d}\Omega + \nu\int_{T_K}\tau f_y\left(\frac{\partial^2 N_j}{\partial x^2} + \frac{\partial^2 N_j}{\partial y^2}\right)\mathrm{d}\Omega - \\
&- \left.\frac{1}{\vartheta}\int_{T_K}\tau u_y^n\left(u_x\frac{\partial N_j}{\partial x} + u_y\frac{\partial N_j}{\partial y}\right)\mathrm{d}\Omega + \frac{\nu}{\vartheta}\int_{T_K}\tau u_y^n\left(\frac{\partial^2 N_j}{\partial x^2} + \frac{\partial^2 N_j}{\partial y^2}\right)\mathrm{d}\Omega\right\}
\end{aligned}
$$

$$
\begin{aligned}
\mathcal{F}(\mathbf{u},p)_{j_3} &= \int_\Omega \left(\frac{\partial u_x}{\partial x}+\frac{\partial u_y}{\partial y}\right) M_j \mathrm{d}\Omega + \sum_K \left\{ \frac{1}{\vartheta}\int_{T_K} \tau \left(u_x\frac{\partial M_j}{\partial x}+u_y\frac{\partial M_j}{\partial y}\right)\mathrm{d}\Omega + \right.\\
&+ \int_{T_K} \tau \left(u_x\frac{\partial u_x}{\partial x}+u_y\frac{\partial u_x}{\partial y}\right)\frac{\partial M_j}{\partial x}\mathrm{d}\Omega + \int_{T_K} \tau \left(u_x\frac{\partial u_y}{\partial x}+u_y\frac{\partial u_y}{\partial y}\right)\frac{\partial M_j}{\partial y}\mathrm{d}\Omega -\\
&- \nu\int_{T_K} \tau \left(\frac{\partial^2 u_x}{\partial x^2}+\frac{\partial^2 u_x}{\partial y^2}\right)\frac{\partial M_j}{\partial x}\mathrm{d}\Omega - \nu\int_{T_K} \tau \left(\frac{\partial^2 u_y}{\partial x^2}+\frac{\partial^2 u_y}{\partial y^2}\right)\frac{\partial M_j}{\partial y}\mathrm{d}\Omega +\\
&+ \int_{T_K} \tau\frac{\partial p}{\partial x}\frac{\partial M_j}{\partial x}\mathrm{d}\Omega + \int_{T_K} \tau\frac{\partial p}{\partial y}\frac{\partial M_j}{\partial y}\mathrm{d}\Omega -\\
&- \left.\int_{T_K} \tau f_x\frac{\partial M_j}{\partial x}\mathrm{d}\Omega - \int_{T_K} \tau f_y\frac{\partial M_j}{\partial y}\mathrm{d}\Omega - \frac{1}{\vartheta}\int_{T_K} \tau \left(u_x^n\frac{\partial M_j}{\partial x}+u_y^n\frac{\partial M_j}{\partial y}\right)\mathrm{d}\Omega \right\}
\end{aligned}
$$

As in Chapter 5.3, after we obtain element stiffness matrix $\mathbf{K}^e$ and element vector of the right hand side $\mathbf{R}^e$ (cf. Figure 5.1) and perform the assemblage procedure of stiffness matrix $\mathbf{K}$ and the right hand side $\mathbf{R}$, we solve the system of linear equations

$$\mathbf{KH} = \mathbf{R}$$

in each iteration of the Newton method.

Once we obtain the solution in a particular time layer, we solve the problem in next time layer and use the previous solution as the initial value for the Newton method. This is repeated, until we reach the desired time.

5.7 Stabilization parameters

It has been already mentioned, that we do not employ stabilization parameter δ. The way to obtain τ is not straightforward. Following the ideas of Franca and Madureira in [15], we compute τ as (cf. (4.7) in Chapter 4.2)

$$\tau = \frac{\xi(\mathrm{Re}_K(\mathbf{x}))}{\sqrt{\lambda_K}\mid \mathbf{u}(\mathbf{x}) \mid_2} \tag{5.15}$$

where

$$
\begin{aligned}
\mathrm{Re}_K(\mathbf{x}) &= \frac{\mid \mathbf{u}(\mathbf{x}) \mid_2}{4\sqrt{\lambda_K}\nu}\\
\xi(\mathrm{Re}_K(\mathbf{x})) &= \begin{cases} \mathrm{Re}_K(\mathbf{x}), & 0 \le \mathrm{Re}_K(\mathbf{x}) < 1 \\ 1, & \mathrm{Re}_K(\mathbf{x}) \ge 1 \end{cases}\\
\lambda_K &= \max_{0\neq \mathbf{v}\in (R_2(T_K)/\mathbb{R})^2} \frac{\|\Delta \mathbf{v}\|^2_{0,T_K}}{\|\nabla \mathbf{v}\|^2_{0,T_K}}\\
\mid \mathbf{u}(\mathbf{x}) \mid_2 &= \left(\sum_{i=1}^{2} \mid u_i(\mathbf{x}) \mid^2\right)^{\frac{1}{2}}
\end{aligned}
$$

Parameter λ_K is computed for each element as the largest eigenvalue of the problem

$$(\Delta\mathbf{w}, \Delta\mathbf{v}) = \lambda_K(\nabla\mathbf{w}, \nabla\mathbf{v}), \quad \forall \mathbf{v} \in (R_2(T_K)/\mathbb{R})^2 \tag{5.16}$$

This is done once, before entering the main computational loop of the Newton method, since λ_K is not a function of velocity and depends only on the computational mesh and space functions on element K.

Let us focus on computing λ_K more precisely. Problem (5.16) can be written as

$$\int_{T_K} \Delta\mathbf{w} \cdot \Delta\mathbf{v} \mathrm{d}\Omega = \lambda_K \int_{T_K} \nabla\mathbf{w} : \nabla\mathbf{v} \mathrm{d}\Omega, \quad \forall \mathbf{v} \in (R_2(T_K)/\mathbb{R})^2 \tag{5.17}$$

In the finite element dialect, similarly to Chapters 5.3 and 5.6, we substitute

$$\begin{aligned} w_x &= \sum_{i=1}^{N_u} w_{xi} N_i \\ w_y &= \sum_{i=1}^{N_u} w_{y_i} N_i \end{aligned}$$

and input the vector basis functions

$$\begin{aligned} \mathbf{v} &= (N_j, 0); \\ \mathbf{v} &= (0, N_j) \end{aligned}$$

as test functions, to get two equations from the scalar one (5.17). It leads to

$$\begin{aligned} \sum_{i=1}^{N_u} \int_{T_K} w_{x_i} \left(\frac{\partial^2 N_i}{\partial x^2} + \frac{\partial^2 N_i}{\partial y^2} \right) \left(\frac{\partial^2 N_j}{\partial x^2} + \frac{\partial^2 N_j}{\partial y^2} \right) \mathrm{d}\Omega &= \lambda_K \sum_{i=1}^{N_u} \int_{T_K} w_{x_i} \left(\frac{\partial N_i}{\partial x} \frac{\partial N_j}{\partial x} + \frac{\partial N_i}{\partial y} \frac{\partial N_j}{\partial y} \right) \mathrm{d}\Omega \\ \sum_{i=1}^{N_u} \int_{T_K} w_{y_i} \left(\frac{\partial^2 N_i}{\partial x^2} + \frac{\partial^2 N_i}{\partial y^2} \right) \left(\frac{\partial^2 N_j}{\partial x^2} + \frac{\partial^2 N_j}{\partial y^2} \right) \mathrm{d}\Omega &= \lambda_K \sum_{i=1}^{N_u} \int_{T_K} w_{y_i} \left(\frac{\partial N_i}{\partial x} \frac{\partial N_j}{\partial x} + \frac{\partial N_i}{\partial y} \frac{\partial N_j}{\partial y} \right) \mathrm{d}\Omega \end{aligned}$$

Let us create element matrices $\mathbf{A}$ and $\mathbf{B}$ for the purpose of computation of the largest eigenvalue of this problem.

$$\begin{aligned} \mathbf{A}_{ji} &= \begin{bmatrix} \int_{T_K} \left(\frac{\partial^2 N_i}{\partial x^2} + \frac{\partial^2 N_i}{\partial y^2} \right) \left(\frac{\partial^2 N_j}{\partial x^2} + \frac{\partial^2 N_j}{\partial y^2} \right) \mathrm{d}\Omega & 0 \\ 0 & \int_{T_K} \left(\frac{\partial^2 N_i}{\partial x^2} + \frac{\partial^2 N_i}{\partial y^2} \right) \left(\frac{\partial^2 N_j}{\partial x^2} + \frac{\partial^2 N_j}{\partial y^2} \right) \mathrm{d}\Omega \end{bmatrix} \\ \mathbf{B}_{ji} &= \begin{bmatrix} \int_{T_K} \left(\frac{\partial N_i}{\partial x} \frac{\partial N_j}{\partial x} + \frac{\partial N_i}{\partial y} \frac{\partial N_j}{\partial y} \right) \mathrm{d}\Omega & 0 \\ 0 & \int_{T_K} \left(\frac{\partial N_i}{\partial x} \frac{\partial N_j}{\partial x} + \frac{\partial N_i}{\partial y} \frac{\partial N_j}{\partial y} \right) \mathrm{d}\Omega \end{bmatrix} \end{aligned}$$

Now, we need to find the largest eigenvalue of the generalized matrix eigenvalue problem

$$\mathbf{A}\mathbf{w}_K = \lambda_K \mathbf{B}\mathbf{w}_K \tag{5.18}$$

for each element. Here, λ_K is the desired eigenvalue and $\mathbf{w}_K$ is the corresponding eigenvector, which is not used in stabilization.

Recommended method for solving this problem in [15] is the power method. But several difficulties are hidden behind it

1. The power method is designed for finding of the largest eigenvalue and the corresponding eigenvector of the problem $\mathbf{A}\mathbf{w} = \lambda_K \mathbf{w}$ and not for the generalized problem. We need to transform problem (5.18) to the ordinary problem of eigenvalues. Possible way without necessity of inverting full matrix is sketched. We decompose matrix $\mathbf{B}$ by Choleski's method, i.e. find $\mathbf{L}$ so that

$$\mathbf{B} = \mathbf{L}\mathbf{L}^T$$

and $\mathbf{L}$ is lower triangular matrix. Its inversion is simpler, and when we have it, we get

$$\mathbf{L}^{-1}\mathbf{A}\mathbf{w}_K = \lambda_K \mathbf{L}^T \mathbf{w}_K.$$

Let us denote $\mathbf{z}_K = \mathbf{L}^T\mathbf{w}_K$ or $\mathbf{w}_K = \mathbf{L}^{-T}\mathbf{z}_K$. After substitution, we have

$$\mathbf{L}^{-1}\mathbf{A}\mathbf{L}^{-T}\mathbf{z}_K = \lambda_K \mathbf{z}_K.$$

If we denote $\mathbf{G} = \mathbf{L}^{-1}\mathbf{A}\mathbf{L}^{-T}$, we can solve the ordinary problem of eigenvalues

$$\mathbf{G}\mathbf{z}_K = \lambda_K \mathbf{z}_K.$$

It is clear, that applied transformations do not take effect on eigenvalues of the generalized problem.

2. During realizing Choleski's decomposition (as for computing an inverse matrix), we need $\mathbf{B}$ to be nonsingular. But obtained matrix, which is similar to element stiffness matrix without application of boundary conditions, is singular.

   Recommended way to regularize it is to fix corresponding number of degrees of freedom. But since this is done by putting units on diagonal and zeros on relevant columns and rows of matrix $\mathbf{B}$, this way could affect the largest eigenvalue, if it is less then one.

   We experienced, that more suitable way to regularize the matrix is to 'cut off' two rows and columns from both matrices $\mathbf{A}$ and $\mathbf{B}$. As far as we have tested this way, it has taken no effect on the largest eigenvalue for different omited rows and columns. The only restriction is to omit one for each component of velocity.

Let us investigate the dependence of τ on local Reynolds number $\mathrm{Re}_K(\mathbf{x})$ given by (5.15). We can observe that $\mathrm{Re}_K(\mathbf{x})$ is a linear function of $\mid \mathbf{u}(\mathbf{x}) \mid_2$ for constant viscosity on element K, i.e.

$$\mathrm{Re}_K(\mathbf{x}) = C_1 \mid \mathbf{u}(\mathbf{x}) \mid_2 \tag{5.19}$$

where $C_1 = \frac{1}{4\sqrt{\lambda_K}\nu}$.

Substituting (5.19) in (5.15) we get

$$\tau(\mathrm{Re}_K(\mathbf{x}), \mathbf{x}) = \begin{cases} C_2, & 0 \leq \mathrm{Re}_K(\mathbf{x}) < 1 \\ \frac{C_3}{|\mathbf{u}(\mathbf{x})|_2} = \frac{C_2}{\mathrm{Re}_K(\mathbf{x})}, & \mathrm{Re}_K(\mathbf{x}) \geq 1 \end{cases}$$

where $C_2 = \frac{1}{4\lambda_K\nu}$ and $C_3 = \frac{1}{\sqrt{\lambda_K}}$, cf. Figure 5.2.

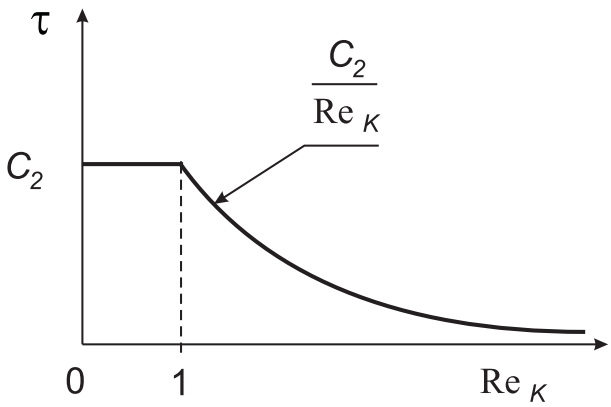

Figure 5.2: Plot of $\tau(\mathrm{Re}_K)$

An unpleasant effect of stabilization can be discovered. In Chapter 5.3 as well as in Chapter 5.6, we violated the continuity equation through the non-zero term of element matrix

$$K_{ji_{33}}(\mathbf{u}, p) \;=\; \sum_K \int_{T_K} \tau \left(\frac{\partial M_i}{\partial x}\frac{\partial M_j}{\partial x} + \frac{\partial M_i}{\partial y}\frac{\partial M_j}{\partial y} \right) \mathrm{d}\Omega.$$

This term introduces dependence on pressure into the continuity equation and affects the presumed incompressibility. Since derivatives of shape functions in $K_{ji_{33}}$ are independent of solution, and since τ is never zero (cf. Figure 5.2), $K_{ji_{33}}$ does not vanish for converged solution.

But Figure 5.2 gives a hope: we can observe, that τ is decreasing for higher local Reynolds number, therefore described perturbation of the continuity equation is also decreasing for higher Re.

5.8 Numerical implementation

The algorithm was implemented using Fortran programming language. Block scheme of the program follows. Main part of programmer's work consisted in writing routines for computing eigenvalues on elements and computing finite element matrices.

For the solution of the system of linear equations, resulting from the Newton method, frontal solver is used. This solver was provided by the consultant of my thesis.

Program was tested and benchmarks were run on Compaq AlphaServerES47 in the Institute of Thermomechanics.

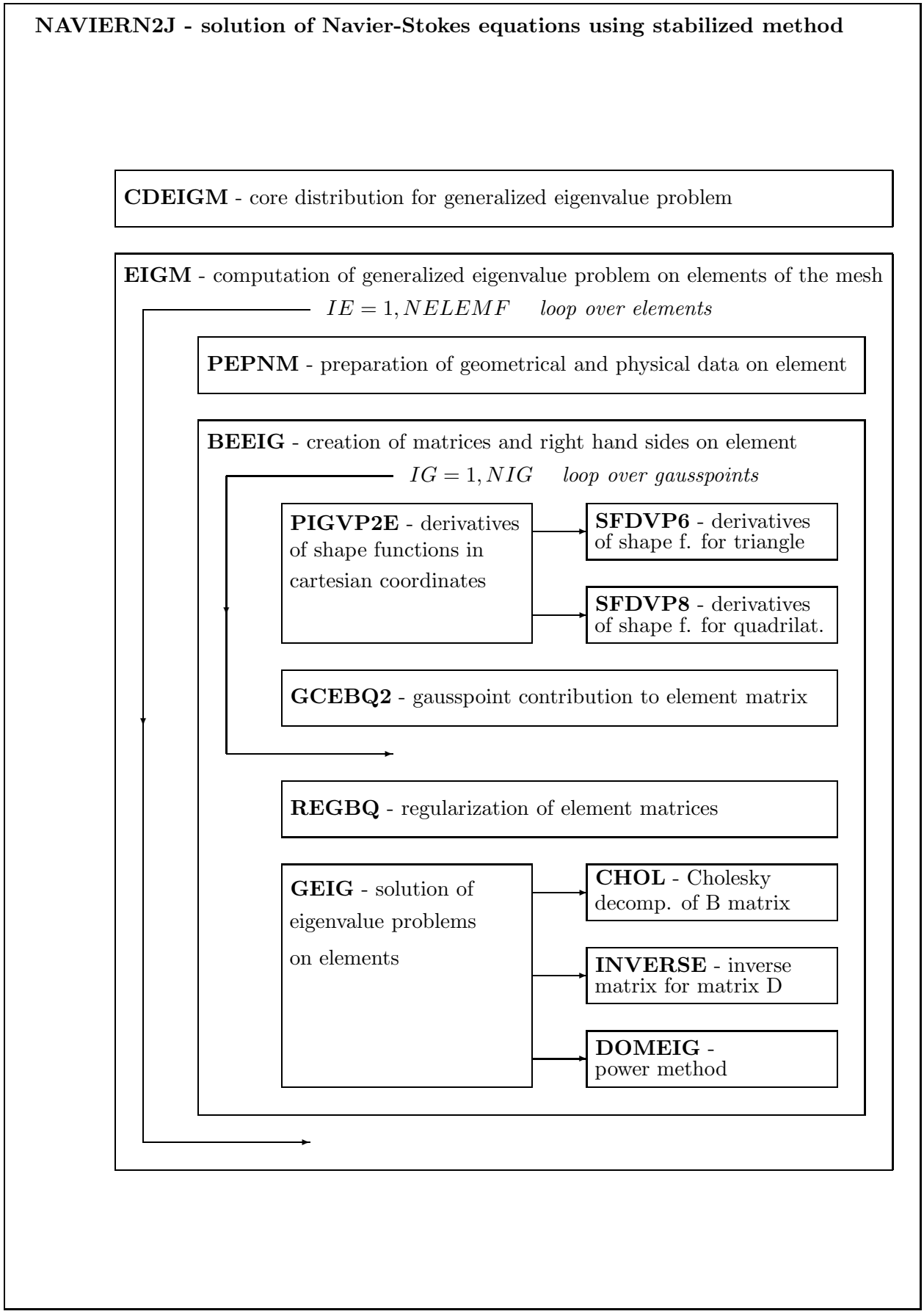
NAVIERN2J - solution of Navier-Stokes equations using stabilized method
CDEIGM - core distribution for generalized eigenvalue problem
EIGM - computation of generalized eigenvalue problem on elements of the mesh
$IE = 1, NELEMF$ loop over elements
PEPNM - preparation of geometrical and physical data on element
BEEIG - creation of matrices and right hand sides on element
$IG = 1, NIG$ loop over gausspoints
PIGVP2E - derivatives of shape functions in cartesian coordinates
SFDVP6 - derivatives of shape f. for triangle
SFDVP8 - derivatives of shape f. for quadrilat.
GCEBQ2 - gausspoint contribution to element matrix
REGBQ - regularization of element matrices
GEIG - solution of eigenvalue problems on elements
CHOL - Cholesky decomp. of B matrix
INVERSE - inverse matrix for matrix D
DOMEIG - power method

NAVIERN2J - solution of Navier-Stokes equations using stabilized method

$ITIME = 1, NTIME$ *loop over time-steps*

$ITER = 1, MITER$ *loop over iterations of the Newton method*

CDMRNJ - core distribution for element matrices and right hand sides

MRHSNJ - creation of matrices and right hand sides for Navier-Stokes eq.

$IE = 1, NELEMF$ *loop over elements*

PEPNM - preparation of geometrical and physical data on element

BESTABN2 - creation of matrices and right hand sides on element

$IG = 1, NIG$ *loop over gausspoints*

PIGSTABN2 - derivat. of shape functions in cartesian coordinates

SFDVP6 - derivatives of shape f. for triangle

SFDVP8 - derivatives of shape f. for quadrilat.

GCSTABMN2 - gausspoint contrib. to element matrix

GCSTABRN2 - gausspoint contrib. to right hand side

FRODSU - direct step of unsymmetric frontal solver

FRSCOR - resolution and backsubstitution of unsymmetric frontal solver

if prescribed accuracy is reached, end of iterations of the Newton method

IF (RESNORM < EPS) GOTO 100

now MITER iterations were computed, method does not converge, STOP

100 CONTINUE

convergence of the Newton method

6 Numerical experiments

The method introduced in Chapter 5 was tested on several problems for verification and to review its behaviour. The results are presented in this chapter. They are accompanied by author's comments and observations, which are supposed to be worth reporting. Results obtained by the algorithm of Chapter 5 are marked as GLS algorithm results.

6.1 Steady solution of lid driven cavity

Popular benchmark problem for testing numerical schemes is the 'lid driven cavity'. Computational domain is of square shape with unit lenght of side. Dirichlet boundary conditions are prescribed on the boundary: value of horizontal velocity is prescribed on the upper side, zero boundary conditions on the rest of the boundary representing a wall.

Many solutions of this problem were presented by various authors. Here are some representatives: in [19], there are presented solutions for Reynolds numbers 1,000, 3,200, and 5,000 obtained on nonuniform grid of approximately 8,800 elements; in [16], there is presented result for Reynolds number 7,500 on quasi-uniform mesh of 96×96 elements; solutions for Reynolds number 10,000 obtained by several methods on the mesh of 64×64 elements are published in [28], and in [13], outstanding results for Reynolds number 500,000 on the mesh of 30×30 elements are presented.

Solution by the developed algorithm was performed on three uniform meshes – of 32×32 (1,024) elements, of 64×64 (4,096) elements, and of 128×128 (16,384) elements.

Reynolds number 10,000 was chosen to compare obtained results to those in [28] (Figure 6.1).

To observe the effect of stabilization, solution obtained by the Newton method without stabilization is presented in Figure 6.2. Solutions computed on all three meshes by the GLS algorithm are presented in Figures 6.2-6.3 to review the sensitivity to the fineness of the computational mesh.

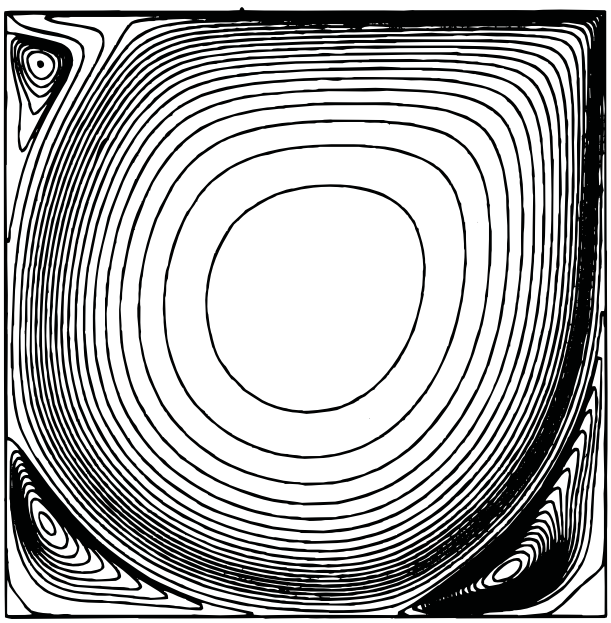

Figure 6.1: Streamlines by S. Turek [28] on the mesh 64×64 by streamline-diffusion approximation, Re = 10,000

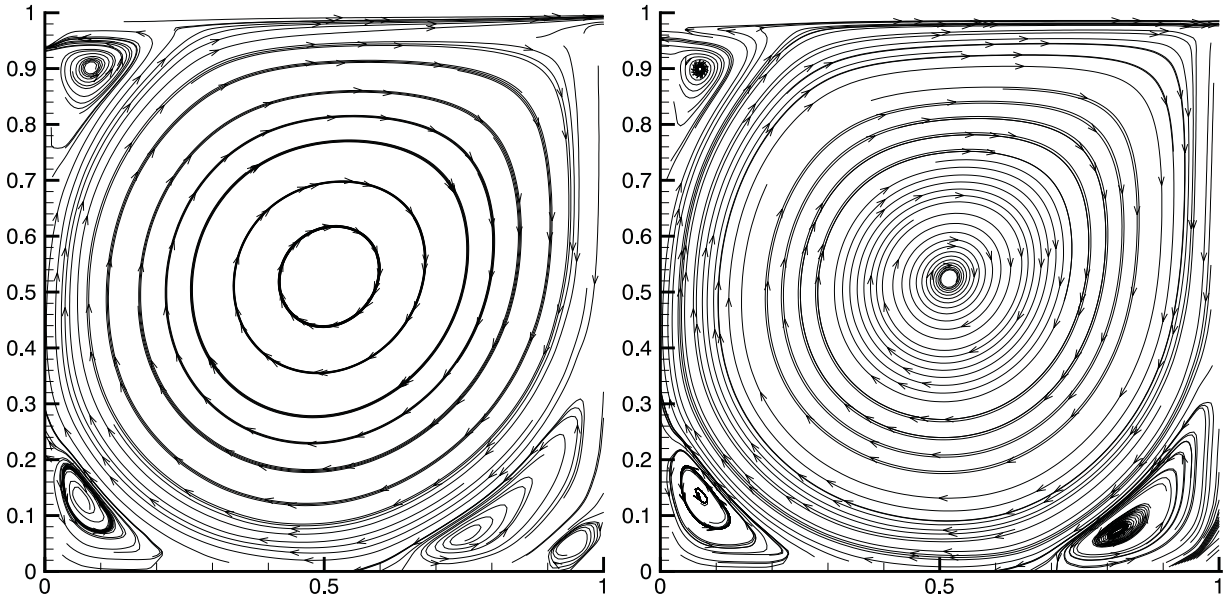

Figure 6.2: Streamlines on the mesh 32×32 by the Newton method without stabilization (left) and streamlines on the mesh 32×32 by the GLS algorithm (right), Re = 10,000

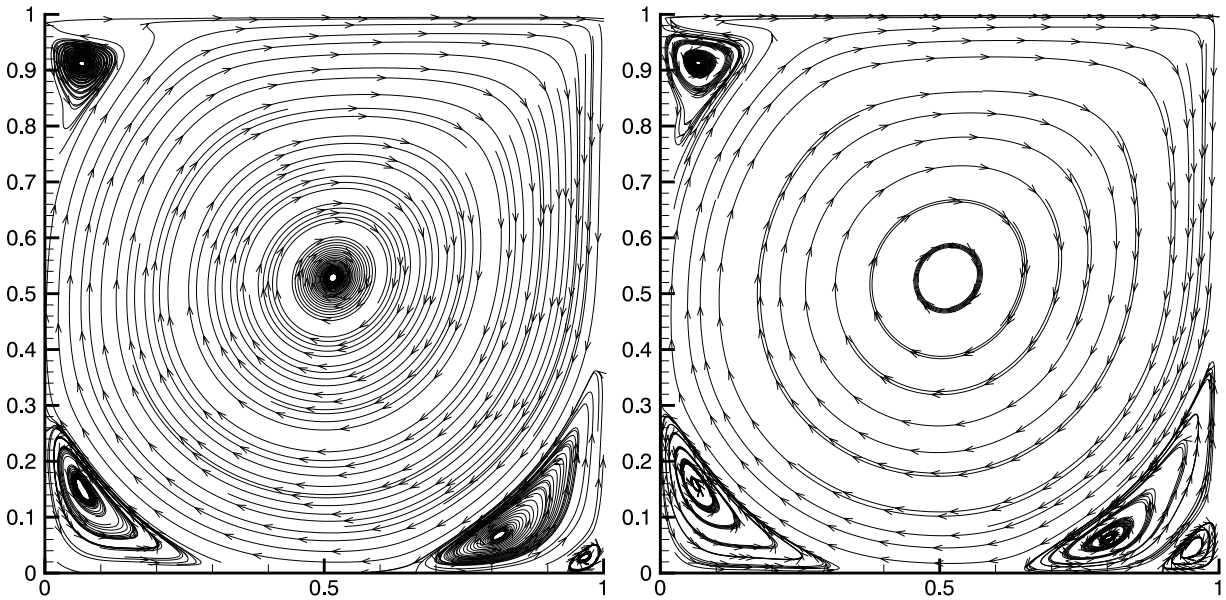

Figure 6.3: Streamlines on the mesh 64×64 (left) and on the mesh 128×128 (right) by the GLS algorithm, Re = 10,000

We can observe, that streamlines are not encircled for the GLS method. It corresponds to the perturbation of incompressibility in the continuity equation described in Chapter 5.7. This defect is decreasing with refining of the mesh.

To extend results to higher Reynolds numbers, solutions for Re = 20,000 on the mesh 32×32 and for Re = 50,000 on the mesh 64×64 are presented in Figure 6.4, and for Re = 100,000 and Re = 120,000 on the mesh 128×128 are presented in Figure 6.5.

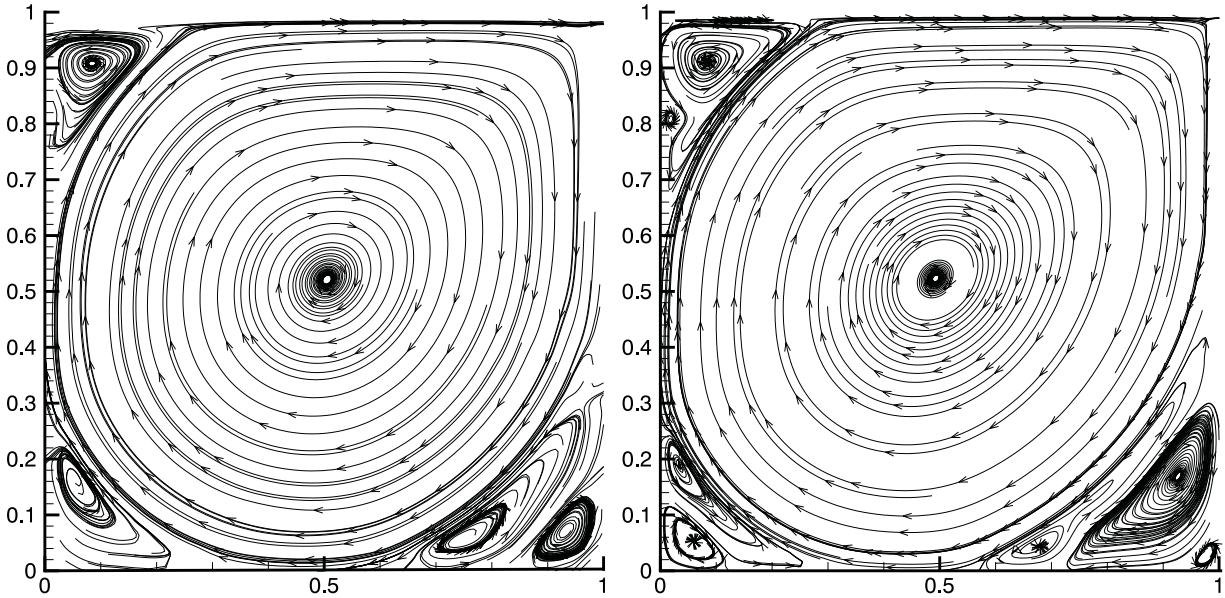

Figure 6.4: Streamlines for Re = 20,000 on the mesh 32×32 (left) and for Re = 50,000 on the mesh 64×64 (right) by the GLS algorithm

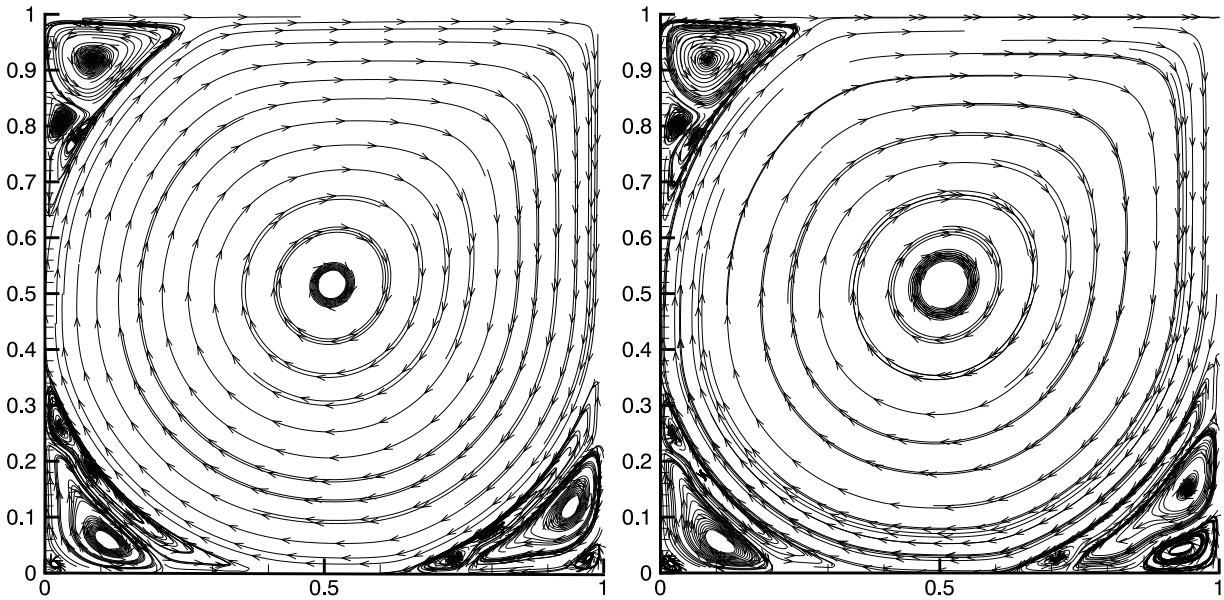

Figure 6.5: Streamlines for Re = 100,000 (left) and for Re = 120,000 (right) on the mesh 128×128 by the GLS algorithm

The effect of decreasing of the incompressibility perturbation with increasing velocity through $\tau(\mathrm{Re})$ (Chapter 5.7) is not apparent in Figure 6.5 in comparison to Figure 6.3.

To comlete the report on investigating of this problem, plots of pressure are presented in Figures 6.6-6.7.

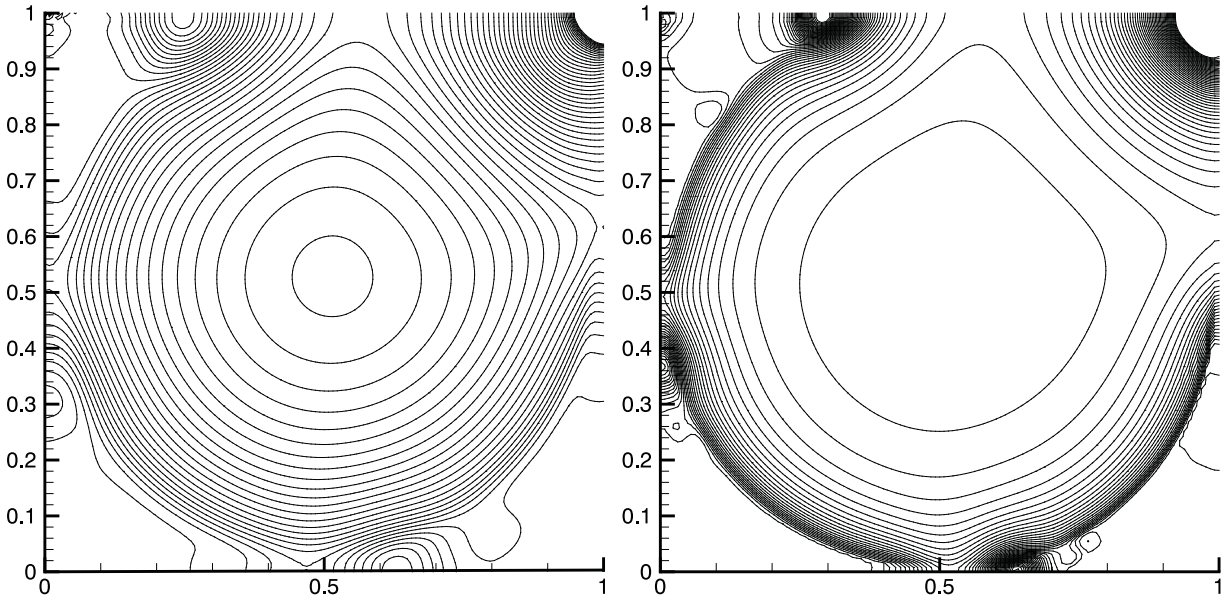

Figure 6.6: Pressure contours for Re = 10,000 (left) and for Re = 100,000 (right) on the mesh 128×128 by the GLS algorithm

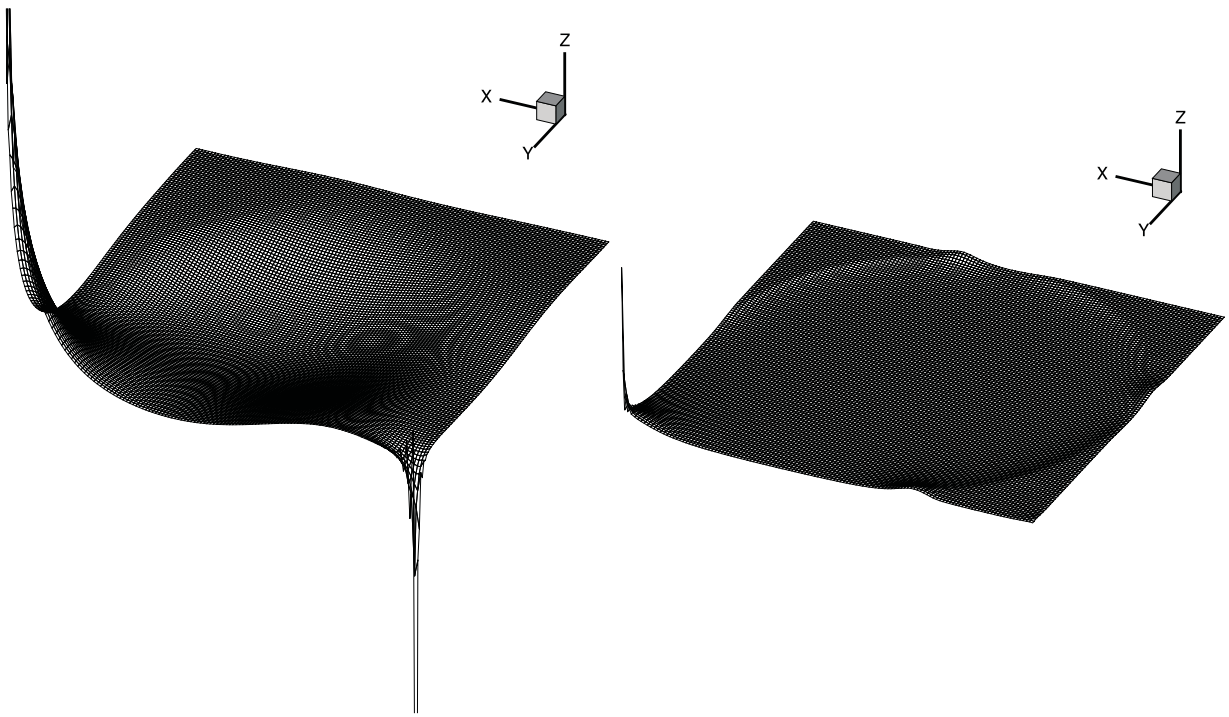

Figure 6.7: Pressure elevation for Re = 500 (left) and for Re = 100,000 (right) on the mesh 128×128 by the GLS algorithm

Althought the continuation method was applied to achieve higher Reynolds numbers, we detected limits of convergence of the Newton method for all three meshes. We observed, that on the mesh 32×32, we were not able to get results over Re ≈ 28,000, on the mesh 64×64 over Re ≈ 50,000, and on the mesh 128×128 over Re ≈ 120,000. For comparison, such limit was around Re ≈ 12,500 on the mesh 32×32 for the method without stabilization ($\tau = 0$).

Another striking effect was observed during the computations. Since it is known, that stabilized methods are, in general, sensitive to stabilization parameters, we tried to modify the computed parameter τ by a quotient 0.7 to 1.5. This improved the convergence, and we were able to reach higher Reynolds numbers, e.g. Re = 70,000 on the mesh 64×64 elements.

Finer mesh is able to catch more vortices and provides better resolution, moreover presented experiments showed another important conclusion – suitable refinement of the mesh significantly improves stability of solution, i.e. convergence.

6.2 Unsteady solution of lid driven cavity

The problem of lid driven cavity described in Chapter 6.1 was solved also as an unstedy problem. The initial condition considered was $\mathbf{u} = \mathbf{0}$ in Ω at time $t = 0$ for all computations. Therefore, we can observe developement of the flow in the cavity.

Solution was performed on three uniform meshes – of 32×32 (1,024) elements, of 64×64 (4,096) elements, and of 128×128 (16,384) elements.

Reynolds number 50,000 and time layers $t = 3.5s$ and $t = 10s$ were chosen to compare obtained results on different meshes to investigate the sensitivity to mesh fineness – Figures 6.8-6.10.

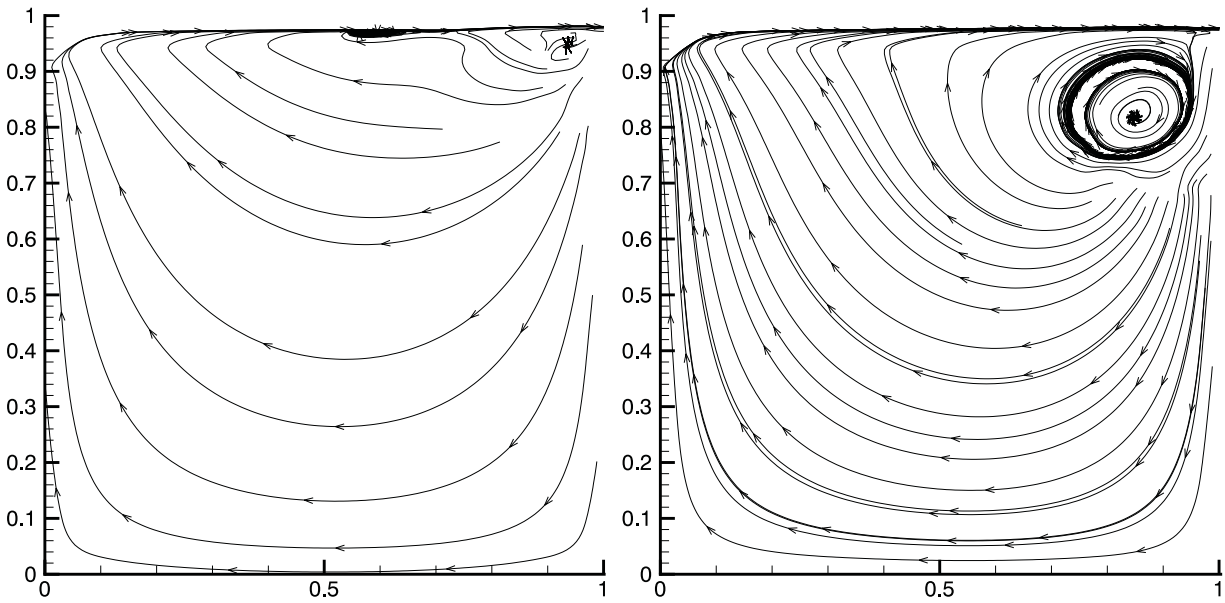

Figure 6.8: Streamlines at time $t = 3.5s$ (left) and $t = 10s$ (right) by the GLS algorithm, mesh 32×32, Re = 50,000

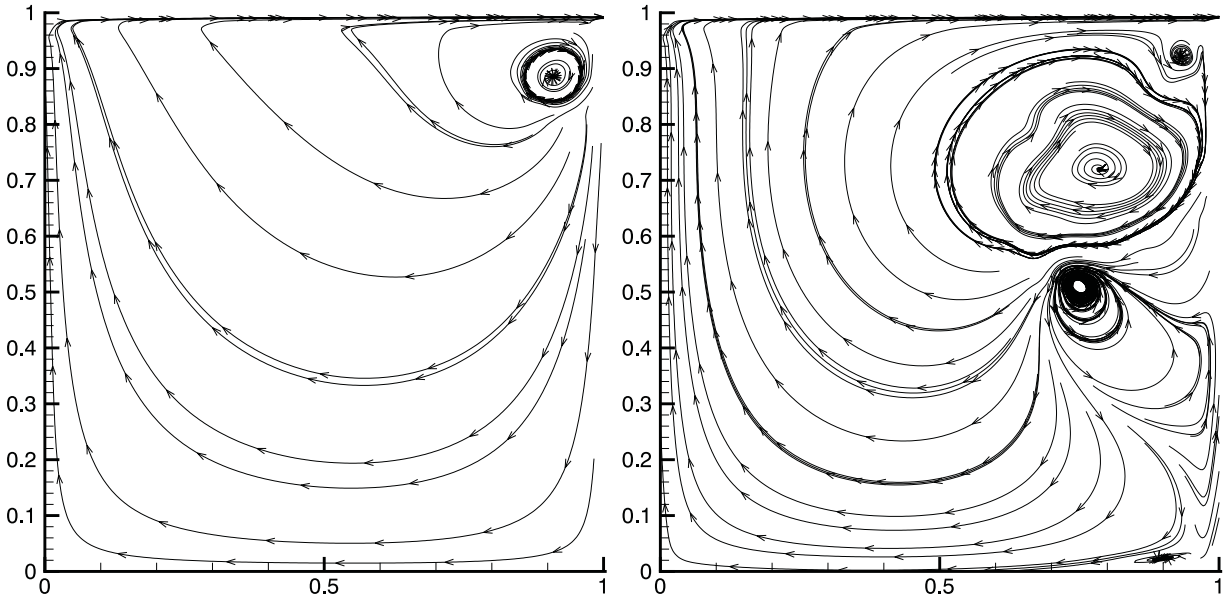

Figure 6.9: Streamlines at time $t = 3.5s$ (left) and $t = 10s$ (right) by the GLS algorithm, mesh 64×64, Re = 50,000

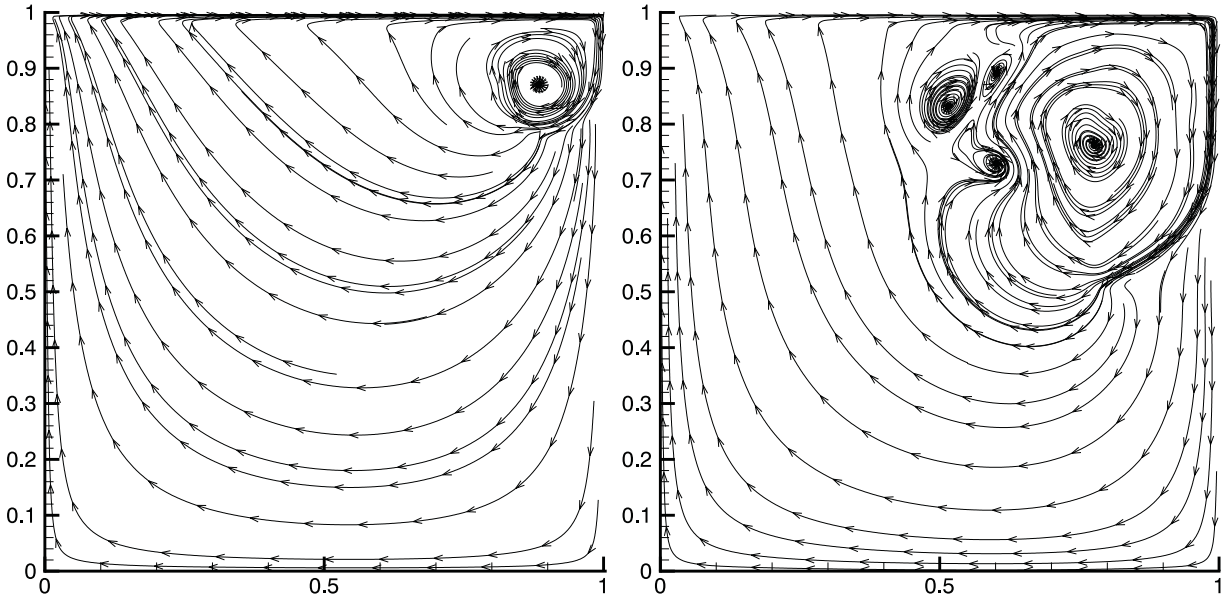

Figure 6.10: Streamlines at time $t = 3.5s$ (left) and $t = 10s$ (right) by the GLS algorithm, mesh 128×128, Re = 50,000

We can observe in Figures 6.8-6.10, that the development of the flow (position of the main vortex) as well as resolution of the solution (shape of the vortex) strongly depends on fineness of the mesh from the start of the solution, cf. solutions at $t = 3.5s$. Moreover, the fineness of the mesh causes serious differences in the solution at later time (cf. solutions at $t = 10s$).

In Figure 6.11, streamlines computed on the mesh 64×64 elements at time $t = 8s$ for Reynolds numbers 400 and 50,000 are presented, and we can observe the effect of Reynolds number on the development of the flow.

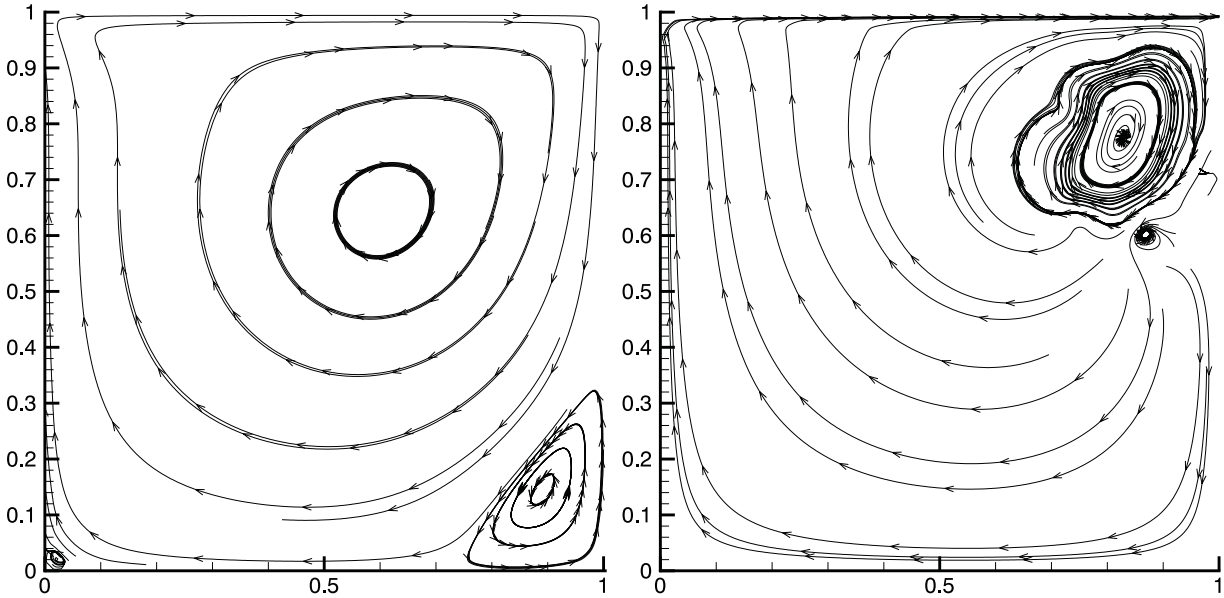

Figure 6.11: Streamlines for Re = 400 (left) and Re = 50,000 (right) by the GLS algorithm, mesh 64×64, $t = 8s$

Reynolds number has significant influence on the speed of development of the flow. In Figure 6.11, one can observe, that the solution for Re = 400 at $t = 8s$ nearly reached the steady state, while the solution for Re = 50,000 is at $t = 8s$ almost in the beginning of the developement. Keep on mind, that the development of the flow for this 'cavity problem' is arranged by the shear stress in the fluid. Since this is linear function of viscosity for Newtonian fluid, the development has to be slower for higher Reynolds numbers.

6.3 Unsteady solution of flow past NACA 0012 airfoil

Unsteady flow past NACA 0012 airfoil was investigated as a more practical application. Results of this problem for angle of incidence of 34 $^\circ$ and Reynolds number 1,000 obtained by the unconditionaly stable projection FEM were presented by Guermond and Quartapelle in [19]. In Figures 6.14-6.18, these results are compared to ours obtained by the GLS algorithm. The computational mesh is shown in Figures 6.12-6.13. It contains 6,220 elements, 18,478 nodes, and 43,085 degrees of freedom.

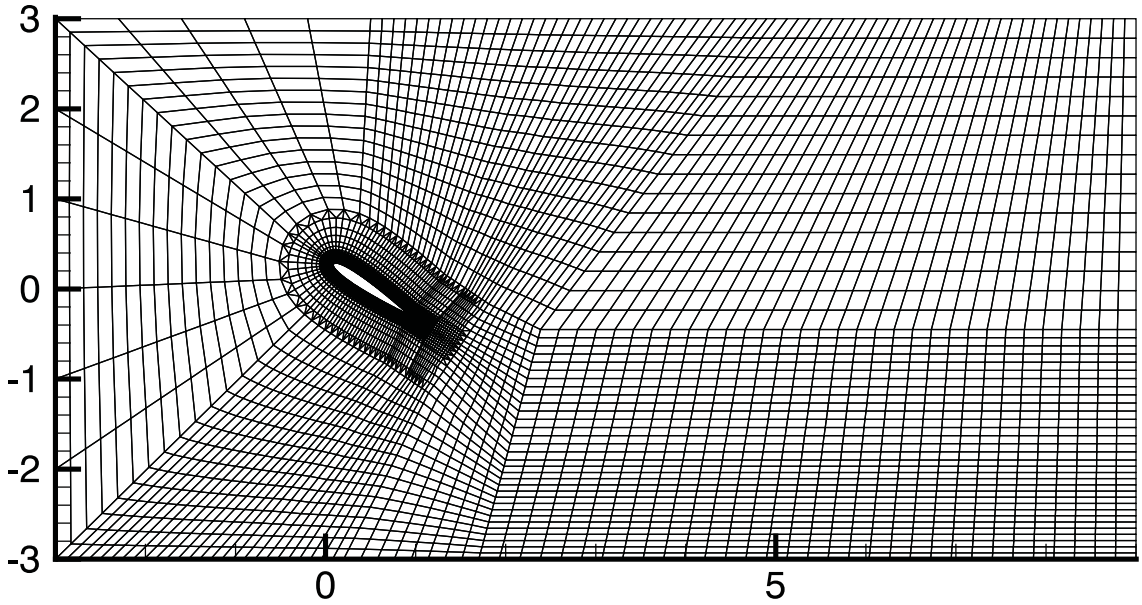

Figure 6.12: Computational mesh for NACA 0012 problem, angle of incidence of 34 °

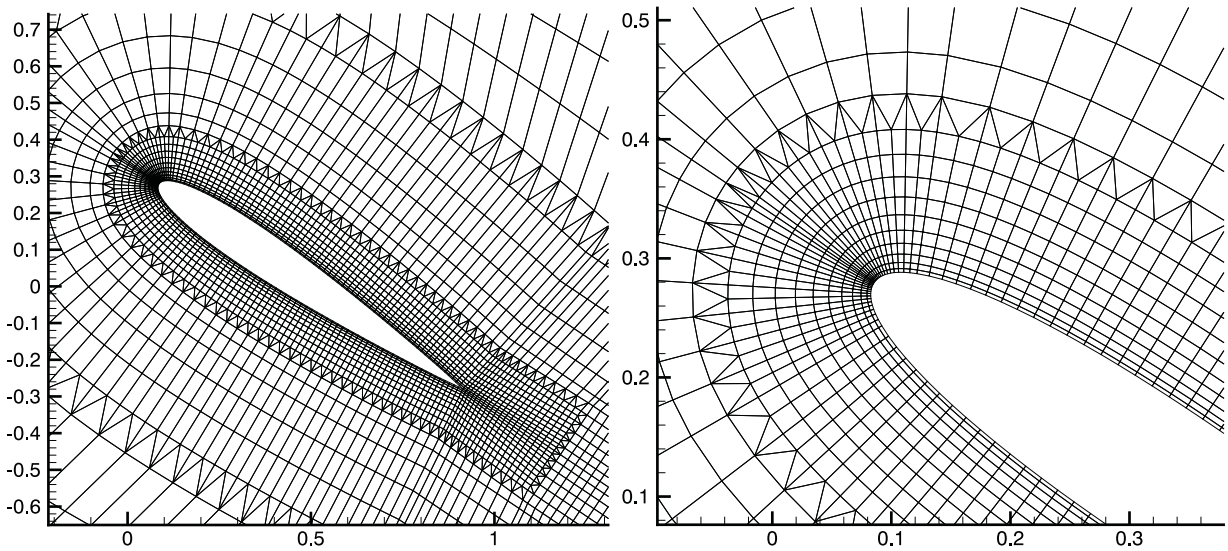

Figure 6.13: Computational mesh for NACA 0012 problem - details

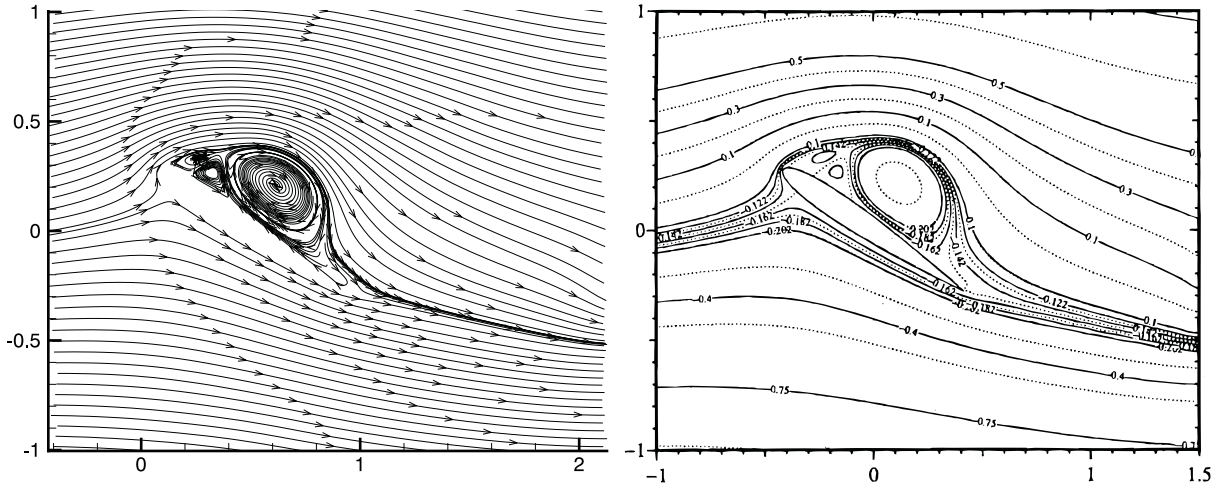

Figure 6.14: Streamlines by the GLS algorithm (left) and by [19] (right), $t = 1.6s$, Re = 1,000

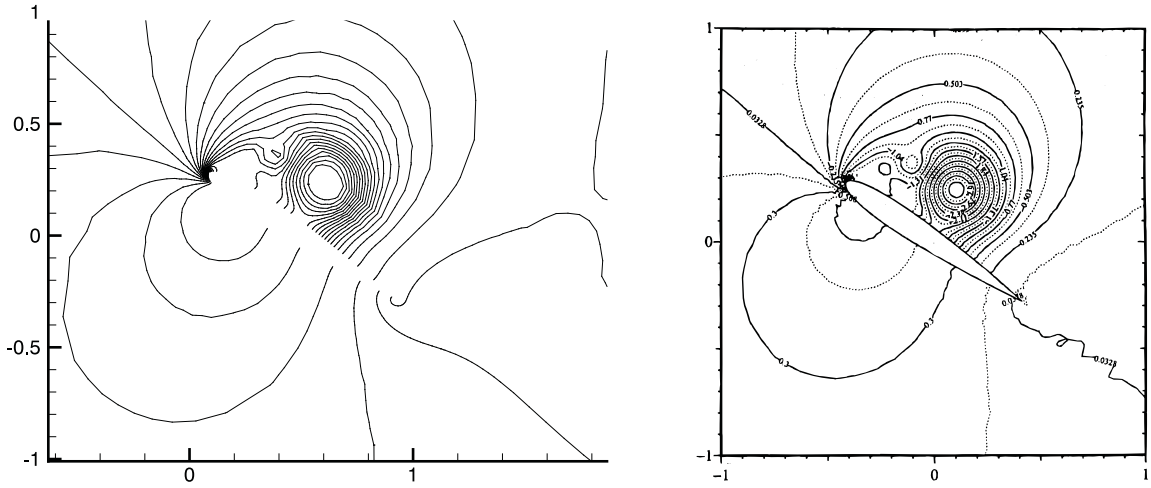

Figure 6.15: Pressure contours by the GLS algorithm (left) and by [19] (right), $t = 1.6s$, Re = 1,000

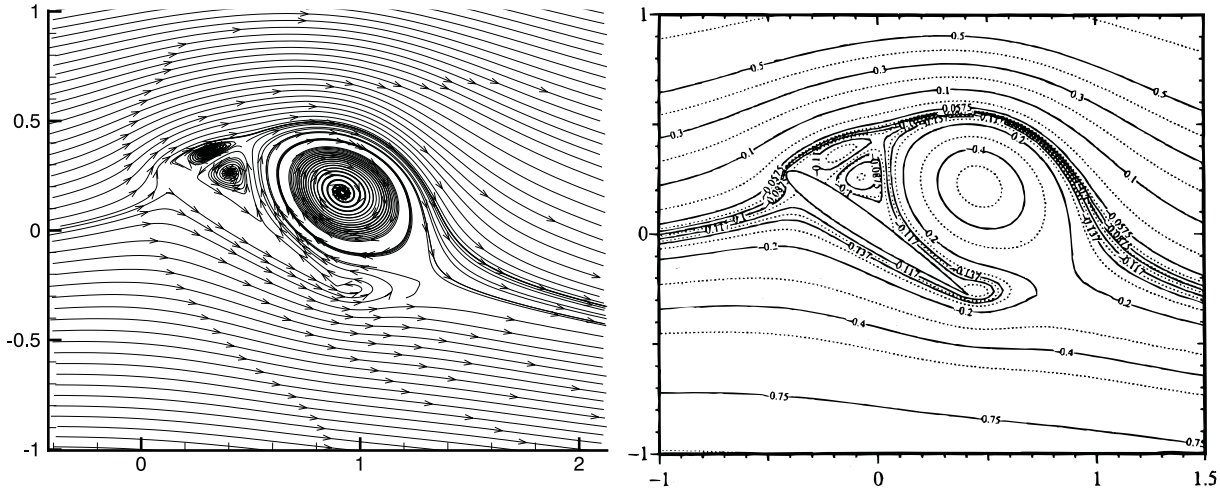

Figure 6.16: Streamlines by the GLS algorithm (left) and by [19] (right), $t = 2.6s$, Re = 1,000

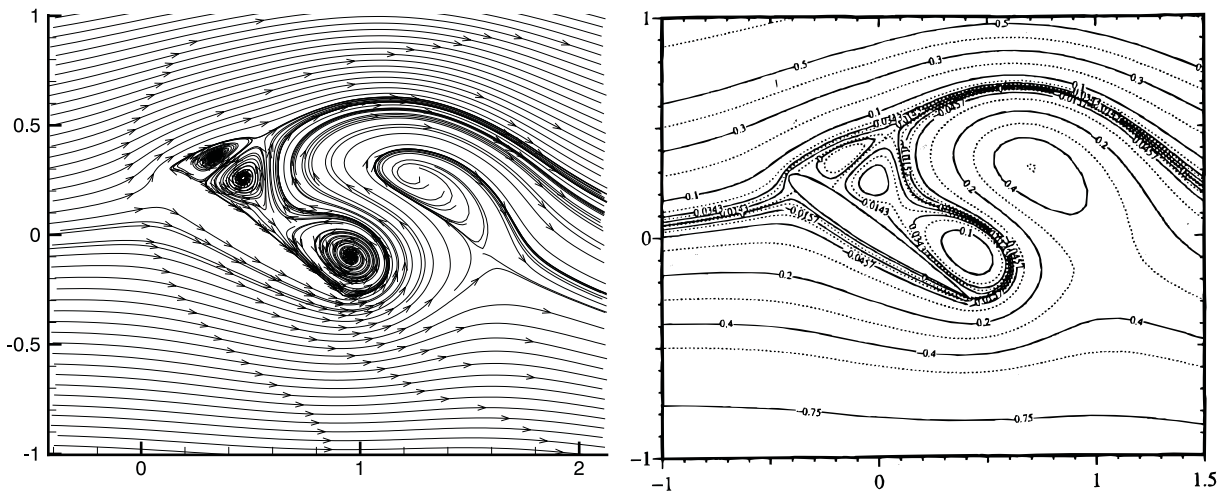

Figure 6.17: Streamlines by the GLS algorithm (left) and by [19] (right), $t = 3.6s$, Re = 1,000

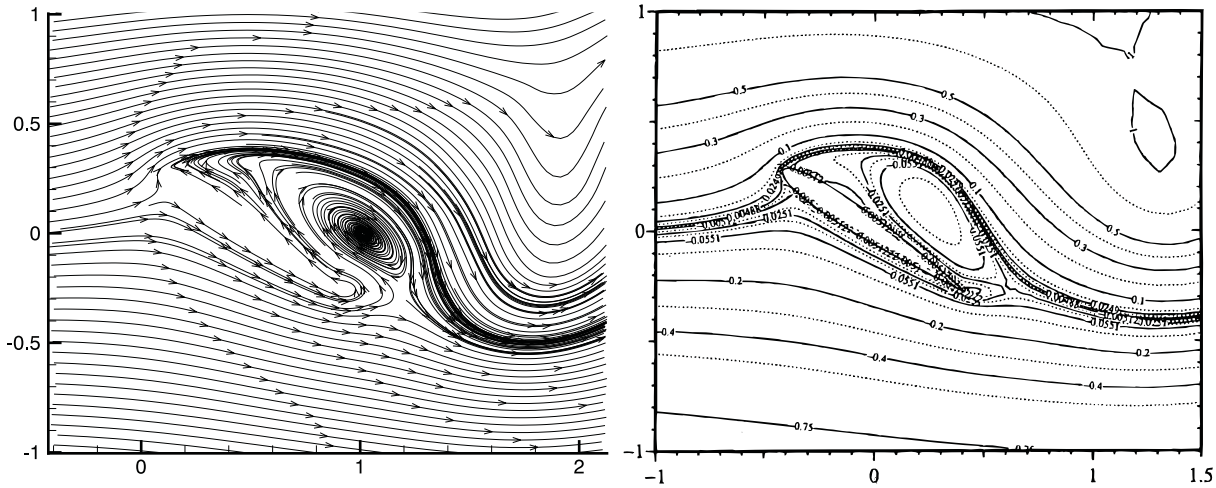

Figure 6.18: Streamlines by the GLS algorithm (left) and by [19] (right), $t = 6.0s$, Re = 1,000

Streamlines and pressure contours for the problem with Reynolds number 100,000 are presented in Figures 6.19-6.22 at the same time layers as for Re = 1,000.

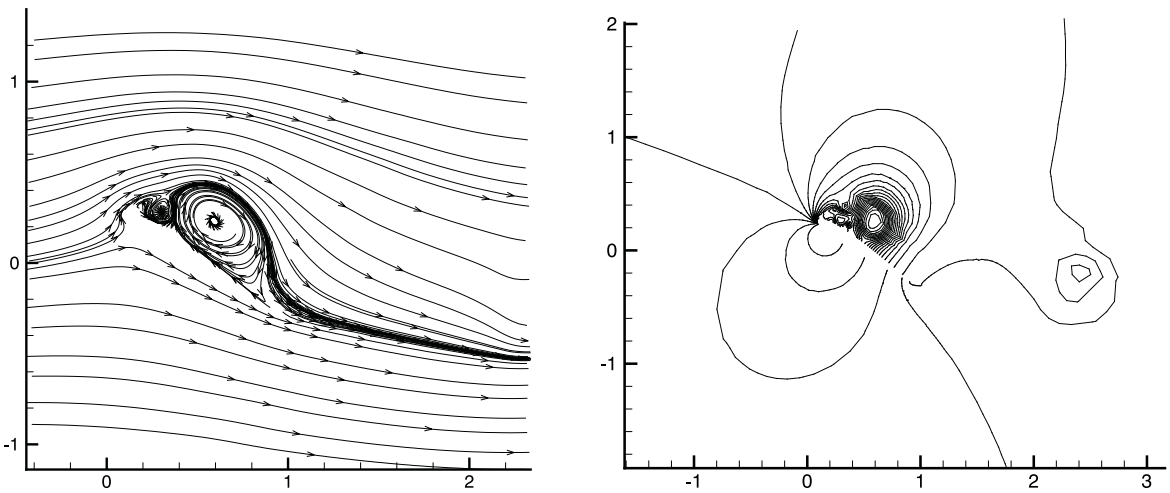

Figure 6.19: Streamlines (left) and pressure contours (right) by the GLS algorithm, $t = 1.6s$, Re = 100,000

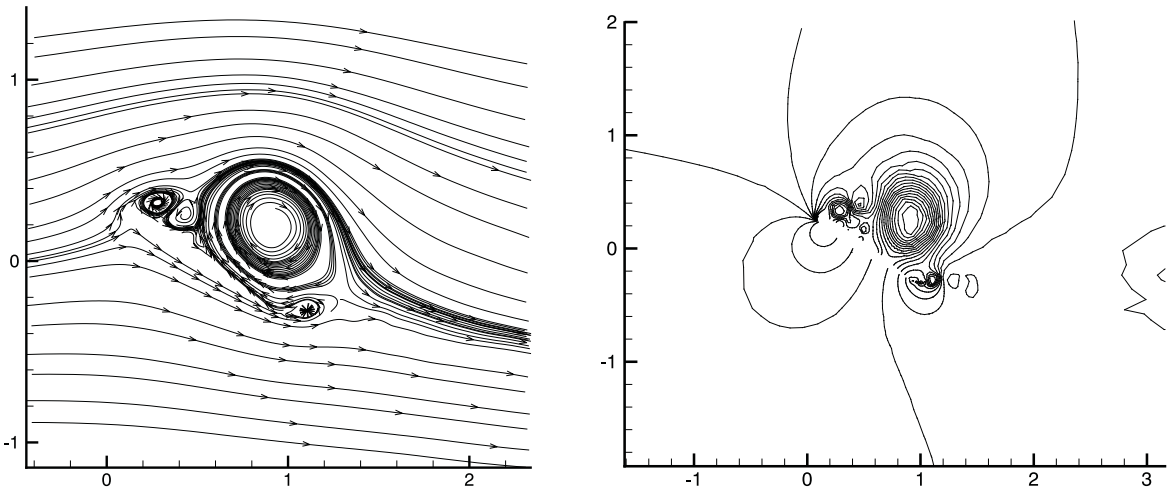

Figure 6.20: Streamlines (left) and pressure contours (right) by the GLS algorithm, $t = 2.6s$, Re = 100,000

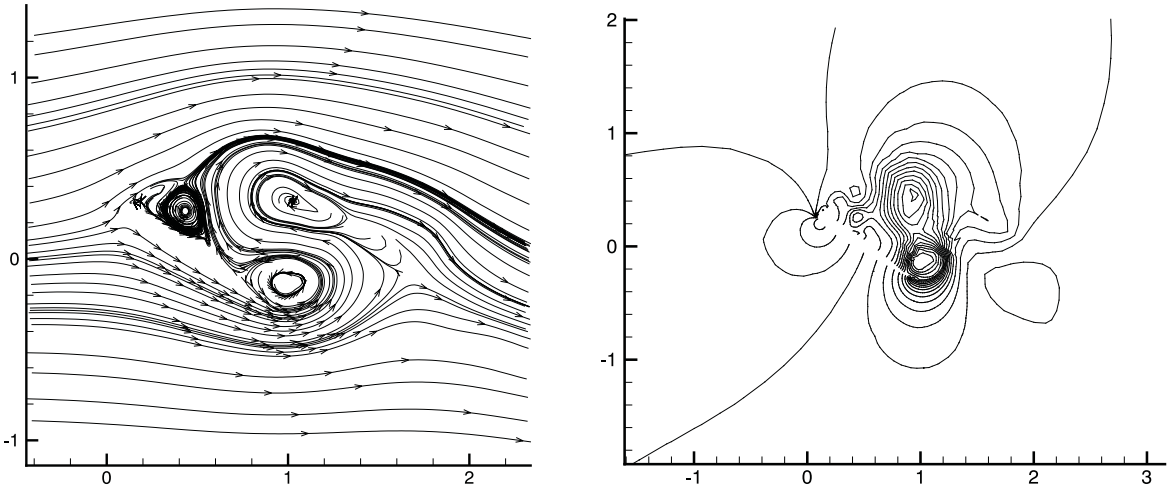

Figure 6.21: Streamlines (left) and pressure contours (right) by the GLS algorithm, $t = 3.6s$, Re = 100,000

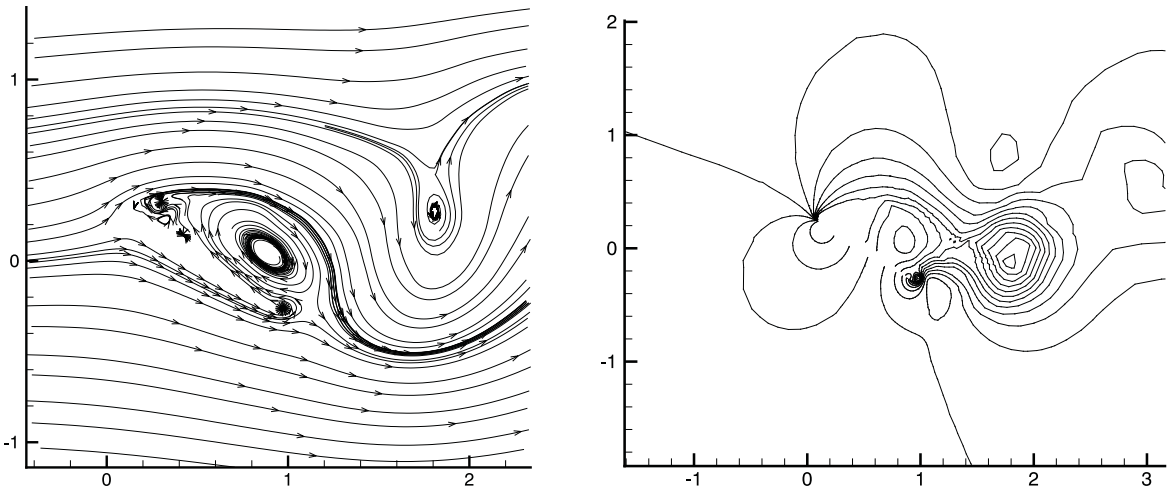

Figure 6.22: Streamlines (left) and pressure contours (right) by the GLS algorithm, $t = 6.0s$, Re = 100,000

7 On the application of a priori error estimates for Navier-Stokes equations

The goal of this chapter is to summarize author's experience with the application of a priori error estimates of the finite element method in computational fluid dynamics. This approach is applied to generation of the computational mesh in the purpose of uniform distribution of error on elements and is used in precise solution on domains with corner-like singularities. Incompressible viscous flow modelled by the steady Navier-Stokes equations (2.24)-(2.26) is considered.

Usual way to improve accuracy of solution by the FEM is the refinement of the mesh near places, where singularity can appear. Another way is the adaptive refinement based on a posteriori error estimates or error estimators. This method could be quite time demanding, since it needs several runs of solution. Completely different method is applied in this chapter. Computational mesh is prepared before the first run of the solution.

Numerical results are presented for flows in a channel with sharp obstacle and in a channel with sharp extension.

7.1 Algorithm for generation of computational mesh

In the derivation of the algorithm, two main 'tools' are used. The first is a priori estimate of the finite element error for the Navier-Stokes equations (2.24)-(2.26) (cf. [17])

$$\|\nabla(\mathbf{u}-\mathbf{u_h})\|_{L_2(\Omega)} \leq C\Big[\Big(\sum_K h_K^{2k} \mid \mathbf{u} \mid^2_{H^{k+1}(T_K)}\Big)^{1/2} + \Big(\sum_K h_K^{2k} \mid p \mid^2_{H^k(T_K)}\Big)^{1/2}\Big] \tag{7.1}$$

$$\|p-p_h\|_{L_2(\Omega)} \leq C\Big[\Big(\sum_K h_K^{2k} \mid \mathbf{u} \mid^2_{H^{k+1}(T_K)}\Big)^{1/2} + \Big(\sum_K h_K^{2k} \mid p \mid^2_{H^k(T_K)}\Big)^{1/2}\Big] \tag{7.2}$$

where h_K is the diameter of triangle T_K of a triangulation $\mathcal{T}$, and $k = 2$ for Hood-Taylor elements, which are applied in presented numerical experiments.

The second tool is the asymptotic behaviour of the solution near the singularity. In [2], it was proved for the Stokes flow in axisymmetric tubes, that for internal angle $\alpha = \frac{3}{2}\pi$, the leading term of expansion of the solution for each velocity component is

$$u_i(\rho,\vartheta) = \rho^{0.5445}\varphi_i(\vartheta) + \ldots,\ i = 1,2 \tag{7.3}$$

where ρ is the distance from the corner, ϑ the angle and φ_i is a smooth function. The same expansion is known to apply to the plane flow (cf. [23]), and similar results were also proved for the Navier-Stokes equations. Differentiating by ρ, we observe $\frac{\partial u_i(\rho,\vartheta)}{\partial\rho} \to \infty$ for $\rho \to 0$.

Taking into account the expansion (7.3), we can estimate

$$\mid \mathbf{u} \mid^2_{H^{k+1}(T_K)} \approx C \int\limits_{r_K-h_K}^{r_K} \rho^{2(\gamma-k-1)}\ \rho\ d\rho = C\ \Big[-r_K^{2(\gamma-k)} + (r_K-h_K)^{2(\gamma-k)}\Big] \tag{7.4}$$

where r_K is the distance of element T_K from the corner, cf. Figure 7.1.

Putting estimate (7.4) into the a priori error estimate (7.1) or (7.2), we derive that we should guarantee

$$h_K^{2k}\Big[-r_K^{2(\gamma-k)} + (r_K-h_K)^{2(\gamma-k)}\Big] \approx h_{ref}^{2k} \tag{7.5}$$

in order to get the error estimate of order $O(h_{ref}^k)$ uniformly distributed on elements. From this expression, we compute element diameters using the Newton method in accordance to chosen h_{ref}. Similar idea was presented by C. Johnson for an elliptic problem in [22].

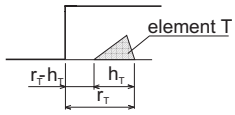

Figure 7.1: Description of element variables

7.2 Geometry and design of the mesh

The algorithm was applied to two different computational domains in 2D. The first is the channel with sudden intake of diameter (Figure 7.2), the second is the channel with abruptly extended diameter (Figure 7.3). Since these are symmetric, the problem was solved only on the upper half of the channels.

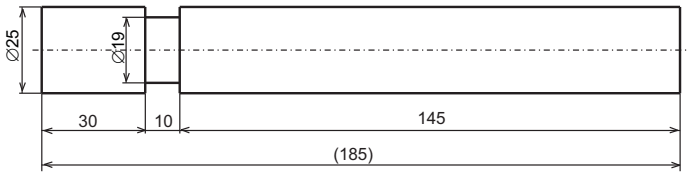

Figure 7.2: The first geometry

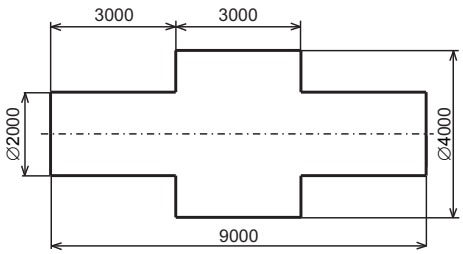

Figure 7.3: The second geometry

In the first case of geometry, diameters of elements were computed for values $h_{ref} = 0.1732$ mm, $k = 2$, $\gamma = 0.5444837$. We started in the distance $r_1 = 0.25$ mm from the corner. This corresponds to cca 3% of relative error on elements. Fourteen diameters of elements were obtained (Table 7.1).

For the second channel, we used $h_{ref} = 0.1732$ m, $k = 2$, $\gamma = 0.5444837$ and started in the distance $r_1 = 300$ mm from the corner. Fifteen diameters of elements were obtained (Table 7.1).

Note, that those are '1D' data. An experiment with three meshes with different refined details (Figure 7.4) was performed (cf. [8],[24] for details). Type C of refinement in Figure 7.4 provided the best uniformity of the error on elements, therefore was chosen for further applications. This type of refinement corresponds to the polar coordinate system used in the derivation of the algorithm, and is applied in the two experiments described in this chapter.

The refined detail is connected to the rest of the coarse mesh. In Figures 7.5-7.6, final meshes after the refinement are shown for both geometries.

i	r_i (mm)	h_i (mm)
1	0.25000	0.06004
2	0.18996	0.04808
3	0.14189	0.03795
4	0.10394	0.02947
5	0.07447	0.02245
6	0.05202	0.01674
7	0.03527	0.01217
8	0.02311	0.00858
9	0.01453	0.00584
10	0.00869	0.00380
11	0.00489	0.00234
12	0.00255	0.00134
13	0.00121	0.00070
14	0.00050	0.00050

i	r_i (m)	h_i (m)
1	0.30000	0.06956
2	0.23044	0.05621
3	0.17423	0.04483
4	0.12940	0.03522
5	0.09419	0.02720
6	0.06699	0.02059
7	0.04640	0.01524
8	0.03116	0.01098
9	0.02017	0.00767
10	0.01250	0.00515
11	0.00735	0.00330
12	0.00405	0.00199
13	0.00206	0.00112
14	0.00094	0.00057
15	0.00038	0.00038

Table 7.1: Resulting refinement for the first (left) and the second (right) cases of geometry

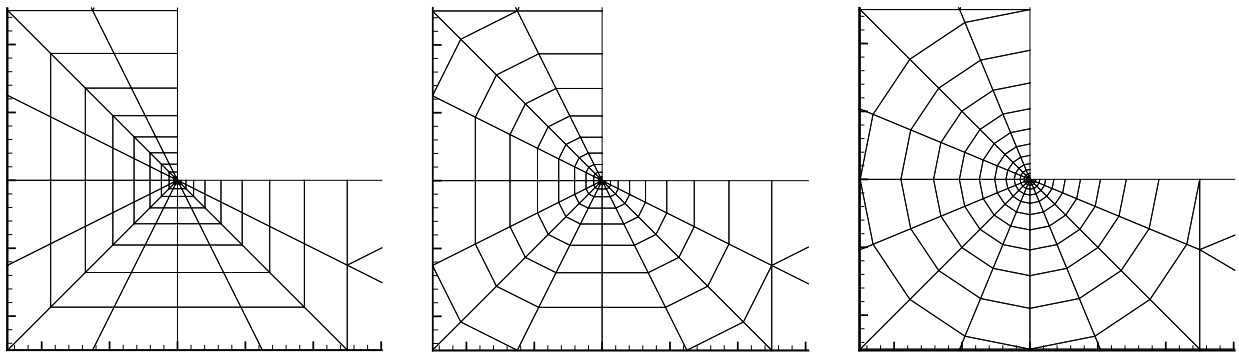

Figure 7.4: Details of refined mesh - type A (left), type B (middle), type C (right)

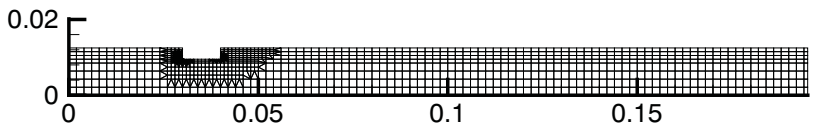

Figure 7.5: Final computational mesh for the first channel

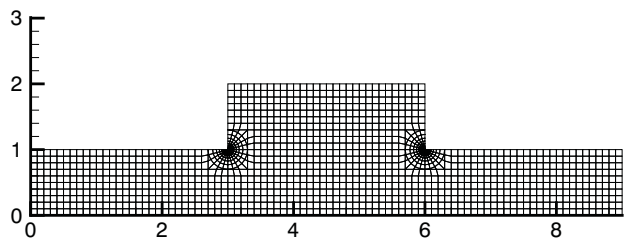

Figure 7.6: Final computational mesh for the second channel

7.3 Measuring of error

To review the efficiency of the algorithm, we use a posteriori error estimates to evaluate the obtained error on elements. Suppose now, that the exact solution of the problem is denoted as (u_1, u_2, p) and the approximate solution obtained by the FEM as (u_{1h}, u_{2h}, p_h). The exact solution differs from the approximate solution in the error $(e_{u_1}, e_{u_2}, e_p) = (u_1 - u_{1h}, u_2 - u_{2h}, p - p_h)$. For the solution (u_1, u_2, p) we denote

$$\mathcal{U}^2(u_1, u_2, p) = \|(u_1, u_2)\|^2_{H^1(T_K)} + \|p\|^2_{L_2(T_K)} =$$

$$= \int_{T_K} \left(u_1^2 + u_2^2 + \left(\frac{\partial u_1}{\partial x_1}\right)^2 + \left(\frac{\partial u_1}{\partial x_2}\right)^2 + \left(\frac{\partial u_2}{\partial x_1}\right)^2 + \left(\frac{\partial u_2}{\partial x_2}\right)^2 \right) \mathrm{d}\Omega + \int_{T_K} p^2 \mathrm{d}\Omega$$

The following estimate of error is used (see e.g. [3])

$$\mathcal{U}^2(u_1 - u_{1h}, u_2 - u_{2h}, p - p_h) \leq \mathcal{E}^2(u_{1h}, u_{2h}, p_h) \tag{7.6}$$

where

$$\begin{aligned}
\mathcal{U}^2(u_1 - u_{1h}, u_2 - u_{2h}, p - p_h) &= \|(e_{u_1}, e_{u_2})\|^2_{H^1(T_K)} + \|e_p\|_{L_2(T_K)} \\
\mathcal{E}^2(u_{1h}, u_{2h}, p_h) &= C\Big[h_K^2 \int_{T_K} \big(\Re_1^2(u_{1h}, u_{2h}, p_h) + \Re_2^2(u_{1h}, u_{2h}, p_h)\big)\, \mathrm{d}\Omega + \\
&+ \int_{T_K} \Re_3^2(u_{1h}, u_{2h}, p_h) \mathrm{d}\Omega\Big]
\end{aligned}$$

where $\Re_1$, $\Re_2$, and $\Re_3$ stand for the residuals

$$\begin{aligned}
\Re_1(u_{1h}, u_{2h}, p_h) &= f_{x_1} - \left(u_{1h}\frac{\partial u_{1h}}{\partial x_1} + u_{2h}\frac{\partial u_{1h}}{\partial x_2}\right) + \nu\left(\frac{\partial^2 u_{1h}}{\partial x_1^2} + \frac{\partial^2 u_{1h}}{\partial x_2^2}\right) - \frac{\partial p_h}{\partial x_1} \\
\Re_2(u_{1h}, u_{2h}, p_h) &= f_{x_2} - \left(u_{1h}\frac{\partial u_{2h}}{\partial x_1} + u_{2h}\frac{\partial u_{2h}}{\partial x_2}\right) + \nu\left(\frac{\partial^2 u_{2h}}{\partial x_1^2} + \frac{\partial^2 u_{2h}}{\partial x_2^2}\right) - \frac{\partial p_h}{\partial x_2} \\
\Re_3(u_{1h}, u_{2h}, p_h) &= \frac{\partial u_{1h}}{\partial x_1} + \frac{\partial u_{2h}}{\partial x_2}
\end{aligned}$$

and constant C is determined from a numerical experiment (cf. [6]).

Usual way to 'measure' the obtained error on elements is to compute the error related to the computed solution, i.e. relative error. This is given by the ratio of absolute norm of the solution error related to unit area of element T_K

$$\frac{1}{|T_K|}\, \mathcal{E}^2(u_{1h}, u_{2h}, p_h, T_K)$$

to the solution norm on the whole domain Ω related to unit area of domain Ω

$$\frac{1}{|\Omega|}\, \mathcal{U}^2(u_{1h}, u_{2h}, p_h, \Omega)$$

i.e.

$$\mathcal{R}^2(u_{1h}, u_{2h}, p_h, T_K) = \frac{|\Omega|\ \mathcal{E}^2(u_{1h}, u_{2h}, p_h, T_K)}{|T_K|\ \mathcal{U}^2(u_{1h}, u_{2h}, p_h, \Omega)} \tag{7.7}$$

But for the similarity with a priori error estimate, we use the modified absolute error defined as

$$\mathcal{A}_m^2(u_{1h}, u_{2h}, p_h, T_K, \Omega, n) = \frac{|\Omega|\mathcal{E}^2(u_{1h}, u_{2h}, p_h, T_K)}{|\overline{T_K}|\ \mathcal{U}^2(u_{1h}, u_{2h}, p_h, \Omega)} \tag{7.8}$$

where $|\overline{T_K}|$ is the mean area of elements obtained as $|\overline{T_K}| = \frac{|\Omega|}{n}$, where n denotes the number of all elements in the domain.

7.4 Numerical results

Channel with sudden intake of diameter (results for Re = 1000)

In Figures 7.7-7.8, plots of entities that characterize the flow in the channel are presented. In Figure 7.7, there are streamlines and plot of velocity component u_x. Plots of velocity component u_y and pressure are in Figure 7.8. Note, that the fluid flows from the right to the left on plots of u_x, u_y, and p, to have better view.

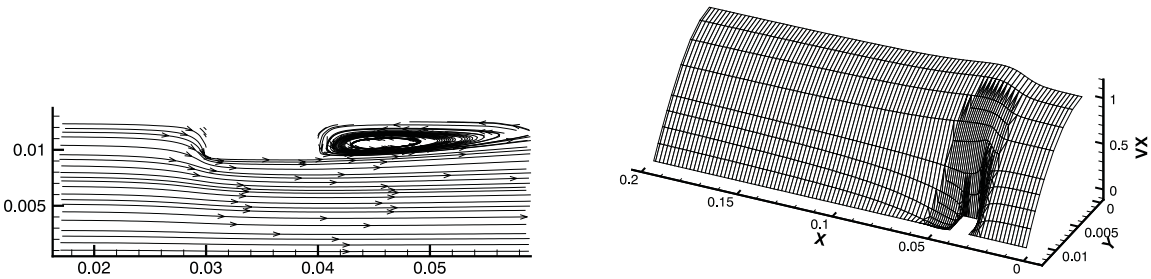

Figure 7.7: Detail of streamlines (left) and velocity component u_x (right)

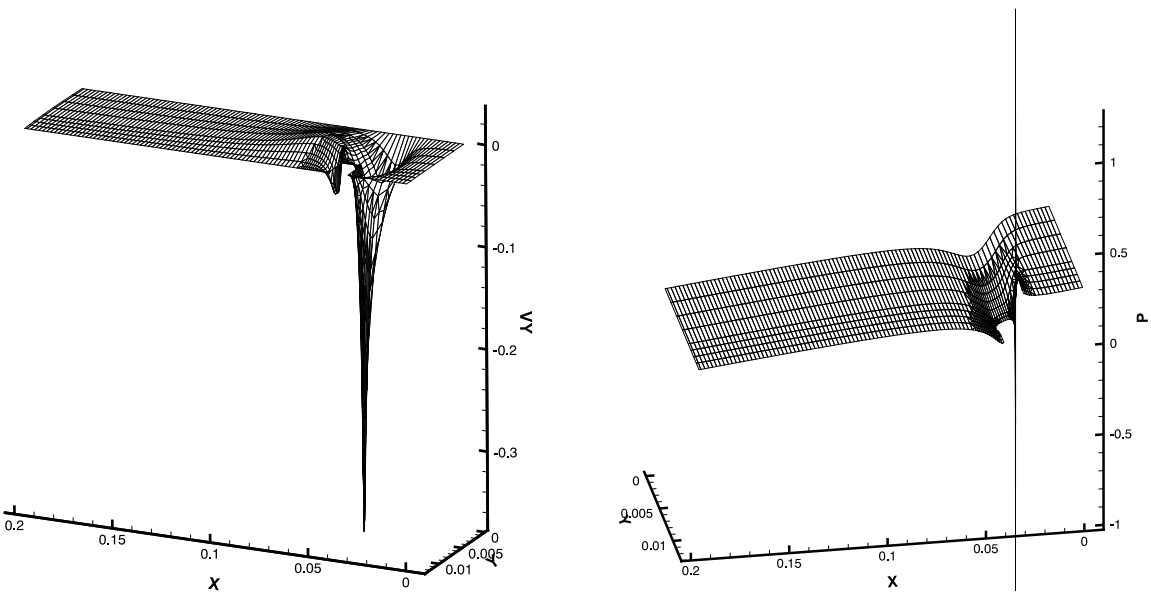

Figure 7.8: Velocity component u_y (left) and pressure (right)

In Figure 7.10, there are values of obtained error on elements in refined area. All values are listed in Table 7.2. Marking of elements in the table is described in Figure 7.9, together with plot of contours of velocity u_y close to the corner.

Figure 7.9: Contours of u_y (left) and marking of elements for Tables 7.2 and 7.3 (right)

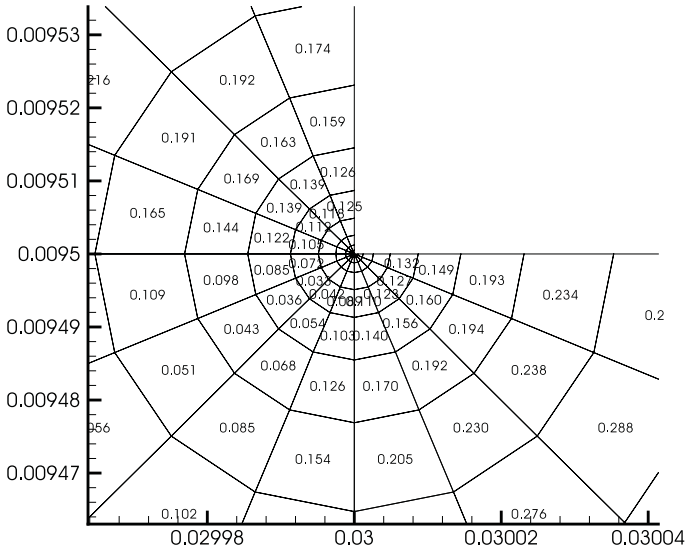

Figure 7.10: FEM error on elements in the refined area for the first case of geometry

	A	B	C	D	E	F	G	H
1	1.858	0.652	0.229	0.103	0.132	0.149	0.193	0.234
2	2.221	0.664	0.135	0.105	0.127	0.160	0.194	0.238
3	2.427	0.513	0.122	0.103	0.123	0.156	0.192	0.230
4	2.292	0.407	0.110	0.095	0.110	0.140	0.170	0.205
5	1.574	0.261	0.083	0.069	0.087	0.103	0.126	0.154
6	0.523	0.104	0.034	0.037	0.042	0.054	0.068	0.085
7	0.585	0.093	0.032	0.030	0.033	0.036	0.043	0.051
8	1.544	0.274	0.079	0.064	0.072	0.085	0.098	0.109
9	2.223	0.404	0.115	0.091	0.105	0.122	0.144	0.165
10	2.409	0.521	0.126	0.098	0.112	0.139	0.169	0.191
11	2.277	0.654	0.134	0.101	0.118	0.139	0.163	0.192
12	1.912	0.665	0.237	0.102	0.125	0.126	0.159	0.174
	I	J	K	L	M	N	con.	-
1	0.283	0.345	0.399	0.499	0.530	0.793	1.222	-
2	0.288	0.341	0.408	0.482	0.596	0.782	1.380	-
3	0.276	0.329	0.392	0.476	0.570	1.353	2.495	-
4	0.245	0.289	0.343	0.390	0.471	0.577	1.996	-
5	0.185	0.216	0.242	0.252	0.222	0.499	1.754	-
6	0.102	0.120	0.122	0.142	0.151	0.419	1.813	-
7	0.056	0.066	0.082	0.126	0.388	1.070	3.776	-
8	0.124	0.140	0.168	0.194	0.363	0.896	1.733	-
9	0.189	0.215	0.243	0.268	0.309	0.488	0.957	-
10	0.216	0.245	0.265	0.285	0.277	0.610	1.558	-
11	0.212	0.237	0.237	0.284	0.411	1.021	2.786	-
12	0.199	0.186	0.209	0.172	0.311	0.496	1.970	-

Table 7.2: Obtained errors on elements for the first case of geometry

Channel with abruptly extended diameter (results for Re = 400)

Similarly, streamlines, plots of velocity components u_x and u_y, and pressure are presented in Figures 7.11-7.12.

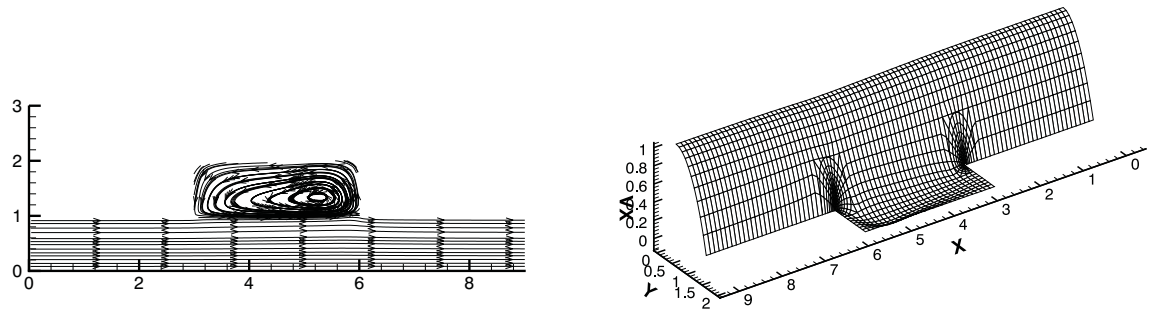

Figure 7.11: Streamlines (left) and velocity component u_x (right)

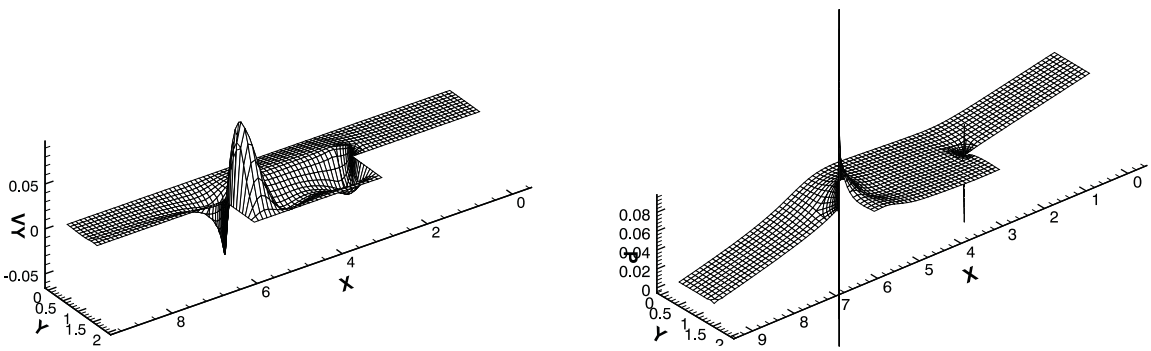

Figure 7.12: Velocity component u_y (left) and pressure (right)

In Figure 7.13, there are, again, values of obtained error on elements in refined area. All obtained values are listed in Table 7.3, where elemets of the refined detail are marked in the same way as in Figure 7.9.

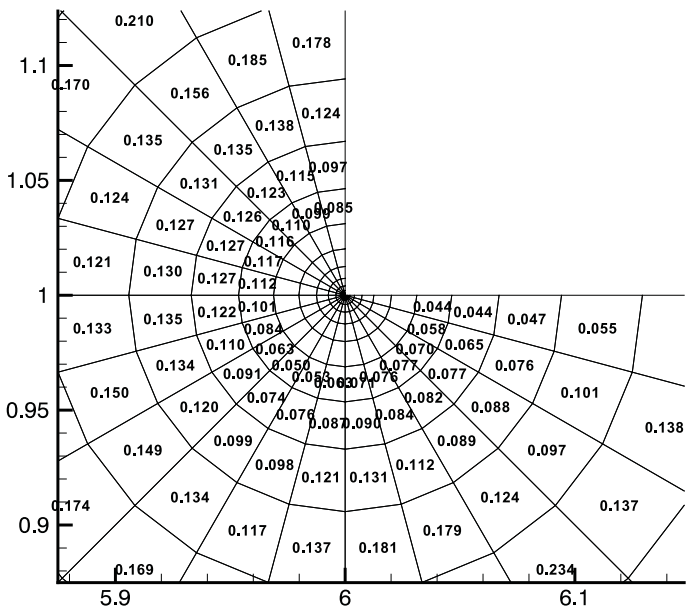

Figure 7.13: FEM error on elements in the refined area for the second case of geometry

	A	B	C	D	E	F	G	H
1	1.276	0.446	0.134	0.049	0.037	0.034	0.040	0.042
2	1.413	0.461	0.083	0.035	0.039	0.044	0.048	0.053
3	1.561	0.411	0.079	0.045	0.048	0.054	0.059	0.065
4	1.610	0.354	0.077	0.051	0.056	0.062	0.067	0.072
5	1.582	0.304	0.076	0.053	0.058	0.063	0.067	0.071
6	1.423	0.251	0.070	0.049	0.054	0.057	0.061	0.065
7	1.115	0.189	0.055	0.039	0.044	0.046	0.042	0.053
8	0.699	0.116	0.037	0.025	0.028	0.030	0.033	0.039
9	0.229	0.044	0.016	0.013	0.015	0.018	0.023	0.032
10	0.262	0.045	0.017	0.019	0.022	0.027	0.033	0.044
11	0.073	0.112	0.036	0.034	0.038	0.038	0.052	0.064
12	1.129	0.186	0.054	0.047	0.052	0.059	0.068	0.082
13	1.434	0.245	0.066	0.055	0.061	0.070	0.080	0.095
14	1.574	0.299	0.072	0.058	0.063	0.074	0.086	0.101
15	1.633	0.350	0.071	0.056	0.061	0.072	0.085	0.101
16	1.511	0.402	0.072	0.051	0.054	0.066	0.079	0.094
17	1.398	0.450	0.073	0.044	0.049	0.059	0.071	0.085
18	1.266	0.441	0.133	0.054	0.049	0.053	0.065	0.074

	I	J	K	L	M	N	O	con.
1	0.044	0.044	0.047	0.055	0.087	0.123	0.258	0.184
2	0.058	0.065	0.076	0.101	0.138	0.193	0.284	0.444
3	0.070	0.077	0.088	0.097	0.137	0.269	0.509	1.474
4	0.077	0.082	0.089	0.124	0.234	0.383	0.577	0.430
5	0.076	0.084	0.112	0.179	0.270	0.309	0.340	0.295
6	0.071	0.090	0.131	0.181	0.201	0.183	0.285	0.075
7	0.063	0.087	0.121	0.137	0.148	0.150	0.225	0.155
8	0.053	0.076	0.098	0.117	0.142	0.190	0.416	0.456
9	0.050	0.074	0.099	0.134	0.169	0.208	0.299	0.611
10	0.063	0.091	0.120	0.149	0.174	0.175	0.360	0.592
11	0.084	0.110	0.134	0.150	0.149	0.212	0.222	0.391
12	0.101	0.122	0.135	0.133	0.137	0.156	0.283	0.277
13	0.112	0.127	0.130	0.121	0.116	0.197	0.176	0.385
14	0.117	0.127	0.127	0.124	0.122	0.292	0.386	0.939
15	0.116	0.126	0.131	0.135	0.170	0.214	0.401	0.737
16	0.110	0.123	0.135	0.156	0.210	0.264	0.635	0.618
17	0.099	0.115	0.138	0.185	0.253	0.435	0.617	0.107
18	0.085	0.097	0.124	0.178	0.286	0.477	0.789	0.522

Table 7.3: Obtained errors on elements for the second case of geometry

8 Conclusion

Presented work is mainly focused on stabilization techniques for FEM for solving flows of incompressible viscous fluids. The motivation for such research leads from the desire of solving problems for higher Reynolds numbers.

The work fulfils its main goal – to develop an applicable algorithm based on the FEM stabilized by the Galerkin least-squares method. The algorithm has been verified by several numerical experiments (cf. the comparison to results by Guermond and Quartapelle in Chapter 6.3) and performed progressive results.

Main contributions are the transformation of the GLS stabilization method for the formulation of the Navier-Stokes equations given by (2.3)-(2.4), the derivation of the FEM algorithm for the steady and the unsteady cases, its implementation in the finite element program, and performing comprehensive numerical experiments with the algorithm.

It was observed in the problem of cavity in Chapter 6.1, that presented stabilization technique leads to improvement of stability of the Newton method to approximately 'double' Reynolds number. In the same chapter, similar effect was observed for the refinement of the computational mesh with half element size. Moreover, it was shown that the stabilization introduces perturbation into the Navier-Stokes system.

This results in recommendation, that for solving flows for higher Reynolds numbers, applying of stabilization techniques should be efficiently combined with a suitable refinement. An unusual approach to refinement is described in Chapter 7.

Further concluding remarks are presented in Chapter 6 accompanied by corresponding figures, and also in Chapter 5.

Although presented technique provides contributive results, investigating of stabilized methods offers several other possibilities, which are left to be tested and compared. Taking it as a challenge, I would like to continue this research in future.

Chapter 7 deepens the idea of using information about solution behaviour for efficient generating of computational mesh in the vicinity of corners with singularity. The two examples confirm the achievement of the goal – to obtain solution tinged with errors on elements satisfactorily small and uniformly distributed. The uniformity is apparent in Figures 7.10 and 7.13, and in Tables 7.2 and 7.3.

Presented approach to refinement is an alternative to the 'common' one, which uses a posteriori error estimates to refine elements with errors exceeding prescribed value. The latter is more robust, but in certain cases, we can save a lot of computational time using mesh 'prepared' for expected solution.

Results of Chapter 7 were presented by the author on the following international conferences:

- IMMAM 2003, Rožnov pod Radhoštěm, June 30 – July 4, 2003, cf. [7]
- Topical Problems of Fluid Mechanics 2004, Prague, February 25, 2004, cf. [25]
- ICFD International Conference on Numerical Methods for Fluid Dynamics 2004, University of Oxford, March 29 – April 1, 2004, cf. [26]

On the following international conferences, the results were presented by co-authors:

- ENUMATH 2003, Prague, August 18 – 22, 2003, cf. [8]
- ICCFD3, Toronto, July 12 – 16, 2004, cf. [9]

9 Appendix

Operator notations

Since a lot of calculations with vector fields in $\mathbb{R}^2$ are used in the thesis, it is considered to be useful to write down what is understood by them:

$$
\begin{aligned}
\mathbf{u} \cdot \mathbf{v} &= u_x v_x + u_y v_y \\
\nabla \mathbf{u} &= \begin{bmatrix} \frac{\partial u_x}{\partial x} & \frac{\partial u_x}{\partial y} \\ \frac{\partial u_y}{\partial x} & \frac{\partial u_y}{\partial y} \end{bmatrix} \\
\nabla \cdot \mathbf{u} &= \frac{\partial u_x}{\partial x} + \frac{\partial u_y}{\partial y} \\
\nabla \mathbf{u} : \nabla \mathbf{v} &= \frac{\partial u_x}{\partial x}\frac{\partial v_x}{\partial x} + \frac{\partial u_x}{\partial y}\frac{\partial v_x}{\partial y} + \frac{\partial u_y}{\partial x}\frac{\partial v_y}{\partial x} + \frac{\partial u_y}{\partial y}\frac{\partial v_y}{\partial y} \\
\Delta \mathbf{u} &= \nabla \cdot (\nabla \mathbf{u})^T = \begin{bmatrix} \frac{\partial^2 u_x}{\partial x^2} + \frac{\partial^2 u_x}{\partial y^2} \\ \frac{\partial^2 u_y}{\partial x^2} + \frac{\partial^2 u_y}{\partial y^2} \end{bmatrix} \\
(\mathbf{u} \cdot \nabla)\mathbf{u} &= \begin{bmatrix} u_x \frac{\partial u_x}{\partial x} + u_y \frac{\partial u_x}{\partial y} \\ u_x \frac{\partial u_y}{\partial x} + u_y \frac{\partial u_y}{\partial y} \end{bmatrix}
\end{aligned}
$$

References

[1] Brezzi, F., Fortin, M. *Mixed and Hybrid Finite Element Methods*, Springer, Berlin, 1991

[2] Burda, P. *On the FEM for the Navier-Stokes equations in domains with corner singularities*. In: Křížek, M., et al., editors. Finite Element Methods, Supeconvergence, Post-Processing and A Posteriori Estimates, Marcel Dekker, New York, 1998, 41-52

[3] Burda, P. *A posteriori error estimates for the Stokes flow in 2D and 3D domains*. In: Neittaanmäki, P., Křížek, M., editors. Finite Element Methods, 3D.(GAKUTO Internat. Series, Math. Sci. and Appl., Vol. 15), Gakkotosho, Tokyo, 2001, 34-44

[4] Burda, P. *On the Stability in the Finite Element Solution of the Navier-Stokes Equations for Incompressible Flows*. In: Proceedings of the XVth summer school Software and Algorithms of Numerical Mathematics 2004, 2004, 41-52

[5] Burda, P., Kořenář, J. *Numerical solution of pulsatile flow in a round tube with axisymmetric constrictions*. In: COMMUNICATIONS, Vol. 19, Institute of Hydrodynamics, Prague, 1992, 87-110

[6] Burda, P., Novotný, J., Sousedík, B. *A posteriori error estimates applied to flow in a channel with corners*, Mathematics and Computers in Simulation, **61** (2003), 375-383

[7] Burda, P., Novotný, J., Sousedík, B., Šístek, J. *Comparison of a posteriori and a priori error estimates of FEM for Navier-Stokes equations near singularity*. IMMAM 2003 Conference, Rožnov pod Radhoštěm, Czech Rep., 2003, to appear in the Proceedings

[8] Burda, P., Novotný, J., Sousedík, B., Šístek, J. *Finite Element Mesh Adjusted to Singularities Applied to Axisymmetric and Plane Flow*. In: Feistauer M, et al., editors. Numerical Mathematics and Advanced Applications, ENUMATH 2003, Springer, Berlin, 2004, 186-195

[9] Burda, P., Novotný, J., Šístek, J. *Accurate solution of corner singularities in axisymmetric and plane flows using adjusted mesh of finite elements*. ICCFD3 Conference, Toronto, 2004, Book of Abstracts, 1-2, to appear in the Proceedings by Springer

[10] Douglas, J., Jr., Wang, J. *An absolutely stabilized Finite Element Method for the Stokes problem*, Math. Comp., **52** (1989), 495-508

[11] Evans, L., C. *Partial Differential Equations*, Graduate Studies in Mathematics, Vol. 19, American Mathematical Society, 1998

[12] Franca, L., P., Frey, S., L. *Stabilized finite element methods: II. The incompressible Navier-Stokes equations*, Comp. Meth. Appl. Mech. Eng., **99** (1992), 209-233

[13] Franca, L., P., Frey, S., L., Madureira, A., L. *Two- and Three-Dimensional Simulations of the Incompressible Navier-Stokes Equations Based on Stabilized Methods*. In: Computational Fluid Dynamics '94, John Wiley & Sons Ltd, 1994, 121-128

[14] Franca, L., P., Hughes, T., J., R. *Convergence analyses of Galerkin least-squares methods for symmetric advective–diffusive forms of the Stokes and incompressible Navier–Stokes equations*, Comp. Meth. Appl. Mech. Eng., **105** (1993), 285-298

[15] Franca, L., P., Madureira, A., L. *Element diameter free stability parameters for stabilized methods applied to fluids*, Comp. Meth. Appl. Mech. Eng., **105** (1993), 395-403

[16] Gelhard, T., Lube, G., Olshanskii, M., A., Starcke, J.,H. *Stabilized finite element schemes with LBB-stable elements for incompressible flows*, Preprint, 2004

[17] Girault, V., Raviart, P., G. *Finite Element Method for Navier-Stokes Equations*, Springer, Berlin, 1986

[18] Glowinski, R. *Finite Element Methods for Incompressible Viscous Flow*, Handbook of Numerical Analysis, Vol. IX, Elsevier, 2003

[19] Guermond, J., L., Quartapelle, L. *Calculation of viscous incompressible viscous flow by an unconditionally stable projection FEM*, J. Comp. Phys., **132** (1997), 12-33

[20] Hughes, T., J., R., Franca, L., P., Balestra, M. *A new finite element formulation for computational fluid dynamics: V. Circumventing the Babuška-Brezzi condition: A stable Petrov-Galerkin formulation of the Stokes problem accommodating equal-order interpolations*, Comp. Meth. Appl. Mech. Eng., **59** (1986), 85-99

[21] Hughes, T., J., R., Franca, L., P., Hulbert, G., M. *A new finite element formulation for computational fluid dynamics: VIII. The Galerkin/least-squares method for advective-diffusive equations*, Comp. Meth. Appl. Mech. Eng., **73** (1989), 173-189

[22] Johnson, C. *Numerical Solution of Partial Differential Equations by the Finite Element Method*, Cambridge University Press, 1994

[23] Kondratiev, V., A. *Asimptotika rešenija uravnienija Nav'je-Stoksa v okrestnosti uglovoj točki granicy*, Prikl. Mat. i Mech., **1** (1967), 119-123

[24] Šístek, J. *Solution of the fluid flow in a tube with singularity using suitable mesh refinement (in Czech)*. In: Student Conference STČ 2003, ČVUT, Prague, 2003

[25] Šístek, J., Burda, P., Novotný, J. *Application of a priori error estimates of finite element method for mesh refinement near singularity in incompressible viscous flow*. In: Příhoda, J., Kozel, K., editors. Seminar Topical Problems of Fluid Mechanics 2004, Proceedings of the conference, Institute of Thermomechanics, Prague, 2004, 153-158

[26] Šístek, J., Burda, P., Novotný, J. *Precise FEM solution of corner singularity using adjusted mesh applied to axisymmetric and plane flow*. In: ICFD Conference on Numerical Methods for Fluid Dynamics, Univ. Oxford, 2004, Proceedings on CD

[27] Tezduyar, T., E. *Adaptive determination of the finite element stabilization parameters*. In: ECCOMAS Computational Fluid Dynamics Conference 2001, 1-17

[28] Turek, S. *Efficient Solvers for Incompressible Flow Problems*, Springer, Berlin, 1999